Journal of the
OPTICAL SOCIETY
of AMERICA

VOLUME 32 SEPTEMBER, 1942 NUMBER 9

A Method for Investigating the Thickness, Chemical Properties, and Surface Structure of Thin Biological Objects[1]

DAVID F. WAUGH[2]
The Department of Zoology, Washington University, St. Louis, Missouri
(Received July 6, 1942)

A method is described for determining thickness, refractive index, and chemical properties of objects which are submicroscopic in one dimension and microscopic in the other dimensions. Designed primarily for use in biology, the method depends upon the modifications in reflectivity of a glass surface produced by the deposition of a thin transparent film. The object is viewed with a microscope fitted with a vertical illuminator. Thickness is determined by matching the intensity of light reflected from the object with that reflected from a standard step film of barium stearate viewed in an identical companion system. The sensitivity is approximately ±12A. The method finds application in the biological field particularly in the investigation of thin cellular structures. In such cases information may also be obtained regarding the relative chemical composition by the use of solvents which remove certain of the components. The existence of patterns due to surface discontinuities (differences in optical thickness) may be detected and structure of this sort has been observed in the case of the limiting envelope of the mammalian red blood corpuscle.

MOLECULAR structure determinations on the limiting envelopes of cells and nuclei are particularly difficult since these structures have one dimension submicroscopic. The customary polarization, x-ray, and electron optical methods are not particularly applicable, although polarization optics has approximated the relative proportions of lipide and protein and has shown the general orientation of these components within the mammalian red cell envelope (for reviews see Schmidt,[3] and Schmitt[4, 5]).

The present communication describes a method which obtains information concerning the thickness, chemical composition, and surface structure of laminar envelopes and interfacial films. It depends upon the modifications in reflectivity of a glass surface produced by the presence of thin transparent films. The size of the objects to be studied necessitates the employment of microscopes and vertical illuminators. A comparison is made between the reflection modifications produced by the object and by a film of known properties. Since the instrument is of general use in biology it has, for convenience, been given the descriptive name, leptoscope (from *leptos*, a very thin object, and *skopeo*, to examine).

[1] The material described herein represents part of a thesis submitted to The School of Graduate Studies, Washington University, in partial fulfillment of the requirements for the degree of Doctor of Philosophy.

[2] Present address: Department of Biology and Biological Engineering, Massachusetts Institute of Technology, Cambridge, Massachusetts.

[3] W. J. Schmidt, *Die Doppelbrechung von Karyoplasma, Zytoplasma, and Metaplasma* (Berlin, 1937). See also Protoplasma **29**, 300, 435 (1937) and Nova Acta Leopoldina, N. F. **7**, 1 (1939). Polarisationsoptische Erforschung des Submikroskopischen Baues tierischer Zellen und Gewebe, Verh. d. Dtsch. Zool. Ges. (1939).

[4] F. O. Schmitt, Physiol. Rev. **19**, 270 (1939). See also J. App. Phys. **9**, 109 (1938).

[5] F. O. Schmitt, R. S. Bear, and E. Ponder, J. Cell. and Comp. Physiol. **9**, 89 (1936); **11**, 309 (1938).

BOSTON UNIVERSITY
COLLEGE OF LIBERAL ARTS
LIBRARY

THEORY OF REFLECTIVITY

The theory of the reflection of light from a glass surface covered by a thin transparent film is given by Blodgett and Langmuir[6] and Blodgett.[7] The ray reflected from the air-film boundary interacts with the ray reflected from the film-glass boundary to form a resultant ray of intensity I_R, where

$$I_R = B^2 + C^2 + 2BC \cos 2\pi D/\lambda, \qquad (1)$$

and B and C are the amplitudes of the rays reflected from the air-film and film-glass boundaries, respectively. The symbol D denotes the optical path difference between the B and C rays and is given by

$$D = 2n_1 t \cos r_1, \qquad (2)$$

where n_1 and r_1 are the refractive index and angle of refraction of light in the film when light is incident at an angle i and t is the thickness of the film.

The amplitude (ρ) of the light reflected at normal incidence from the interface between two isotropic media of refractive indices n_a and n_b is, according to the Fresnel theory,

$$\rho = (n_a - n_b)/(n_a + n_b), \qquad (3)$$

where the amplitude of the incident light is taken as unity. When $n_b > n_a$, ρ is negative and the phase of the light waves is reversed upon reflection. There is no reversal if ρ is positive.

Equation (1) neglects multiple reflections within the film. For perpendicular incidence, the correction to be applied to Eq. (1) has been derived by Blodgett and Langmuir[6] for the case $D = a\lambda$ and $D = \lambda(2a+1)/2$, where a is an integer,

when $D = a\lambda$,

$$I_+ = \left[\frac{B+C}{1+BC}\right]^2 = \left[\frac{n_0 - n_g}{n_0 - n_g}\right]^2, \qquad (4)$$

when $D = \lambda\dfrac{(2a+1)}{2}$,

$$I_- = \left[\frac{B-C}{1-BC}\right]^2 = \left[\frac{n_0 n_g - n_1^2}{n_0 n_g + n_1^2}\right]^2. \qquad (5)$$

When $n_1 < n_g$, I_+ and I_- are the maximum and minimum intensities of light reflected from the glass surface. When $n_1 > n_g$, the conditions are reversed, I_- being greater than I_+. When $n_1 = n_g$, the intensities of light reflected from the clean glass surface and any thickness of film are equal. The latter fact was utilized by Blodgett and Langmuir in determining the refractive index of built-up films of barium stearate.

In the present work glass of refractive index 1.69 was used for comparison purposes. The refractive index of built-up films of barium stearate, using film-trough solution A of Blodgett and Langmuir,[6] is 1.495 and $n_1 < n_g$. When observed in air, using normal incidence, the maximum intensity of light reflected from the surface given by Eq. (4) is 0.067 when the intensity of incident light is unity. The minimum intensity of reflected light is 0.018 by Eq. (5).

The thickness of one double layer of barium stearate is 48.8A. In most of the experiments a flat tungsten ribbon filament source was used in conjunction with a green filter transmitting a wave-length band from 4800 to 5400A having its center of gravity at 5000A. The type of illumination described below in connection with the microphotometer determinations of built-up films would be more desirable. For $\lambda = 5000$A and normal incidence the first minimum will occur at $t = 839$A or between step 16 and step 17, assuming 0.5 double layer to be due to the ferric stearate with which the slide was rubbed down.

Glasses having refractive indices greater than 1.7 are available. Glass of $n_g = 1.9$ would provide the greater intensity range 0.096 (I_+) to 0.006 (I_-) which would be highly desirable. However, such glasses tarnish readily and were not used extensively.

The use of the microscope objective both as the condenser which focuses the light on the object, and the objective which gathers a certain cone of rays reflected by the object necessitated proof that this system records faithfully the intensities of light reflected from a glass surface covered with films of different thickness. Evidence that such is the case may be deduced from Fig. 1. The maximum intensity of light reflected from clean glass is taken as unity in each case. Ordinates, therefore, represent the fraction of this intensity which is reflected by film thicknesses, in double layers, represented by the abscissae. The solid

[6] K. B. Blodgett and I. Langmuir, Phys. Rev. **51**, 964 (1937).
[7] K. B. Blodgett, Phys. Rev. **55**, 391 (1939).

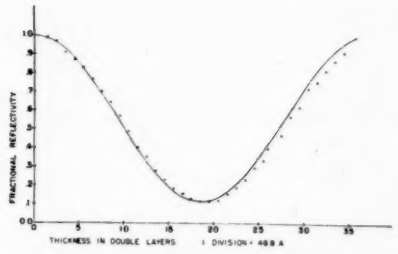

FIG. 1. A comparison of the theoretical reflectivity of a glass surface of $n_g = 1.82$ covered with a step film of $n_1 = 1.495$ with the reflectivity as measured with a microscope objective and vertical illuminator. Ordinates: fractional reflectivity taking the reflectivity of the clean glass as unity. Abscissae: film thicknesses in double layers. Solid curve calculated from Eq. (1) using $\lambda = 5460$A. Crosses obtained by microphotometering a step film of barium stearate.

line of Fig. 1 represents the thickness-fractional reflected intensity curve for a film of $n_1 = 1.495$ deposited on glass of $n_g = 1.82$. This curve was calculated from Eq. (1), using $\lambda = 5460$A, and assuming unit intensity of perpendicular incidence. The crosses were obtained by microphotometering steps from 0 to 34 double layers deposited on glass of $n_g = 1.82$ which had previously been rubbed down with ferric stearate, the ferric stearate contributing 0.5 double layer. The illuminating system consisted of a General Electric H-4 mercury vapor lamp and collimating system. The light was passed through Corning glass filters numbers 350, 430, and 512, cemented in series with gum Damar, transmitting the green line $\lambda = 5460$A. A Leitz Spaltmikrophotometer,[8] employing a vertical illuminator and 6_a objective, was used to observe the film steps. The slight deviations are due to small differences between the assumed and the actual values of the film and glass refractive indices and the fact that the objective does not give perpendicular incidence but incidence angles between 0° and about 15°. These differences are small and should disappear when comparisons are made using identical illuminating systems.

PREPARATION OF MATERIAL

Methods of preparation must be suited to the characteristics of the material to be studied. These methods (and results) have been described in detail elsewhere.[9] A short summary is introduced here as an aid in the discussion to follow.

A few ml of a dilute defibrinated blood cell suspension are placed upon a glass slide, $n_g = 1.69$. After a period of two minutes, during which a large number of the cells adhere to the ferric stearate surface, the excess cells are removed by immersion in isotonic saline. The adhering cells are immersed in 400 ml of $10^{-4}M$ buffer solution causing the cells to liberate their hemoglobin, salts, etc., into the hemolysing buffer. The limiting envelopes, however, remain attached to the glass surface. While the slide is totally immersed a monolayer of egg albumen is spread upon the cleaned surface of the buffer solution. The slide is then withdrawn through the film and dried in a vertical position. During the withdrawal the hydrous slide and adhering envelopes (osmotically hemolyzed erythrocytes) are covered with a monolayer of albumen. This lowers the surface tension so that the adhering envelopes are drawn into flat disks and they dry thus, the two membranes being tightly applied on each other (dried envelope disks). The slide carrying the object whose thickness is to be measured will be termed the preparation slide.

When viewed with a microscope and vertical illumination the portions of the field covered by the dried envelope disks reflect less light than the surrounding glass surface.[9] The dried disks can be extracted in alcohol or other organic solvents without altering their form. However, they now reflect more light than before, the difference being a measure of the amount of material lost.

DETERMINATION OF OPTICAL THICKNESS

The optical thickness of the envelope disk, normal or extracted, is obtained by determining that thickness of barium stearate film which reflects the same intensity of light as the envelope disk when both are deposited on glass of the same refractive index. The diameter of the envelope disk is approximately 8μ; hence, matching must be carried out at magnifications of 200–500.

A number of matching techniques have been investigated, the apparatus shown in Fig. 2 being found suitable. A ribbon filament lamp (General

[8] Thanks are due to Professor Newhouse of M. I. T. for the use of this instrument.

[9] D. F. Waugh and F. O. Schmitt, Cold Spring Harbor Symposia on Quantitative Biology **8**, 233 (1940).

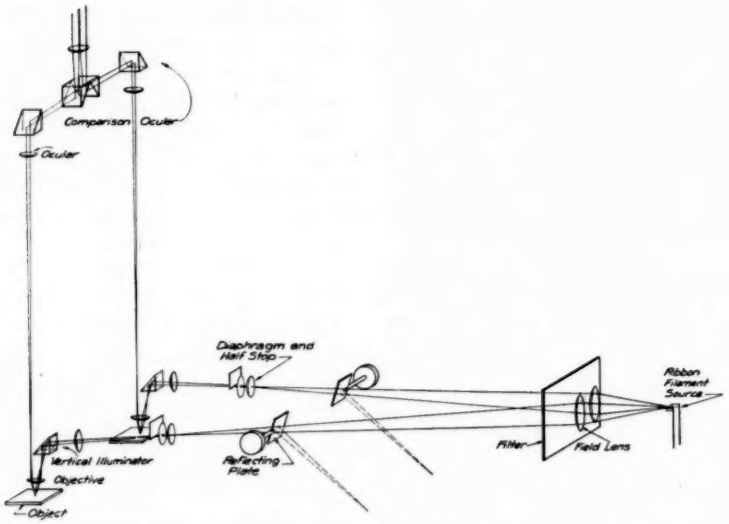

FIG. 2. Diagrammatic representation of the light paths in the leptoscope.

Electric SR-6a) provides a uniform source. The two light gathering field lenses[10] have equal focal lengths (about 7 cm).

The paths of the two light beams from the source are indicated by the solid lines. The prism vertical illuminators (Leitz, improved large model) reflect the incident beams to the objectives (Leitz 6a, short mounted) which act as condensers, focusing the light upon the objects. The objects reflect a certain amount of light back into the objectives and from thence to the oculars. The intensities of light reflected by the objects are compared by means of the comparison ocular.

A photograph of the apparatus is shown in Fig. 3. The glass slides are placed upon micrometer stages attached to microscope stages permitting vertical motion. The illuminating system, including the diaphragms and half-stops, is enclosed in a light-tight duraluminum box painted black on the inside to absorb stray reflections. Light-tight doors permit convenient adjustment of the individual units.

Correct alignment of the optical system is essential. All duplicate parts, including microscopes, objectives, illuminators, oculars, diaphragms and half-stops, and field lenses must be matched. Alignment is then carried out in the following steps. The optimal positions and distances between the parts of one-half of the system (source, field lens, diaphragm and half-stop, and microscope with vertical illuminator) are first determined. The two microscopes are fastened to metal plates having holes in the axial positions. These articulate with pins in the aligning base spaced so that the comparison ocular fits over the microscope tubes. Rotation of either microscope around its pin does not, therefore, affect the placement of the comparison ocular. The lamp, mounted on rack and pinion, is then fixed at the proper position and height, equidistant from the optic axes of the microscopes. Rotation of each microscope brings the filament and entrance tube exactly in line. The other parts are then introduced at their predetermined positions. After alignment, the movable stage alone is used for changing objects and for rough focusing. This avoids large changes in the position of the vertical illuminator. The work should be done in a dark room and sufficient time allowed after adjustments to permit the eyes to become dark adapted.

After alignment the procedure is as follows. The envelope preparation is placed upon the micrometer stage of the right-hand microscope and a comparison barium stearate film, built up in 2-mm steps according to the technique of

[10] In the newer apparatus the light beam is divided by means of 90° prisms facilitating alignment.

Blodgett, is placed upon the stage of the left-hand microscope.

The matching technique requires that each envelope disk be individually compared with several step thicknesses of the standard built-up film. The positions of the step boundaries are, therefore, determined on the micrometer scale at the start, permitting a rapid determination of the step under observation.

The contrast between the 0 and 1 double layer step predicted from Eq. (1), using $n_0 = 1.69$, is only 1 percent when $\lambda = 5400$A. Nevertheless, after dark adaptation, and with care, this boundary can be observed.

The intensities of light reflected from the glass surfaces must first be matched. The built-up film is moved so that the 0 step (no double layers) is in view. A field of envelope disks suitable for matching is then obtained and a portion of this field which is relatively free from the disks is brought to the boundary in the comparison ocular. With the Bertrand lenses[11] the apertures of the objectives are made equal by adjusting the diaphragms and half-stops.

The Bertrand lenses are then removed and the intensities of light reflected from the surfaces of the glass slides are matched by changing the intensities of incident light. This is done by rotating the differential reflecting glass plates (0.03 cm thick, $n_0 = 1.5$) shown in Fig. 2. The intensity of light which the plate transmits is a function of the angle of incidence of the light and the total reflecting area of the beam on the plate. These two factors, working together, permit the plate to be used as an intensity vernier.

The presence of the protein film on the envelope disk slide means that the intensity of light reflected from the surface of the rubbed-down standard comparison slide surface is being matched against the intensity of light reflected from the rubbed-down surface plus protein film of the preparation slide, thus introducing an error. The thickness of an egg albumen monolayer deposited at 15 dynes/cm is approximately 20A, (Langmuir, Schaefer, and Wrinch).[12] From Eq. (1) the intensities of light reflected from the rubbed-down slide and rubbed-down slide plus protein film, assuming the same refractive index for stearate films and protein monolayers, are 0.0688 and 0.0686, respectively. The difference in intensities is 0.3 percent which is below the minimal difference discernible by the eye. The error (due to protein) introduced in matching the initial intensities by the above matching technique can, therefore, be considered as negligible. At greater film thicknesses (see Fig. 1) the intensity difference due to the presence of the protein monolayer is larger. The thickness contribution of the protein monolayer is, therefore, subtracted from the actual thickness found for the unknown object. The method of obtaining actual thickness will be discussed below. Experimental determinations on known material showed the above to be quite accurate.

After matching the reflectivities of the glass slides, the envelope disk, whose optical thickness is to be measured, is moved to the boundary in the comparison ocular. Built-up film steps are then compared until a step is found which just matches the disk in intensity of reflected light or the envelope disk may be found to lie between two steps. The optical thickness of the envelope disk is thus determined within ± 12A of barium stearate film (since the step increment is 50A.)

The optical thickness of an object is accurately determined, using nearly monochromatic light. However, with monochromatic light, reflections from film steps in the second, or higher order,

FIG. 3. Photograph of the leptoscope.

[11] The Bertrand lens focuses on the back surface of the objective and indicates the extent to which the aperture of the objective is being utilized. From the position and size of the spot of light, and knowing the N. A. of the objective, one may calculate the average angle of incidence of light striking the object.

[12] I. Langmuir, V. J. Schaefer, and D. Wrinch, Science **85**, 76 (1937).

minima or maxima can be matched with reflections from film steps in the corresponding positions of the first-order range. The order of thickness of an unknown is first determined by using white light to match the unknown against built-up films having 4 double-layer step increments. A film having step increments of one double layer is then built up in the critical range, the green filter introduced, and the object accurately matched.

Mammalian envelope disks have optical thicknesses which place them in the first-order range, below 12 double layers. For exact matching, a film having steps of 0-1-2---15 double layers in thickness is used.

The determination of actual thickness will be discussed after the section concerning the measurement of refractive index.

MEASUREMENT OF REFRACTIVE INDEX

If a film having a refractive index n_1 is deposited on a number of glasses whose refractive indices form a series, the contrast between the film-covered glass and clean glass varies in a characteristic manner (unless as shown by Eq. (4), $D=2n_1t=a\lambda$, in which case the film always reflects the same intensity of light as the clean glass). Examination of Eqs. (4) and (5) shows that when $n_1<n_0$, I_+, which also equals the intensity of light reflected by the clean glass surface, is maximum, and the intensity of light reflected by any thickness of film will either be equal to or less than this value. When $n_1>n_0$, the situation is reversed; I_+ is the minimum value, and the intensity of light reflected by any thickness of film is always equal to or greater than this value. When $n_1=n_0$ the film always reflects the same intensity of light as the clean glass.

1. Optically Thick Microscopic Objects

The series of slides of different refractive indices is not rubbed down with ferric stearate but is cleaned with Shamva and kept hydrophilic until used. Observation with the leptoscope indicates the slide on which the contrast between the object and glass is a minimum. This method is suitable for objects having an optical thickness above that of 4 double layers of barium stearate.

2. Insoluble Microscopic Objects

In certain cases the microscopic object may be too thin to give sufficient contrast for the determination of refractive index as given under 1. In this case if the object is insoluble the contrast may be greatly intensified by depositing over the whole slide a number of double layers of barium stearate. The effect of the added double layers is to intensify the contrast between the glass and a thin object having a refractive index near that of the glass. Figure 1 shows that for a given increment in optical thickness, the contrast increases with increasing total thickness.

It should be pointed out that in methods 1 and 2 the refractive index of a weight of material less than 10^{-14} g may be obtained.

3. Macroscopic Objects

The refractive index of dry substance in bulk may be obtained as follows. A series of glass slides is carefully cleaned, washed with distilled water, and allowed to dry. A drop of solution (for protein about a 0.2 percent aqueous solution, for lipide about a 0.2 percent benzene solution) is then applied to the slide held in a vertical position. As it drains the drop wets the length of the slide and forms a band a few mm wide. After a short time, drying at the edges will cause a thin film (perhaps 1000A thick) of the dissolved substance to deposit in a coherent fashion on the glass surface. The contrast between the edge of the film and the glass, and interference colors in the body of the film immediately indicate whether the refractive index of the film is greater than, equal to, or less than that of the glass.

Films prepared from solutions in this manner may be used as a micro-solubility test. After preparation all but a narrow width of the thinnest part is wiped off and this strip of material is immersed for one-half its length in the solvent to be tested. Solubility is indicated by a change in interference color and a recession of the film glass boundary which has been immersed in the solvent.

THE DETERMINATION OF ACTUAL THICKNESS AND SPECIAL METHODS

Little difficulty is experienced in those cases in which the refractive indices of object and com-

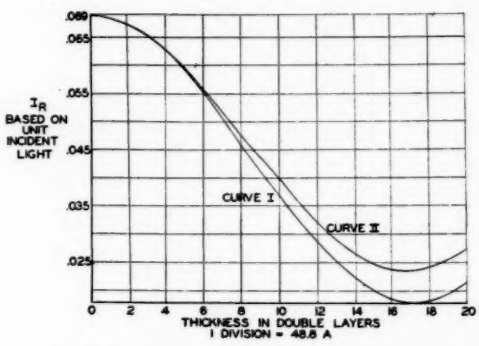

FIG. 4. Curves used in obtaining actual thickness from matching thickness when the object and film have different refractive indices. Ordinates: intensity of reflected light based on unit incident intensity. Abscissae: film thickness in double layers, one division being 48.8A. Both curves calculated from Eq. (1), using $n_g = 1.70$, and $\lambda = 5000$A. Curve I for stearate film of $n_1 = 1.495$. Curve II for an unknown object having a measured $n_1 = 1.525$.

parison film are equal for here the thickness of the object is equal to that of the matching step of the comparison film. When a refractive index difference is encountered, this difference must be taken into account in calculating the actual thickness from the optical thickness. There is no difficulty in making measurements on objects which are optically thick (above that of 4 double layers of barium stearate). However, when the object is thin some method of intensifying contrast is necessary. These factors are discussed below.

1. Determination of Actual Thickness

Films of materials having refractive indices within the range shown by biological objects (1.48 to 1.65) will reflect sensibly the same intensity of light when their thickness is less than 4 double layers. This may be seen from the curves of Fig. 4 calculated from Eq. (1) for films of $n_1 = 1.495$ (Curve I) and $n_1 = 1.525$ (Curve II) deposited on glass of $n_g = 1.69$ and assuming $\lambda = 5000$A. No corrections for refractive index differences need be made, therefore, when the equivalent thicknesses fall below 4 double layers (*ca.* 200A).

If the optical thickness is above 4 double layers, corrections for the refractive index difference may be made as follows. Two intensity-thickness curves are plotted as in Fig. 4, assuming glass of the same refractive index and unit normal intensity, but using the comparison film refractive index for one curve and the object refractive index for the other. The thickness of an object reflecting the same intensity of light as a given thickness of comparison film may then be readily obtained.

2. Special Methods

a. Optically Thin Objects

Objects which have optical thicknesses below about 4 double layers are difficult to match due to the lack of contrast between them and the surrounding glass surface. If the object is insoluble in water, contrast may be increased and matching greatly facilitated by applying to the preparation slide a number of double layers of barium stearate. This increases the thickness to the point where intensity differences for small thickness increments are large. If the refractive index of the object and comparison film is the same, no corrections are necessary other than to subtract the thickness of the film (both protein and stearate) added to the object.

Even in those cases where the object has a refractive index different from that of the comparison film, it has been found helpful to increase contrast by depositing double layers of barium stearate. The regions of the envelope disks, however, now form a layered structure, the layers having different refractive indices and thicknesses. Corrections for this factor have not been attempted for little is known concerning the reflection of light within a layered structure such as is present in this case. It is possible, however, to obtain the difference in measured thickness before and after the deposition of, say, 5 double layers of barium stearate in a few test cases. Assuming that the value measured directly is correct, a reasonable correction for the measured thickness after the deposition of 5 double layers of barium stearate is obtained. Further investigation is required to obtain a precise correction factor.

b. Soluble Objects

The deposition of stearate layers over an object which will be affected by hydration leads to relatively large errors, for during deposition a film of water usually will be trapped between the

hydrophylic object and the stearate film. It is possible to increase contrast in this case by depositing the object on a slide covered with a number of initial double layers of barium stearate film. The object may be deposited directly or after conditioning the stearate surface according to the technique of Langmuir and Schaefer.[13] In the foregoing discussion it has been assumed that the preparation slide will be treated with some reagent, such as an organic solvent, after the initial thickness measurements have been made. If barium stearate film has been deposited on the slide, it is inadvisable to treat with organic solvents, for the free fatty acid molecules will be leached out of the underlying stearate film to an unknown extent.[6,7] Where only one thickness determination is to be made, however, the deposition of initial barium stearate film is a valuable aid in increasing contrast. The objections to it are those mentioned under the section on optically thin objects. When the film and object have different refractive indices, a layered structure is formed which cannot at present be treated theoretically.

[13] I. Langmuir and V. J. Schaefer, J. Am. Chem. Soc. **59**, 1406 (1937); **59**, 1763 (1937). This opportunity is taken for acknowledging deep appreciation to Dr. Irving Langmuir for valuable information concerning the technique of built-up films and for his generosity in offering stimulating suggestions.

SURFACE STRUCTURE

Local differences in molecular constitution on a microscopic and submicroscopic level have been demonstrated in components such as the fibrous structures of muscle, chromosomes, and collagen. It is to be expected that similarly a specific molecular distribution will be found in the laminar structures of cells and tissues. Surface structure of this type would be manifest as regional differences in optical thickness which, in turn, would be resolved into differences in absolute thickness and refractive index; the latter originating in regional deviations in the distribution of the component molecules.

The ability of the leptoscope to detect surface structure will depend upon the resolving power of the microscopes used and the minimum contrast discernible by the eye. This method has been applied to an analysis of the structure of the red cell envelope.[9]

The author is deeply indebted to Professor F. O. Schmitt for aid and advice throughout the course of this work.

SEPTEMBER, 1942 J. O. S. A. VOLUME 32

Corrections for Residual Impurity and Background in Spectrochemical Analysis

JACOB CHOLAK AND ROBERT V. STORY
Kettering Laboratory of Applied Physiology, College of Medicine, University of Cincinnati, Cincinnati, Ohio
(Received July 14, 1942)

IT was formerly our custom, when dealing with weak lines in spectrochemical analysis, to correlate opacity data with concentration.[1] This procedure was sufficiently accurate when the backgrounds of the test spectra were of the same order of magnitude as those obtained in spectrograms of the standards, but large variations in background resulted in poor reproducibility of findings in the extremely low range of concentration and particularly in the case of weak lines in spectra with little or no background fog. Thus the need for greater precision in this range led to the development of a method which corrects not only for background but also for residual impurity in the standard mixtures. Use of this method has resulted in an appreciable increase in the reproducibility of the analytical findings even when dealing with concentrations of metal of the order of 0.00001 percent.

[1] J. Cholak and R. V. Story, J. Opt. Soc. Am. **31**, 730 (1941).

METHOD OF CORRECTING FOR BACKGROUND EFFECT

In order to correct for the residual impurity of reagents, the background effect must first be

eliminated. When dealing with lines of low intensity, this is accomplished in a manner similar to that described by Pierce and Nachtrieb,[2] with the additional precaution of using for comparison a standard line in the same range of intensity as the test line. The latter is important in evaluating weak lines which are influenced to a greater extent by variations in background than are lines of intermediate or heavy blackness. The use of such lines for comparison does not necessitate change in the usual chemical preparation of samples for analysis or in the spectrographic procedure, since the quantity of metal usually added to supply the standard line will give a number of lines of different intensities. In certain spectral regions the line chosen need not be in the immediate neighborhood of the test line. Any suitable line in the region 2500A to 3150A may be used for comparison in the determination of elements that give analytically useful lines in this region. (Pierce and Nachtrieb have reported that Eastman Process and Eastman Spectrum No. 1 plates show no change in plate gamma for the region 2500A–3100A[2] and we have found that this observation holds true also for Eastman No. 33 plates.)

The metal used to supply comparison lines is bismuth, the line at 2898A being employed in the usual routine procedure,[1] and that at 2993A serving when background corrections are necessary. Five milligrams of the metal per 100 ml of prepared solution are used. With such an amount of bismuth the average transmittancy of the former line is 0.50 (0.30 density) and that of the latter is 0.85. All analytical spectra are obtained with the rotating step sector, the interval of log exposure separation[1] being employed whenever possible. This method partially corrects for variations in background, except in the case of the very weak lines; consequently background corrections are applied only when the latter are used. In such cases, only the maximum exposure step is employed, the intensities of the standard and test lines being corrected for the backgrounds in which they lie, by the method described by Pierce and Nachtrieb.[2] The calibration mark is obtained from any suitable line in any stepped spectrum in which the transmittancy of the line in the minimum exposure step is greater than 0.95. The calibration curve of the plate is ordinarily obtained once for each box of plates.

[2] W. C. Pierce and N. H. Nachtrieb, Ind. Eng. Chem. Anal. Ed. **13**, 774 (1941).

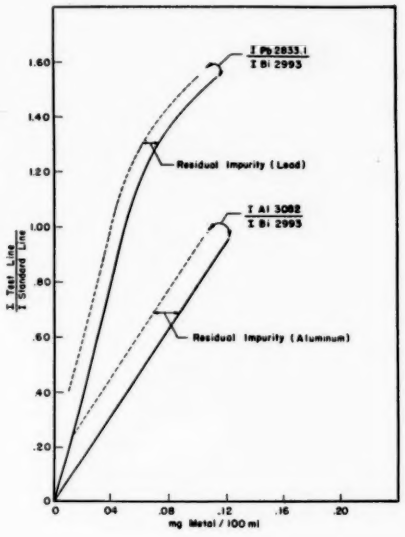

FIG. 1.

CORRECTION FOR RESIDUAL IMPURITY

To illustrate the technique employed in correcting working curves for residual impurity in the synthetic standard mixture and reagents, the method for aluminum is here described. Although the lines at 2898A and 2993A can be used, we have employed the lines at 3024A and 2993A. In obtaining a suitable density of the 3024A line for use in the interval log exposure separation method, 15 mg of bismuth per 100 ml of prepared samples are used. Spectra of a number of synthetic standard solutions containing known added amounts of aluminum (0.01, 0.05, and 0.10 mg Al/100 ml solution) are taken repeatedly on a number of plates. The intensities of the aluminum line at 3082A and of the bismuth line at 2993.4A are obtained and corrected for background as described above. The intensity ratios of the two lines (I Al 3082/I Bi 2993) are then determined for each spectrum and the average value for each concentration is plotted directly against the concentration, as is shown by the dotted line in Fig. 1. Since the initial blackenings of photographic plates vary almost linearly with the ex-

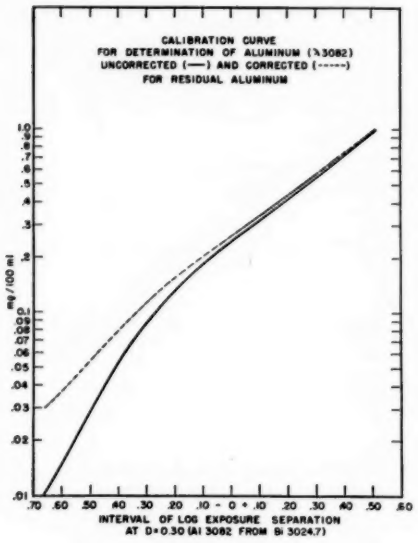
CALIBRATION CURVE
FOR DETERMINATION OF ALUMINUM (λ3082)
UNCORRECTED (—) AND CORRECTED (-----)
FOR RESIDUAL ALUMINUM
mg/100 ml
INTERVAL OF LOG EXPOSURE SEPARATION
AT D=0.30 (Al 3082 FROM Bi 3024.7)

FIG. 2.

posure,[3] it is obvious that the point where the linear portion of the plotted curve intercepts the intensity ratio axis depends on the amount of residual aluminum present in the materials used to prepare the standard solutions. The amount of lateral shift of this line away from a parallel line drawn through zero then represents the quantity of aluminum present as impurity in the standard. Further confirmation of the quantity thus determined is obtained by testing the standard solution itself. When this is done the intensity ratio should fit the proper concentration as read from the corrected curve (solid line in Fig. 1).

When quantities of aluminum above 0.10 mg per 100 ml of solution are present, background corrections are not made and the working curve (solid line) illustrated in Fig. 2 is employed (except in the case of samples of urine). The bend in the lower section of this curve is due both to residual aluminum in the standards and to the effect of background. That the latter is of little consequence, however, in dealing with quantities above 0.10 mg per 100 ml of solution, may be seen from the figure. The dashed line represents the working curve after it has been corrected for residual aluminum in the standard solutions, and although some bending, principally due to background, is still present, it is obvious that above 0.08 mg/100 ml the deviation from linearity is so slight as to be insignificant.

[3] H. Lundegardh, *Die Quantitative Spektralanalyse der Elemente*, Vol. 2 (Gustav Fischer, Jena, 1934).

DISCUSSION

Although it is not always possible to check the amount of impurity present by chemical means, it has been possible to do this with very sensitive and accurate methods in the case of aluminum and lead. In the case of aluminum, the residual impurity as determined by the method just described was 0.02 mg per 100 ml of solution, as compared with the result of 0.022 mg per 100 ml obtained by chemical analysis. As applied to lead (see Fig. 1), the values determined by these independent means were 0.01 mg per 100 ml and 0.006 mg per 100 ml, respectively, for the spectrographic and chemical methods.

Corrections for impurities need not be made when the synthetic standard solution is added to

TABLE I. Comparison of reproducibility of ratios employing standard lines of different intensity. (2993 = low intensity, 2898 higher intensity) (d.c. arc from 110-v line—10 amp., 50-volt drop across electrodes)

Concentration/100 ml	$\frac{I \text{ Pb } 2833.1}{I \text{ Bi } 2993}$	$\frac{I \text{ Pb } 2833.1}{I \text{ Bi } 2898}$
0.02 mg	0.42	0.13
	0.40	0.09
	0.33	0.065
	0.43	0.075
	0.50	0.035
	0.45	0.085
Average ratio	0.42	0.08
Mean error of individual value	±0.06	±0.03
% mean error	±14.0	±37
0.06 mg	1.31	0.20
	1.15	0.22
	1.15	0.22
	1.20	0.16
	1.20	0.23
	1.13	0.26
Average ratio	1.19	0.22
Mean error of individual value	±0.065	±0.028
% mean error	±5.5	±12.7
0.11 mg	1.51	0.30
	1.60	0.33
	1.54	0.31
	1.55	0.30
Average ratio	1.55	0.31
Mean error of individual value	±0.037	±0.014
% mean error	±2.4	±4.5

samples in order to control their inorganic salt composition. They are required only in the case of urine samples, which the standard salt solution was originally designed to simulate.[4] The other important use of such working curves is in the analysis of any material which itself has provided the standard mixture base.

The reproducibility of the ratios obtained from lines in which the background effect has been eliminated is shown in Table I. The data in this table have been taken from the spectra of standard concentrations used to derive the lead curve of Fig. 1. The average value for each concentration, the mean deviation of an individual ratio from the average (and the percentage of error) have also been listed for the various concentrations tested. The increased precision obtainable by the use of properly chosen lines for the internal standard may be seen by comparing the mean percentage of error in an individual finding obtained by this method with that given by the ratio obtained when the more intense 2898A line is used. In the latter case the calibration curve is so shallow that small differences in ratio give proportionally large errors.

The reproducibility of analytical results is further illustrated in Table II, in which there are data obtained from ten spectra of the same urine sample analyzed for aluminum. The general practice of using the average of the ratios for two spectra results in some increase in precision and this practice therefore is followed routinely in the analysis of all material known to be low in aluminum.

Standard comparison lines of a low scale of intensity have also been used by others,[5] but in these methods background corrections were not employed. Instead it was assumed that if the chosen test and standard lines were near enough together they would be affected to the same extent by background variation. This may be true in certain spectral regions, but in others, especially those above 3150A, the background intensity builds up toward the longer wavelength region (particularly when carbon or graphite electrodes must be used) and consequently the lines do not lie in backgrounds of equal intensity. If, however, the individual line is corrected for the background in which it lies, the reproducibility of analysis is quite satisfactory. In this region—with our method—because of the continual change of the gamma of the plate, it is not possible to use the same standard line for the measurement of widely separated test lines, and some difficulty may be encountered in obtaining two comparison lines of the proper intensity close enough to the test line to be of service. In such cases a single line must be applied according to the observed conditions, and the analysis must be repeated by adding or decreasing the amount of internal standard as the case may require.

TABLE II. Illustrating reproducibility of analytical result obtained by single spectrograms as compared with that obtained from the average of two spectra.

Spectrum number	$\frac{I \text{ Al } 3082}{I \text{ Bi } 2993}$	Mg Al/L from curve	Mg Al/L Using average ratios of two spectra
1	0.30	0.040	
2	0.50	0.064	0.052
3	0.43	0.054	
4	0.32	0.042	0.048
5	0.40	0.052	
6	0.32	0.042	0.047
7	0.39	0.050	
8	0.42	0.054	0.052
9	0.40	0.052	
10	0.40	0.052	0.052
Average	0.39	0.050	0.050
Mean error of an individual analysis	±0.06	±0.007	±0.005

[4] J. Cholak, Ind. Eng. Chem. Anal. Ed. **7**, 287 (1935).
[5] E. A. Boettner, Ind. Eng. Chem. Anal. Ed. **13**, 861 (1941).

Luminous Characteristics of Two Phosphorescent Materials

A. H. TAYLOR
Lighting Research Laboratory, General Electric Company, Nela Park, Cleveland
(Received July 6, 1942)

IN many locations where artificial light may be suddenly cut off by interruption of electric power, phosphorescent materials can be used to advantage to indicate obstructions, exits, etc. In view of their present importance in "blackout" applications as well as others, it appeared worth while to study the characteristics of two materials now on the market.* One of these materials, designated as P-10, exhibits a blue phosphorescence, while the other, P-11, shows a green phosphorescence.

It is well known that when a phosphorescent material is exposed to light of proper spectral character it stores up some radiant energy and re-radiates it. When the exciting energy is cut off the material remains luminous but decreases in brightness rapidly at first and more gradually thereafter. Its usefulness is dependent upon its brightness immediately after activation ceases and upon its rate of decay. These are affected by two well-known visual characteristics, dark adaptation and the Purkyne effect (usually incorrectly referred to as the *Purkinje* effect).

If the eye is adapted to reasonably high brightness levels such as are encountered in daylight and modern artificial lighting, it will rapidly increase in sensitivity in total darkness. Its sensitivity at any moment is measurable in terms of the minimum perceptible brightness of a luminous field of definite visual angle and location. It is found that the minimum brightness which can be seen decreases rapidly for the first ten minutes in darkness and more slowly thereafter; it may continue to decrease for an hour or more. This adaptation to some extent compensates for the brightness decay of the phosphorescent material. The rate of dark adaptation of the eye depends upon many factors, some important ones being the state of adaptation just prior to the start of the test, the color, angular extent, position, etc., of the low brightness field to be observed.

Dark adaptation data which might be applicable to the use of these phosphorescent materials in artificially lighted interiors are presented in Table I. These are averages for two normal subjects, as recently determined in our laboratory.

TABLE I. Average darkness adaptation data for two observers with so-called normal vision, viewing a uniform field one foot square from a distance of ten feet (6-degree field). Data apply to binocular central vision. Pre-adaptation for several minutes in a well-lighted office, indirectly illuminated to 30 footcandles on the working plane.

Minutes in darkness	Minimum perceptible brightness in micro-foot-lamberts (1×10^{-6} ft.-l)†
1	65
2	28
3	16
4	10
5	7.5
6	6
8	3.2
10	2.5
15	1.4
20	0.8
30	.45
40	.35
50	.32
65	.27

† The average brightness of the clear night sky is approximately 200 micro-foot-lamberts or 0.0002 foot-lambert.

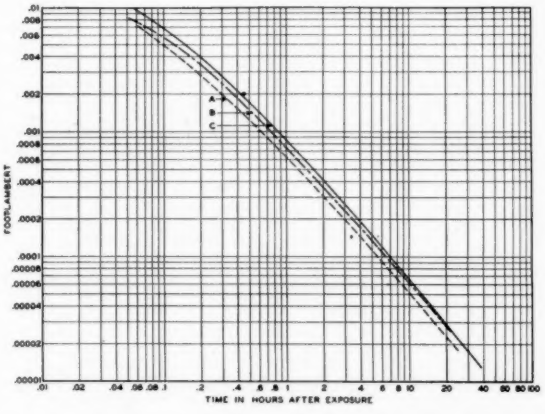

FIG. 1. Brightness decay curves for P-10 (blue) phosphorescent material exposed for 4 minutes to a 500-watt tungsten-filament lamp at (*A*) 15, (*B*) 25, and (*C*) 50 footcandles. (Exposures for 4 minutes to 100 and 200 footcandles gave results practically the same as 50 footcandles.)

* Manufactured by the Continental Lithograph Company, Cleveland, Ohio.

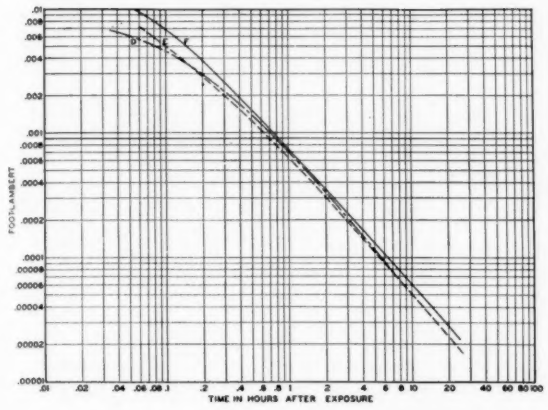

FIG. 2. Brightness decay curves for P-10 (blue) phosphorescent material exposed for (*D*) 16½ hours to 5 footcandles, (*E*) 4 minutes to 15 footcandles, and (*F*) 20 minutes to 1200 footcandles from a tungsten-filament lamp.

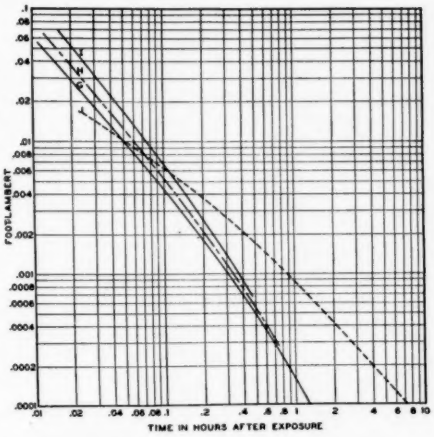

FIG. 3. Brightness decay curves, after exposures sufficient to produce saturation, for (*J*) P-10 (blue) exposed to tungsten-filament lamps and for P-11 (green) phosphorescent material exposed to (*G*) tungsten-filament lamps, (*H*) 3500° White Mazda *F* (fluorescent), and (*I*) Type H-4 high pressure mercury lamp with "black-light" filter.

The test field was an opal glass, one-foot square, illuminated from behind by a tungsten-filament lamp. The observer, seated ten feet away, used central binocular vision. It was always possible to see the test field by peripheral vision before it was seen by central vision, but the data in the table are those for central vision. Prior to starting the adaptation test the observer spent several minutes in a well-lighted office, the illumination being 30 footcandles at desk level. Thus his state of adaptation was comparable to that of a worker in a factory which might be "blacked out."

At low brightness levels the eyes become relatively much more sensitive to the blue than to the red region of the spectrum. This is the Purkyne effect, named after the man who discovered it. This phenomenon especially favors one of the materials for which data are to be given, the blue one designated P-10.

The brightness of the phosphorescent materials immediately after activation and the subsequent decay rates may depend on a number of factors such as temperature of the material, spectral distribution of the energy from the light-source, energy incident per unit area, length of exposure, etc. All of our tests have been made with the material at room temperature, approximately 75°F.

The spectral region most effective in activating the two materials was studied qualitatively by exposing them to a tungsten-filament lamp through filters cutting off at various wave-lengths in the near-ultraviolet and visible spectrum. This test showed that most of the activation was produced by ultraviolet energy of wave-lengths shorter than λ4000.

"Saturation" may be defined as that degree of activation which produces the maximum brightness of the material immediately after excitation ceases. In order to study this characteristic the P-10 (blue) material was exposed to different intensities of illumination from a 500-watt tungsten-filament lamp for equal lengths of time, and the rate of decay measured with a Taylor Model A Low Brightness Meter.[1] Curves *A*, *B*, and *C* of Fig. 1 show the brightness of the P-10 material at various times after the termination of exposure, which was for four minutes to illuminations of 15, 25, and 50 footcandles, respectively. Other exposures to 100 and 200 footcandles for four minutes gave results almost exactly the same as *C*, which was for 50 footcandles.

It might seem possible that a long exposure to low illumination could produce the same phosphorescent result as a shorter exposure to higher

[1] A. H. Taylor, "Brightness and brightness meters," Illum. Eng. **37**, 19 (January, 1942).

illumination. To study this factor the same P-10 material was exposed to 5 footcandles for 16½ hours, to 15 footcandles for 4 minutes, and to 200 footcandles for 20 minutes. The results are shown, respectively, by curves *D*, *E*, and *F* of Fig. 2. Apparently the long exposure to low illumination produced a result not greatly different from the shorter exposures to higher illumination, except in the first 10 to 15 minutes after the exposure stopped.

The results described above were all obtained with a tungsten-filament lamp as the illuminant. Tests were also made with a 3500° white fluorescent (Mazda F) lamp and an H-4 high pressure mercury lamp with black glass filter. If the exposure was sufficient to produce saturation, the decay curves were practically the same as those obtained with tungsten-filament lamps.

From Fig. 3 it will be noted that the brightness of the P-11 (green) material is higher when activated by the H-4 (high pressure mercury) "black-light" lamp than when a tungsten-filament lamp is used, by a factor of approximately two in the first ten minutes. Although the initial brightness of the P-11 is higher than that of the P-10, its decay rate is much more rapid. If they are both saturated by light from a tungsten-filament lamp, they are equal in brightness about three minutes after activation and thereafter the P-10 remains the brighter. If a "black-light" source such as the H-4 lamp and filter is used, the P-11 (green) material is the brighter for the first six minutes after activation and is darker thereafter. The P-10 (blue) is still bright enough, several days after activation, to be seen by a thoroughly dark-adapted observer. One specimen of this material, three days after exposure, had a brightness of approximately 5 micro-foot-lamberts (5×10^{-6} ft.-l).

To anyone unfamiliar with low brightness units the data in Figs. 1 to 3 may be meaningless. In order to help one visualize the meaning of such brightnesses let us consider the brightness of certain diffusing surfaces under 0.0002 footcandle which is the approximate level of illumination at the earth's surface due to full starlight on a clear night. Under this level of illumination a diffusing surface having a reflection factor of 10 percent would have a brightness of about 0.00002 foot-lambert (20 micro-foot-lamberts). It is found that the brightness of the P-10 (blue) material decays to 0.00002 foot-lambert approximately 27 hours after excitation ends, whereas the P-11 (green) material reaches this value in three hours. A higher order of brightness would be that of fresh snow in the light from a clear moonless sky, i.e., full starlight. This brightness would be approximately 0.00015 foot-lambert. To a dark-adapted eye this is a very appreciable brightness. The time after exposure when the two materials reach this brightness is approximately five hours for the P-10 and one hour for the P-11.

TABLE II. Approximate brightnesses of two phosphorescent materials, relative to visual threshold, at various times after the activating light is turned off.

Time after exposure and start of dark adaptation	Approximate brightness relative to visual threshold	
	P-10	P-11
3 minutes	600	600
6 minutes	1000	700
10 minutes	1750	900
30 minutes	4000	1100
1 hour	3000	500

Another method of appraising the brightness level of phosphorescent materials at various times is in terms of the visual threshold brightness. Using the data in Table I, which apply specifically to a 6-degree field, we obtain the results in Table II for observation in total darkness beginning immediately after saturation exposure to tungsten-filament lamps. These are approximately the conditions which might be encountered in an office or factory suddenly blacked out.

The exposure required to produce saturation with each of these materials is of especial interest. Using the 500-watt tungsten-filament lamp as the source, an exposure of the P-10 material to 25 footcandles for 4 minutes produced a brightness about 10 percent below saturation, whereas an exposure of 8 minutes produced saturation. An exposure to 200 footcandles for ½ minute produced saturation. From these data it appears that an exposure of 100 footcandle minutes to this source is sufficient to produce approximate saturation, provided the illumination is not less than 25 footcandles. Data are not available to determine whether saturation can be produced by

lower illuminations for periods sufficient to give 100 footcandle minutes.

When the P-11 (green) material was exposed to 200 footcandles from the 500-watt lamp, saturation was obtained with an exposure of 7½ seconds.

Phosphorescent materials such as these have many obvious uses in wartime, since moderate areas furnish sufficient brightness to serve as markers of doorways, passageways, etc., and at the same time they are not bright enough to be seen from the air by enemy planes. No doubt there are also many peacetime uses which will be developed when such phosphorescent materials are readily available.

SEPTEMBER, 1942 J. O. S. A. VOLUME 32

Photoelectric Tristimulus Colorimetry with Three Filters*

RICHARD S. HUNTER
National Bureau of Standards, Washington, D. C.

(Received April 20, 1942)

The term, photoelectric colorimetry, is commonly employed to designate both photoelectric tristimulus colorimetry, used to evaluate the appearance of materials, and abridged spectrophotometry, often used to assist in chemical analyses. This paper is devoted to the first type of measurement. For a photoelectric tristimulus colorimeter, it is desired to find three or more source-filter photo-cell combinations of such spectral character that they duplicate the standard I.C.I. observer for colorimetry. With an instrument having these combinations, tristimulus values would be obtained by direct measurement. Although no one has duplicated the I.C.I. observer perfectly, several investigators have obtained source-filter photo-cell combinations suitable for the measurement of color differences between spectrally similar samples. To measure color differences as small as those which the trained inspectors of paint, textile, plastic, paper, and ceramic products can see, an instrument must have high precision. If the needed precision is available, a photoelectric tristimulus colorimeter may be used to measure: (1) I.C.I. colorimetric values, x, y, and Y, relative to those of a spectrally similar, calibrated standard; (2) relative values of α and β, components of the chromaticity departure from neutral in a new uniform-chromaticness-scale mixture diagram for representing surface colors; (3) amounts of color difference between pairs of spectrally similar samples; (4) amounts of color change accompanying fading; and (5) whiteness of white and near-white surfaces. In giving examples of the measurement of some of these different properties and in describing the errors of color measurement to which the tristimulus method is subject, reference is made to operations with the author's recently developed multipurpose photoelectric reflectometer.

CONTENTS

I. Introduction 510
II. Terms, symbols, and definitions 511
1. Physical 512
2. Psychological 512
3. Psychophysical 512
III. The source-filter photo-cell combinations 513
IV. Reduction of photoelectric tristimulus data 516
1. To I.C.I. values, x, y, and Y 517
2. To (α, β)-uniform-chromaticness-scale coordinates 518
3. To the amount of color difference ΔE perceived between surface colors 519
4. To the coordinates α', β', L' of a solid with an approximately uniform color-perception spacing 521
5. To the hue angle ϕ, the saturation index S, and the lightness index L 522
6. To estimates in N.B.S. units of the hue, saturation, and lightness components, $\Delta H'$, $\Delta S'$, and $\Delta L'$, of a perceived surface-color difference 522
7. To values of whiteness W 522
8. To the yellowness of a white and near-white surface 523
V. Standards for photoelectric tristimulus colorimetry 523
VI. Errors in photoelectric tristimulus measurements 524
1. Errors in tristimulus measurements of chromaticity difference due to spectral inaccuracy of the source-filter photo-cell combinations 525
2. Changes in measured chromaticity resulting from change of photo-cell in an instrument 527
3. Fluorescence errors 528
4. Short cuts in computation which produce only small errors 528
VII. The relation of perceptual impressions and measured values of color 530
VIII. Examples 534
IX. Summary 535
X. References 536

* A preliminary brief account of this project was presented as part of the ASTM-ISCC joint *Symposium on Color* held in Washington, March 5, 1941 [19].

I. INTRODUCTION

THE possibility of using photo-cells to measure color has attracted widespread attention ever since the photoelectric cell became available in practical form. Photoelectric cells have now been used for a number of years in spectrophotometry to measure the spectral reflective and transmissive properties of materials. From the spectrophotometric curves of samples, one may obtain the tristimulus values of color by multiplying the separate spectral values of any sample by the three distribution functions of the standard observer[1] and totaling the three sets of products throughout the visible spectrum (see Eqs. (3), below). Although the use of photo-cells has considerably diminished the time needed to obtain spectrophotometric curves, and although devices such as the one developed by Sears [43][2] are available to facilitate the integration, a considerable expenditure of time and effort is still required [29 p. 259] to obtain the accurate colorimetric specification of a sample by the method of spectrophotometry and integration.

Photoelectric tristimulus colorimetry is direct and rapid because the result of integration with respect to wave-length is found automatically by the use of specially chosen source-filter photo-cell combinations (see Eqs. (5), below). With this type of photoelectric colorimeter, the tristimulus specification of a sample is found by settings upon it using in succession each of the three or more filters in an instrument. This direct method of color measurement has at present somewhat limited application because the best available source-filter photo-cell combinations fail to be spectrally equivalent to the desired combination of I.C.I. standard observer and standard illuminant for colorimetry. Nevertheless, there are many problems of color measurement to which the shorter procedure may be advantageously applied and these will doubtless increase in number as research progresses.

Photoelectric tristimulus colorimetry is frequently confused with photoelectric abridged spectrophotometry [11], and both are popularly called photoelectric colorimetry. Therefore, a short discussion of the two experimental methods and of the differences between them is appropriate. Instruments for both procedures require a source, several filters, and a photo-cell. Instead of the prism or grating used in a true spectrophotometer, three to about eight spectral filters are used in an abridged spectrophotometer to isolate spectral bands. These bands are of wider wave-length ranges and are fewer in number than the bands employed in true spectrophotometry; consequently accurate spectrophotometric curves are not obtained [21]. Nevertheless, an abridged spectrophotometer is often a useful instrument. Frequently, it is known that some particular chemical or physical property of a substance may be studied by using a single spectral range or several spectral ranges which may be isolated by filters. An abridged spectrophotometer may serve adequately for the measurements needed.

A tristimulus colorimeter also requires filters, but it does not primarily measure the variation of any property of samples with respect to wave-length. Instead samples are measured with source-filter photo-cell combinations which spectrally duplicate, as nearly as possible, the three distribution functions characterizing the standard observer combined with some standard illuminant. With one source and photo-cell, three or at most four filters are needed. However, the filters for tristimulus colorimetry differ from those used for abridged spectrophotometry in that they transmit bands of wide wave-length range.

Ives described a thermopile tristimulus colorimeter in 1915 [23], which made use of a spectrum selectively projected through a series of carefully-cut templates in place of the filters employed in the more recent devices. Twyman and Perry showed in 1928 [46] that an instrument which would yield direct tristimulus measurements could be obtained by finding source-filter photo-cell combinations spectrally similar[3] to the standard observer, illuminant combination for colorimetry.[4] However, it was not until 1938 that

[1] For descriptions of the I.C.I. standard observer for colorimetry, see references [15, 20, 22, 25, 31, 33, and 45].

[2] Numbers in brackets, either with or without specific page numbers, indicate references listed at the end of the paper.

[3] For a discussion of what is meant by spectrally similar, see footnote 6 below.

[4] The three ideal source-filter photo-cell combinations would each duplicate in spectral response the relative spectral distribution of one of the three functions of the I.C.I. standard observer combined with chosen standard

TABLE I. Tabular arrangement of some of the terms used to describe the color of a surface.

Category	Physical	Psychophysical (physically measured, psychologically significant)	Psychological
Instrument	Spectrophotometer	Tristimulus colorimeter	Visual mechanism of the observer
Product of the instrument	Spectral apparent-reflectance curve	Designation of the surface color by a set of tristimulus values for it; X, Y and Z; A, G and B; or other.	The perceived surface color
The separate attributes of the surface color, and the perceived surface color		(1) Luminous apparent reflectance $A_{\theta i, \theta v}$ (chiefly designated below by Y), the lightness index L.	(1) Lightness
		(2) Dominant wave-length Λ, or hue angle ϕ	(2) Hue
		(3) Purity p, or saturation index S	(3) Saturation, or "strength"
		(2 and 3 combined) Chromaticity, indicated either by Λ and p, ϕ and S, or by a pair of trilinear coordinates, x and y, α and β, etc.	(2 and 3 combined) Chromaticness

Perry described an actual instrument for photoelectric tristimulus colorimetry. He called his device the Blancometer [40] because of its special suitability for white and near-white samples. Guild described the experimental model of a tristimulus colorimeter in 1934 [14], and Winch and Palmer [50], Dresler and Frühling [4], and Barnes [2], have described devices for the same purpose since that time. Gibson [11] and Van den Akker [47] have discussed the problem of obtaining the source-filter photo-cell combinations giving the closest spectral equivalence to the standard observer.

The present paper describes a 3-filter method for approximate photoelectric tristimulus colorimetry which has so far been used chiefly in conjunction with the author's multipurpose reflectometer [18] to measure surface color. Tristimulus measurements with this instrument have proved to be valuable in studies of the colors of paints, ceramic products, textiles, papers, pigments, inks, and other materials which reflect light. The major part of the present paper is devoted to tristimulus measurements of surface colors, but it should be noted that a number of the methods suggested are equally useful for the study of volume colors by measurements of transmitted energy and for the study of illuminant colors by measurements of emitted energy.

II. TERMS, SYMBOLS, AND DEFINITIONS

It is the purpose of photoelectric tristimulus colorimetry to give by measurement quantities which provide useful information about the appearance of objects and lights. Three different classes of properties must be recognized in the study of the subject: physical, psychological, and psychophysical. Physical properties have no necessary connection with an observer; psychological properties deal directly with the impressions of an observer and are therefore not subject to exact physical measurement; psychophysical properties are an intermediate class which are capable of measurement, but which relate to the impressions of an observer. It is important to distinguish between these three classes of properties and identify the terms which refer to each.

To assist in this differentiation, Table I, which classifies a number of the terms used herein, has been prepared. This table is modeled after Fig. 1 in the Preliminary Draft of a Report on Nomenclature and Definitions for Colorimetry [24] by L. A. Jones, Chairman of the Colorimetry Committee of the Optical Society of America. One term in Table I, chromaticness, has been added to accord with the present draft of the uncompleted report of this committee.

illuminant (as expressed in Eqs. (1), below). A standard illuminant is, in general, relatively non-selective and plays a secondary role in determining the spectral character of the ideal source-filter photo-cell combinations. In the remainder of the paper it has sometimes been convenient to speak of spectral duplication of, or spectral similarity to, the standard observer when actually spectral duplication of, or spectral similarity to, the standard observer combined with a standard illuminant is meant.

The definitions, and in some cases symbols, for a number of the terms used in the present paper are separated below according to the three categories.

1. Physical

A *spectrophotometer* is an instrument which measures transmission or apparent reflectance as a function of wave-length.

A *spectrophotometric curve* is a curve giving transmission T_λ, or apparent reflectance A_λ, of a sample as a function of wave-length.

2. Psychological

A perceived surface color is color experienced as a property of a surface [30]; the three attributes of a perceived surface color are lightness, hue, and saturation.

The lightness of a perceived surface color is that attribute which permits it to be classed as equivalent to some member of the series of grays ranging from black to white [30]. (In the Munsell system, value correlates closely with lightness under usual observing conditions.)

The hue of a perceived color is that attribute which permits it to be classed as red, yellow, green, blue, purple, or an intermediate [30].

Chromatic surfaces are those perceived to possess hue (not to be confused with Munsell chroma) [30].

Achromatic surfaces are those such as whites, grays, and blacks which are perceived to possess no hue [30].

Saturation is that attribute of a perceived surface color which determines the degree of its difference from the gray of the same lightness [30]. (Munsell chroma correlates closely with saturation under usual visual conditions.)

The chromaticness of a perceived color is determined by its hue and saturation taken together.

3. Psychophysical

A *tristimulus colorimeter* is a device which measures a color stimulus in terms of three selected stimuli called primaries. The ideal source-filter photo-cell combinations for a photoelectric tristimulus colorimeter are those which are spectrally equivalent to the 1931 I.C.I. standard observer for colorimetry in combination with an appropriate illuminant.

The 1931 I.C.I. standard observer for colorimetry embodies the average colorimetric characteristics of 17 normal observers studied by Guild [13] and Wright [51]. The definition of the standard observer consists of three functions of wave-length λ, showing the relative amounts ($\bar{x}_\lambda$, $\bar{y}_\lambda$, $\bar{z}_\lambda$) of three primary stimuli required to color match the various parts of the equal-energy spectrum.

A tristimulus designation of an unknown stimulus consists of the amounts (such as X, Y, Z)[5] of the three primary stimuli required to produce a color match for it.

Apparent reflectance is the reflectance which a perfectly diffusing surface would need to have in order to produce, under the same angular conditions of illuminating and viewing, the same instrumental effect as the specimen actually measured. Apparent reflectance given as a function of wave-length is designated *spectral apparent reflectance* $A_{\lambda(\theta i, \theta v)}$, and is most frequently represented by a spectrophotometric curve. Apparent reflectance weighted according to the luminosity function is designated *luminous apparent reflectance* $A_{(\theta i, \theta v)}$, or Y. For apparent-reflectance values weighted according to other spectral functions such as those of the source-filter photo-cell combinations described below, symbols which identify the functions are used.

The Y component of the tristimulus designation of a color represents the luminous component of that color [31, 33]. Thus Y designates the luminous apparent reflectance of a surface color, the luminous transmission of a volume color, and the brightness of an aperture or illuminant color. The methods of measurement described below are in most cases applicable to problems involving volume, aperture, and illuminant colors as well as to the surface colors referred to in the text. For this reason, the symbol Y has been used

[5] It should be noted that there has not been universal agreement on the use of these symbols. The National Bureau of Standards has in the past usually used $\bar{x}$, $\bar{y}$, and $\bar{z}$ to represent the tristimulus designation of an unknown stimulus and X, Y, and Z to represent the trichromatic coefficients of the spectrum. In the present paper, however, this former use of symbols has been discarded in favor of the above usage, which is recommended in the present unpublished draft of the O.S.A. Colorimetry Committee report.

below instead of $A_{\theta i, \theta v}$ where the text refers to luminous apparent reflectance. It should be noted that the symbol A is used herein to designate settings with the multipurpose reflectometer and amber filter.

The settings, A, G, and B, with the multipurpose reflectometer employing, respectively, the amber, green, and blue filters, are, for a surface color, apparent reflectances for illumination at 45° and viewing at 0° relative to MgO. In practice the instrument is adjusted by means of a working standard calibrated in terms of MgO. Illumination at 45° and viewing at 0° have been internationally adopted as standard conditions for the colorimetry of opaque surfaces [22] because they represent a satisfactory average of the directional conditions under which surfaces are observed in everyday life. Because the combination of source, green filter, and photo-cell nearly duplicates the standard luminosity ($\bar{y}$) function times I.C.I. illuminant C, readings obtained with the green-filter combination closely duplicate Y. Because the three source-filter photo-cell combinations are nearly equivalent spectrally[6] to the I.C.I. standard observer, measurements of A, G, and B of a sample constitute an approximate tristimulus description of its color.

The chromaticity of a color is its characterization by either (1) dominant wave-length and purity, (2) hue angle and saturation index, or (3) a pair of trilinear coordinates (x and y, α and β, etc.).

The dominant wave-length Λ [41], and *the hue angle* ϕ, of a color are both computed from the tristimulus specification to indicate hue.

The purity p [41], and *the saturation index* S, of a color are obtained from the tristimulus specification to indicate what is variously called saturation or strength.

The trilinear coordinates (x, y, and z, or α, β, and γ) are the amounts of the three primary stimuli expressed as fractions of their total. Because the three trilinear coordinates of a color are fractions of a total and must necessarily sum to unity, two of them (either x and y, or α and β) are sufficient to define the *chromaticity* of a stimulus.

A chromaticity diagram is a plot according to trilinear coordinates in which position of a point indicates the chromaticity of the stimulus represented.

III. THE SOURCE-FILTER PHOTO-CELL COMBINATIONS

The distinguishing feature of apparatus for photoelectric tristimulus colorimetry is that spectral elements nearly equivalent to the I.C.I. standard observer for colorimetry must be provided. If the device is to be used for the colorimetry of light sources, television screens, or other self-luminous color stimuli, the apparatus will require filters and photo-cells only. If the samples are to be non-self-luminous objects, such as opaque surfaces or transparent media, a source for illuminating the objects must be added to the filter photo-cell combinations. The resulting sets of source, filter, and photo-cell must then be nearly equivalent in spectral response to the standard observer combined with the desired standard illuminant.

The combinations of elements described in the present paper are those which have been used for tristimulus colorimetry with the author's multipurpose reflectometer [18]. Although used for the most part in this one instrument, the source-filter photo-cell combinations described below are applicable to photoelectric tristimulus colorimetry with other photoelectric devices[7] of suitable precision.

If the three spectral response functions of the I.C.I. observer are denoted by $\bar{x}$, $\bar{y}$, and $\bar{z}$ and the spectral energy of the illuminant for equivalent visual analysis is denoted by E_v, then the ideal source-filter photo-cell combinations for photoelectric colorimetry according to the I.C.I. observer will satisfy the following equations:

$$\begin{aligned} E_I T_1 s K_1 &= \bar{x} E_v, \\ E_I T_2 s K_2 &= \bar{y} E_v, \\ E_I T_3 s K_3 &= \bar{z} E_v. \end{aligned} \tag{1}$$

The source in the instrument is represented by

[6] By "nearly equivalent spectrally to the I.C.I. standard observer" it is meant that the spectral distributions of the three source-filter photo-cell combinations can be changed by transformation equations which are linear and homogeneous [31, p. 345] to spectral functions which nearly duplicate the I.C.I. standard observer combined with Illuminant C (see Fig. 1).

[7] These combinations, for example, have been used in the Lumetron Colorimeter, Photovolt Corporation, 95 Madison Avenue, New York, New York.

its spectral energy E_I, the ideal filters by their spectral transmissions T_1, T_2, and T_3, the photocell by its spectral response s, and the constants of proportionality between the two sides of the respective equations by K_1, K_2, and K_3.

An instrument was desired which would give numbers corresponding to those furnished by the I.C.I. observer rating objects under I.C.I. Illuminant C [22],[8] a standard illuminant which is similar in spectral quality to overcast sky. Accordingly E_C, representing I.C.I. Illuminant C, was substituted for E_v in Eqs. (1). Since a source of high efficiency and small area is needed in the apparatus, a Mazda projection-type incandescent lamp was chosen. This is operated at approximately 3100°K and hence the relative spectral irradiance corresponding to 3100°K [44] was used for E_I. The General Electric light-sensitive cell [10] was chosen because[9] of the high current it generates for a given illumination, and the relatively high response to light of the blue region of the spectrum, and because data giving the spectral response of the cells available for the author's instrument were at hand.[10]

It was recognized that ideal filters satisfying Eqs. (1) would not be found. No attempt was made to duplicate with a single source-filter photo-cell combination the complete $\bar{x}$ function with its two components. Instead, the two components were separated as suggested by Gibson [11] and the short-wave component was taken to be spectrally similar to the $\bar{z}$ function.[11] A combination was then sought to duplicate the long-wave component only. This component of the $\bar{x}E_C$ function is approximated by using an amber filter having a spectral transmission T_A. The $\bar{y}E_C$ and $\bar{z}E_C$ functions are approximated by using green (T_G) and blue (T_B) filters, respectively.

Spectral specifications for the source-filter photo-cell combinations chosen, $E_I T_A s k_A$, $E_I T_G s k_G$, and $E_I T_B s k_B$, are given in Table II. Included in the same table are the spectral transmissions of the three filters,[12] the spectral irradiance from a source at 3100°K, and the spectral response of G.E. light-sensitive cell No. 55. The values of k were adjusted so that each of the final three columns would total 100,000. Each filter consists of two components, all six components chosen being from stock manufactured by the Corning Glass Works.[13]

The success with which the source-filter photocell combinations duplicate the I.C.I. standard observer combined with Illuminant C is shown

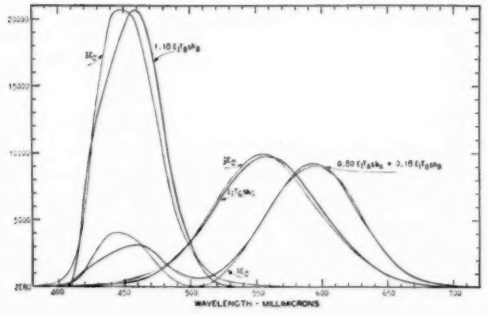

FIG. 1. The I.C.I. observer, represented by the curves $\bar{x}E_C$, $\bar{y}E_C$, and $\bar{z}E_C$, compared to its approximate duplication by the source-filter photo-cell combinations used in the multipurpose reflectometer.

[8] By using one of the color-temperature altering filters described by Gage [9] or Estey [5] with each of the three source-filter photo-cell combinations, it is possible to obtain the effect of raising or of lowering the color temperature of E_v. Thus it is possible to simulate not only visual observations made under I.C.I. Illuminant C, but visual observations made under light from a yellow incandescent lamp, or from blue sky.

[9] For a more detailed account of the selection of the photo-cells used for tristimulus colorimetry in the multipurpose reflectometer, see [18, p. 584 and 18a, p. 538].

[10] Kindly supplied by Dr. B. T. Barnes of the General Electric Company, Nela Park, Cleveland, Ohio.

[11] Guild [14], Perry [40], Dresler and Frühling [4], Barnes [2], and Van den Akker [47] have all pointed out that a fourth source-filter photo-cell combination is preferable to using the $\bar{z}$ combination in order to simulate suitably the short-wave component of the $\bar{x}$ function. However, the author is chiefly interested in the measurement of small differences in color with the simplest procedures possible. If three filters will suffice, a fourth adds undue complexity to the measurements. Until important improvements are made in the degree to which the three present filters duplicate the I.C.I. observer, the use of a fourth filter is unwarranted.

[12] The author is indebted to Mr. H. J. Keegan for numerous spectral transmission curves obtained during the course of this work.

[13] It is possible to obtain suitable tristimulus filters from Corning glass available at the present writing (October, 1941), by using the following designations and thicknesses:

	Catalog number	Melt designation	Thickness (mm)
Yellow component of amber filter	326	190	2.42
Green component of amber filter	978	$\beta_{540}=0.338$ (This Corning β value bears no relation to the trilinear coordinate β.)	1.3
Blue-green component of green filter	428	194	3.65
Yellow component of green filter	330	17	3.30
Blue component of blue filter	554	211	5.00
Yellow component of blue filter	038	206	1.5

TABLE II. Spectral character of the individual components and of the source-filter photo-cell combinations used for photoelectric tristimulus colorimetry with the multipurpose reflectometer [18].

	Spectral transmissions (Corning filters)					Spectral specification of the three source-filter photo-cell combinations. (Each value of k has been chosen so that the sum of the column is 100,000.)		
Wave-length (mμ)	T_A (Amber filter of No. 330 yellow glass and No. 978 green glass)	T_G (Green filter of glass and No. 428 green glass and No. 330 yellow glass)	T_B (Blue filter of No. 554 blue glass and No. 038 yellow glass)	E_I Relative spectral irradiance of source at 3100°K [44]	$\bar{s}$ Spectral response of G.E. cell No. 55 (in micro-amperes per milliwatt)	$E_I T_A \bar{s} k_A$ (amber)	$E_I T_G \bar{s} k_G$ (green)	$E_I T_B \bar{s} k_B$ (blue)
380		0.010	0.000	0.1188	94.5		31	
90		.010	.000	.1425	101.5		39	
400		.011	.000	.1688	107.8		56	
10		.011	.020	.1979	113.9		70	337
20		.012	.298	.2294	119.5		92	6,109
30		.013	.443	.2634	124.7		120	10,885
40		.017	.478	.2998	129.7		185	13,901
450		.023	.482	.3383	134.2		291	16,368
60		.035	.445	.3790	138.8		514	17,511
70		.050	.338	.4215	143.0		842	15,237
80		.077	.195	.4658	147.2		1,476	10,001
90	0.004	.107	.090	.5114	151.3	96	2,315	5,208
500	.010	.138	.045	.5582	155.5	269	3,350	2,922
10	.020	.173	.015	.6061	159.1	596	4,664	1,082
20	.038	.209	.003	.6548	162.3	1,248	6,210	239
30	.063	.235	.000	.7040	164.9	2,258	7,628	
40	.095	.249		.7536	167.0	3,695	8,763	
550	.128	.251		.8033	168.4	5,351	9,496	
60	.164	.243		.8531	168.7	7,291	9,778	
70	.196	.222		.9025	167.4	9,148	9,378	
80	.224	.193		.9516	162.9	10,727	8,366	
90	.237	.163		1.0000	156.3	11,443	7,125	
600	.238	.135		1.0476	147.5	11,363	5,833	
10	.227	.109		1.0945	135.4	10,393	4,516	
20	.206	.086		1.1403	117.3	8,511	3,216	
30	.181	.067		1.1850	97.7	6,472	2,170	
40	.153	.053		1.2284	79.1	4,594	1,440	
650	.122	.040		1.2704	60.8	2,910	864	
60	.099	.032		1.3111	43.7	1,752	512	
70	.077	.025		1.3503	28.5	914	268	
80	.057	.020	.000	1.3880	18.0	439	140	
90	.043	.017	.002	1.4240	11.9	226	81	25
700	.030	.014	.003	1.4584	8.8	117	50	28
10	.022	.012	.004	1.4912	7.2	74	36	32
20	.016	.010	.004	1.5223	6.1	46	25	28
30	.011	.009	.005	1.5517	5.8	31	22	34
40	.008	.008	.004	1.5793	5.7	22	20	27
750	.005	.007	.004	1.6055	5.5	12	17	26
					Σ	99,998	99,999	100,000

graphically in Fig. 1, in which $\bar{x}E_C$, $\bar{y}E_C$, and $\bar{z}E_C$, which inclose areas of approximately 98,000, 100,000, and 118,000, respectively, are plotted as functions of wave-length together with

$$0.80E_I T_A \bar{s} k_A + 0.18E_I T_B \bar{s} k_B,$$
$$1.00E_I T_G \bar{s} k_G, \quad \text{and}$$
$$1.18E_I T_B \bar{s} k_B,$$

which inclose respectively equal areas. The duplication is far from perfect and can be improved by further work. Also, as already noted, the use of a fourth filter would improve the duplication. The following approximate equations designate the relationships shown in Fig. 1 and serve as the basis for comparison of I.C.I. tristimulus values

TABLE III. The uses of photoelectric tristimulus measurements.

Quantities computed from settings	Equations used	Uses of results
The coordinates, x, y, and Y of the I.C.I. standard system	$x \doteq (0.80A+0.18B)/\Sigma$ $y \doteq G/\Sigma$ $\Sigma = 0.80A+G+1.36B$ $Y \doteq G$ (From Eqs. (5) and (6))	To find whether sample meets color requirements specified by x, y, and Y. To represent colors in the standard I.C.I. system.
The chromaticity coordinates α and β of a uniform-chromaticness-scale system	$\alpha \doteq (A-G)/(A+2G+B)$ $\beta \doteq 0.4(G-B)/(A+2G+B)$ (Eqs. (8))	To designate chromaticity in a coordinate system yielding approximately uniform-chromaticness scales for surface color. To indicate changes of chromaticness of specimens with time, exposure, change of composition, change of method of preparation, or other treatment.
The amount of color difference ΔE between two surface colors	$\Delta E = f_\phi\{[7Y^{\frac{1}{2}}[(\Delta\alpha)^2+(\Delta\beta)^2]^{\frac{1}{2}}\cdot 10^2]^2 + [k_1\Delta(Y^{\frac{1}{2}})]^2\}^{\frac{1}{2}}$ (Eq. (13))	To measure the amount of color difference between two surface colors in N.B.S. units. To find whether a sample differs from a standard by more or less than a specified color tolerance. To measure the amount of color change resulting from exposure, change of composition, change of method of preparation, or other treatment of the sample.
The coordinates α', β', and L' of a uniformly-spaced surface-color solid	$\alpha' = 700Y^{\frac{1}{2}}\alpha$ $\beta' = 700Y^{\frac{1}{2}}\beta$ $L' = k_1Y^{\frac{1}{2}}$ (Eqs. (14))	To designate surface color using coordinate scales which give perceptually nearly uniform measures of stimulus difference.
The hue angle ϕ, the saturation index S, and the lightness index L	$\phi \equiv$ angle whose tangent is β/α $S \equiv [(\alpha^2+\beta^2)Y^{\frac{1}{2}}]^{\frac{1}{2}}$ $L \equiv Y^{\frac{1}{2}}$ (Eqs. (16))	To approximate the hue, the saturation, and the lightness of colors by separate numbers.
The hue, saturation, and lightness components $\Delta H'$, $\Delta S'$, and $\Delta L'$, of a surface-color difference in N.B.S. units	$\Delta H' = 12.2Y^{\frac{1}{2}}(\alpha^2+\beta^2)^{\frac{1}{2}}\cdot\Delta\phi$ ($\Delta\phi$ in degrees) $\Delta S' = 700Y^{\frac{1}{2}}\cdot\Delta([\alpha^2+\beta^2]^{\frac{1}{2}})$ $\Delta L' = k_1\Delta(Y^{\frac{1}{2}})$ (Eqs. (17))	To separate a surface-color difference into the hue, saturation, and lightness components of the difference in N.B.S. units.
The whiteness W of a white or near-white surface	$W = 1-\left\{[30(\alpha^2+\beta^2)^{\frac{1}{2}}]^2+\left[\frac{1-Y}{2}\right]^2\right\}^{\frac{1}{2}}$ (Eq. (19))	To designate a white or near-white surface with a number on a scale of whiteness which gives an MgO surface a value of 1.00 and a black surface a value of zero.
Yellowness	Yellowness $= (A-B)/G$ (Eq. (20))	To give a white or near-white surface a number which indicates degree of yellowness if positive, degree of blueness if negative.

and photoelectric tristimulus values:

$$\begin{aligned} \bar{x}E_C &\doteq 0.80E_IT_Ask_A+0.18E_IT_Bsk_B, \\ \bar{y}E_C &\doteq 1.00E_IT_Gsk_G, \\ \bar{z}E_C &\doteq 1.18E_IT_Bsk_B. \end{aligned} \qquad (2)^{14}$$

[14] The author is indebted to Miss N. J. Hendley (now Mrs. E. M. Furness) for assistance in finding transformations of the source-filter photo-cell combinations which were closely equivalent to the standard observer. After experiment with several transformations giving slightly closer equivalence to the standard observer, it was decided that the simple transformations indicated by Eqs. (2) were more practical for ordinary use.

IV. REDUCTION OF PHOTOELECTRIC TRISTIMULUS DATA

Values of A, G, and B obtained from a photoelectric tristimulus colorimeter may be converted to useful information about the colors of the samples measured in a number of different ways. Each procedure for reducing data gives numbers which are useful for a particular purpose. In Table III the quantities which can be computed are identified by the equations for finding them and by their principal uses.

As previously noted, the methods of measurement suggested herein refer chiefly to surface colors. It is believed, however, that several of these suggested methods will prove to be equally applicable to the evaluation of volume colors from transmission measurements and to the evaluation of the colors of self-luminous objects from measurements of radiant flux.

1. To I.C.I. Values, x, y, and Y

The I.C.I. standard system [22] for designating colors has international recognition and is therefore widely used in the specification of colors. The tristimulus specification of a surface color according to the I.C.I. observer is the summation through the spectrum of the spectral apparent reflectance of the sample relative to MgO ($A_{\lambda(\theta i,\theta v)}$ being measured by a spectrophotometer), times the spectral energy E_C of the illuminant, times the respective spectral distribution functions $\bar{x}$, $\bar{y}$, and $\bar{z}$ of the I.C.I. observer:

$$X \equiv \sum_{\lambda=0}^{\lambda=\infty} A_{\lambda(\theta i,\theta v)} E_C \bar{x} \Delta\lambda,$$

$$Y \equiv \sum_{\lambda=0}^{\lambda=\infty} A_{\lambda(\theta i,\theta v)} E_C \bar{y} \Delta\lambda, \qquad (3)$$

$$Z \equiv \sum_{\lambda=0}^{\lambda=\infty} A_{\lambda(\theta i,\theta v)} E_C \bar{z} \Delta\lambda.$$

If the same sample is compared with MgO in a photoelectric tristimulus colorimeter, the following summations through the spectrum are made automatically:

$$\sum_{\lambda=0}^{\lambda=\infty} A_{\lambda(\theta i,\theta v)} E_I T_A s k_A \Delta\lambda \equiv A,$$

$$\sum_{\lambda=0}^{\lambda=\infty} A_{\lambda(\theta i,\theta v)} E_I T_G s k_G \Delta\lambda \equiv G, \qquad (4)$$

$$\sum_{\lambda=0}^{\lambda=\infty} A_{\lambda(\theta i,\theta v)} E_I T_B s k_B \Delta\lambda \equiv B.$$

A, G, and B are, by definition, the settings of the sample relative to those of standard MgO with the amber, green, and blue filters, respectively.

By multiplying both sides of Eqs. (2) by $A_{\lambda(\theta i,\theta v)}$ and making summations through the spectrum, we find by way of Eqs. (3) and (4) that:

$$X \doteq 0.80A + 0.18B,$$
$$Y \doteq 1.00G, \qquad (5)$$
$$Z \doteq 1.18B.$$

The equations are only approximate because the source-filter photo-cell combinations are spectrally somewhat different from the standard I.C.I. observer, as shown in Fig. 1. However, photoelectric tristimulus measurements according to a substitution method using a calibrated standard spectrally similar to the samples are, as is shown below, suitably accurate for many purposes.

Since the $\bar{y}$ function of the I.C.I. observer is the luminosity function, approximate values of luminous apparent reflectance are given directly by settings with the green filter. To indicate chromaticity in the I.C.I. system, the trilinear coordinates of a color are computed as follows:

$$x \equiv X/(X+Y+Z)$$
and $$y \equiv Y/(X+Y+Z). \qquad (6)$$

Figure 2 shows the I.C.I. (x, y) diagram and the corresponding photoelectric approximation to the diagram plotted in the same coordinates. In each diagram are the spectrum locus and points representing twelve differently colored porcelain-enamel plaques,[15] each illuminated by

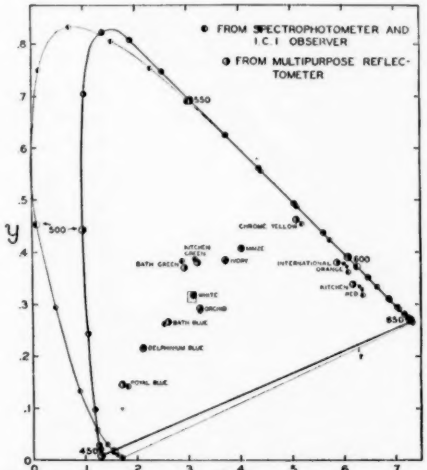

FIG. 2. I.C.I. (x, y) diagram and corresponding photoelectric approximation to the diagram with the point for white (MgO) common to both diagrams. The pairs of points for the eleven chromatic porcelain-enameled plaques show the errors in chromaticity measured by the photoelectric tristimulus method. The small rectangle near the center gives boundaries shown in Fig. 7.

[15] The standards used are ten kitchen and bathroom colors [36], and plaques representing medium chrome yellow [6] and international orange [7].

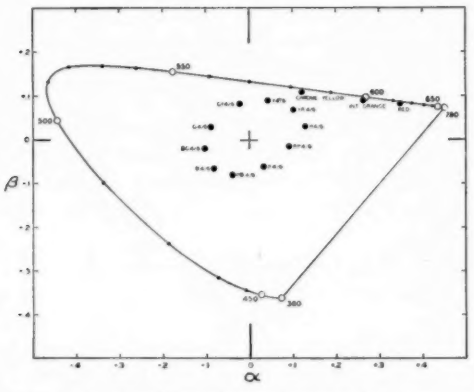

FIG. 3. (α, β)-uniform-chromaticness-scale diagram for surface colors showing the spectrum locus and points representing ten Munsell colors of 4-value and 6-chroma [38] medium chrome yellow, international orange, and toluidine red.

I.C.I. Illuminant *C*. The point $X=0.3101$ and $y=0.3163$, representing a freshly prepared magnesium oxide surface similarly illuminated, is common to both diagrams. Each of the twelve plaques was measured relative to MgO, first with a spectrophotometer and then with a multipurpose reflectometer; the values of x and y obtained from the two sets of data were computed and plotted in Fig. 2.

Coordinates of the spectrum locus of the I.C.I. mixture diagram are published in many places [15, 22, 25, 31, 33, 45]; coordinates of the boundary of the photoelectric approximate chromaticity diagram were computed by applying Eqs. (5) and (6) to the values of $E_I T_A s k_A$, $E_I T_G s k_G$, and $E_I T_B s k_B$ given in Table II. At the ends of the visible spectrum (380 to 420 mμ and 670 to 750 mμ) the source-filter photo-cell combinations imperfectly duplicate the I.C.I. standard observer as the distributions diminish to zero. Therefore the trilinear coordinates which would result from photoelectric measurement of the spectrum for these wave-lengths of low response are highly inaccurate and have been left out of Fig. 2.

2. To (α, β)-Uniform-Chromaticness-Scale Coordinates

The (α, β)-chromaticity diagram shown in Fig. 3 has been planned especially for representing surface colors measured with the multipurpose reflectometer and tristimulus filters. Cartesian coordinates and an origin located at the point representing MgO were used because of the greater convenience for plotting chromaticity, and because of the simple relation afforded thereby between position of point in the diagram and saturation index and hue angle of the color represented. The convenience of these two features was recognized by Breckenridge and Schaub, who used them in their earlier R.U.C.S. triangle [3]. In addition to these features and the advantage of easy computation from settings with a reflectometer, values of α and β have an important advantage as uniform-chromaticness-scale coordinates for representing the colors of paints, papers, textiles, and opaque ceramic products. The equations defining α and β were chosen, as pointed out by Scofield, Judd, and Hunter [42], to give measures of chromaticity in improved accord with visual estimates of the chromaticness of opaque surfaces.

The coordinates of the chromaticity diagram are defined by:

$$\alpha \equiv \frac{2.4266x-1.3631y-0.3214}{1.0000x+2.2633y+1.1054}, \qquad \beta \equiv \frac{0.5710x+1.2447y-0.5708}{1.0000x+2.2633y+1.1054}. \tag{7}$$[16]

Prior to the selection of these equations defining the (α, β) diagram, equations were sought which would make the conversion of multipurpose reflectometer settings to values in the new coordinate system a simple matter. After trial with a number of possible sets,[17] the following

[16] The reverse equations are

$$x=\frac{0.5583\alpha+0.1631\beta+0.2466}{0.0100\alpha-1.4347\beta+0.7951}, \qquad y=\frac{-0.2515\alpha+0.6285\beta+0.2515}{0.0100\alpha-1.4347\beta+0.7951}. \tag{7a}$$

[17] Prior to the choice of Eqs. (8), two earlier pairs were used by the author. The first pair, suggested in 1939 [16] were

$$\alpha \doteq \frac{2A-2G}{2A+5G+3B}, \qquad \beta \doteq \frac{G-B}{2A+5G+3B}, \tag{8a}$$

and the second pair, suggested in 1940 [17] were

$$\alpha \doteq \frac{2.5(A-G)}{A+6G+3B}, \qquad \beta \doteq \frac{G-B}{A+6G+3B}. \tag{8b}$$

simple equations were chosen to give approximate values of α and β in the chromaticity diagram:

$$\alpha \doteq \frac{A-G}{A+2G+B}, \qquad \beta \doteq \frac{0.4(G-B)}{A+2G+B}. \tag{8}$$

Neither Eqs. (8a) nor (8b) give as close approximation to uniform-chromaticness spacing for surface colors as Eqs. (8). Closest accord with the spacing in Judd's U.C.S. diagram [26] is, however, afforded by the use of Eqs. (8b).

Because the settings of A, G, and B for any white or nearly achromatic color are of roughly the same magnitude, suitable values of α and β for these colors may often be found by:

$$\alpha \doteq 2.5(A-G)/10G, \qquad \beta \doteq (G-B)/10G. \tag{9}$$

Values of α and β computed according to Eqs. (7) for spectrum colors at 10-millimicron intervals are recorded in Table IV and plotted in Fig. 3 to form the boundary of the (α, β) diagram. Points representing three colors widely used on signs and markers have also been plotted in Fig. 3. In addition, points have been plotted to show the degree of agreement between the chromaticity scales of the new system and the chromaticness spacing of the Munsell system. Using Nickerson "smoothed" values of x and y for Munsell papers [38], values of α and β were computed by Eqs. (7) for the ten papers representing the hues and intermediate hues of 4-value and 6-chroma under I.C.I. Illuminant C. The points representing these ten papers would be spaced at equal intervals along the circumference of a circle if the Munsell system and the (α, β) diagram both gave perfectly uniform chromaticness spacings.

Since the chromaticness spacing of the Munsell system is known to be fairly good [37], the departure of the actual ten points plotted in Fig. 3 from equal spacing on the circumference of a circle can be considered a rough measure of the degree to which the (α, β) diagram fails to give uniform chromaticness spacing of surface colors. Comparison of the spacing of points in Fig. 3 with the similar spacings of points representing Munsell papers in the (x, y) diagram as shown by Newhall [37, p. 640] indicates a considerable advantage in favor of the (α, β) system.

TABLE IV. Values of α and β, computed according to Eqs. (7), of spectrum colors at 10-millimicron intervals.

Wave-length in millimicrons	α	β
380	+0.0731	−0.3604
90	+ .0725	− .3608
400	+ .0718	− .3612
10	+ .0705	− .3617
20	+ .0679	− .3622
30	+ .0613	− .3611
40	+ .0484	− .3579
450	+ .0265	− .3528
60	− .0095	− .3430
70	− .0729	− .3146
80	− .1876	− .2361
90	− .3373	− .0977
500	− .4440	+ .0446
10	− .4651	+ .1317
20	− .4166	+ .1661
30	− .3387	+ .1688
40	− .2605	+ .1641
550	− .1793	+ .1557
60	− .0924	+ .1451
70	+ .0001	+ .1330
80	+ .0952	+ .1204
90	+ .1879	+ .1082
600	+ .2688	+ .0974
10	+ .3320	+ .0891
20	+ .3754	+ .0833
30	+ .4035	+ .0796
40	+ .4229	+ .0769
650	+ .4352	+ .0753
60	+ .4423	+ .0744
70	+ .4458	+ .0740
80	+ .4483	+ .0736
90	+ .4501	+ .0734
700 to 780 inc.	+ .4506	+ .0733
MgO under I.C.I. illuminant C	.0000	.0000

3. To the Amount of Color Difference ΔE Perceived Between Two Surface Colors

Expressions for estimating the amount of difference perceived between two colors and for estimating the whiteness of a perceived color have recently been set up by Judd [28, 29, 32]. Visual estimates of these two properties are widely used in commerce where it must frequently be decided whether the perceived color of one object is a suitable match for that of another, or whether a

material meets a whiteness specification. By making minor changes in Judd's two expressions, methods are available for rapidly converting photoelectric tristimulus settings to values of ΔE and W which are in good accord with perceived color difference and whiteness, respectively.

To form his empirical equation for ΔE, the approximate amount of perceived color difference, Judd first assumed that color can be represented by a 3-dimensional figure in which distance is a close measure of the perceptibility of the corresponding surface-color difference. In this Euclidian solid the chromaticity and reflectance components of color difference, ΔE_C and ΔE_Y, are vectors at right angles. By expressing these two components in a unit which gives uniform measure of perceived color difference throughout the color solid, the definition of ΔE may be written

$$\Delta E \equiv [(\Delta E_C)^2 + (\Delta E_Y)^2]^{\frac{1}{2}}. \tag{10}$$

Because the square root of luminous apparent reflectance is known to correlate well with observers' estimates of lightness under usual observing conditions, Judd wrote the reflectance component [28, 29]

$$\Delta E_Y = k_1 \Delta(Y^{\frac{1}{2}}), \tag{11}$$

where Y is the luminous apparent reflectance.

The chromaticness difference corresponding to a given chromaticity difference varies with the luminous apparent reflectance of the specimens represented. Judd assumed this variation to be proportional to $Y^{\frac{1}{2}}$:

$$\Delta E_C = k_2 Y^{\frac{1}{2}} \Delta S,$$

where the chromaticity difference ΔS is expressed in the units of Judd's own uniform-chromaticness-scale diagram [26].

TABLE V. Values of k_1, the proximity factor, suggested by Judd [28, p. 425].

Conditions of observation giving equivalent visual estimates of color difference	k_1
Samples separated by a very narrow or non-existent dividing line	120
Samples separated by a contrasting, but narrow dividing line	90
Samples separated by a broad patterned area different from the areas being compared	40
Samples evaluated for whiteness without visual reference to other samples	20
(Convenient value for use when samples are separated by narrow line)	100

For the present work use is made of chromaticity differences measured in the (α, β) coordinate system, represented by $[(\Delta\alpha)^2 + (\Delta\beta)^2]^{\frac{1}{2}}$. In order to find the factor relating chromaticity differences in Judd's U.C.S. diagram and chromaticity differences in the author's (α, β) diagram, points representing eight selected stimuli were plotted in each system. The stimuli were chosen so that the points representing them were distributed throughout each diagram and lines were drawn connecting various pairs of these points. It was found by measurement that the lines in Judd's diagram averaged 1.16 (from 1.10 to 1.27) times the lengths of the corresponding lines in the (α, β) diagram:

$$\Delta E_C = 1.16 k_2 Y^{\frac{1}{2}} [(\Delta\alpha)^2 + (\Delta\beta)^2]^{\frac{1}{2}}. \tag{12}$$

To establish the "N.B.S. unit of color difference"[18] numbers were assigned to the constants k_1 and k_2 in the expressions representing the lightness and chromaticness components of perceived color difference, respectively. These numbers were intended to make the unit of color difference so small that measured differences of less than one unit would represent perceptually unimportant color differences in most commercial transactions. Measured differences of more than one unit, however, were expected to represent color differences which are commercially important. For k_2 the number 600 was chosen [28, 29]. The quantity k_1 is called the proximity factor; the number assigned it must be chosen on the basis of the visual proximity of the surface areas compared for color difference. (See Table V and accompanying text, below.)

By replacing 1.16 times k_2 by its equivalent, 7 times 10^2, in Eq. (12), substituting in Eq. (10), and adding a factor (f_g), explained below, to account for the masking of the perceived color difference by specularly reflected light from glossy surfaces, the equation for ΔE becomes

$$\Delta E = f_g \{[7 Y^{\frac{1}{2}} [(\Delta\alpha)^2 + (\Delta\beta)^2]^{\frac{1}{2}} \cdot 10^2]^2 + [k_1 \Delta(Y^{\frac{1}{2}})]^2\}^{\frac{1}{2}}. \tag{13}$$

As given, Eq. (13) is not in the most conventional form because the chromaticity difference,

[18] This unit has since been called by Balinkin [1] the "judd" after its originator.

$[(\Delta\alpha)^2+(\Delta\beta)^2]^{\frac{1}{2}}$, is within a bracket which is itself squared. One would think that the indicated squaring should be carried out. However, the expression is given in the above form because of the convenience of evaluating it graphically. Twice in computing a value of ΔE according to Eq. (13), it is necessary to find the square root of the sum of two squares. These two operations were purposely provided because they can easily be done graphically with sufficient precision for color-difference measurement by using a pair of dividers and a piece of rectangular cross-section paper to get the length of the hypotenuse of the right triangle whose other two sides are known.

The constant k_1 and the gloss factor f_g remain to be discussed. With respect to k_1, experience has shown that the expression $\Delta(Y^{\frac{1}{2}})$ is proportional to lightness difference only so long as the conditions for observation of the samples remain unchanged. To obtain the best agreement between instrumentally-obtained data substituted in Eq. (13) and the average of visual estimates, it has proved necessary to change values of k_1 to accord with the proximity of the areas visually compared. Thus k_1 has been called the proximity factor. When specimens are compared by holding their colored areas in immediate juxtaposition, differences in $Y^{\frac{1}{2}}$ are found to be readily apparent. The value of k_1 representing this manner of observation must therefore be relatively large and is, in practice, taken as about 100. If, however, specimens must be examined with a border or pattern separating the areas compared, the same differences in $Y^{\frac{1}{2}}$ are found to correspond to less discriminable lightness differences. The value of k_1 representing this manner of observation is therefore smaller, perhaps as low as 40. The values of the proximity factor, k_1, suggested by Judd [28, p. 425] are listed in Table V.

The factor f_g in Eq. (13) was added to account for the masking of perceived color difference by specularly reflected light [28, p. 426]. For matte surfaces, f_g is unity; for glossy surfaces it is assumed to be:

$$f_g = Y/(Y+K_g),$$

where K_g is a constant referring to the conditions under which the samples are examined visually. In situations yielding considerable admixture of specularly reflected light, K_g is made large to give correspondingly small values of ΔE. If, on the other hand, care is taken in the corresponding visual situation to illuminate the samples so that only a small portion of the incident light is specularly reflected into the eyes of the observer, K_g should be small. A value of 0.025 was found by Judd to give satisfactory correspondence between visual estimates under the latter conditions and measured values of ΔE for a number of pairs of glossy porcelain-enameled plaques. In Fig. 4, f_g is plotted against apparent reflectance for $K_g=0.025$.

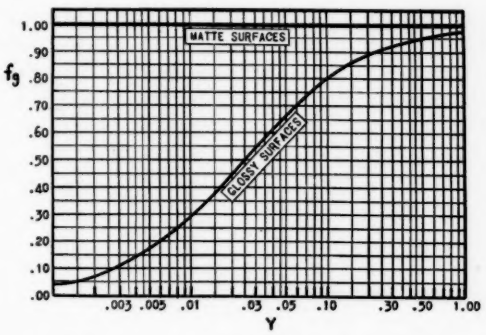

FIG. 4. The gloss factor f_g plotted as a function of Y for $K_g=0.025$.

4. To the Coordinates α', β', L' of a Solid with an Approximately Uniform Color-Perception Spacing

From Eq. (13) rectangular coordinates can be derived for a color solid designed to give spacings which accord with perceptual surface-color differences observed with light gray backgrounds. If the unit of length along each of the rectangular axes is made the N.B.S. unit of color difference, if the point representing black is made the origin for these axes, and if the components of color parallel to the α, the β, and the $Y^{\frac{1}{2}}$ axes are designated by α', β', and L', respectively, then from Eq. (13) it may be shown that

$$\begin{aligned} \alpha' &= 700\,Y^{\frac{1}{2}}\alpha, \\ \beta' &= 700\,Y^{\frac{1}{2}}\beta, \\ L' &= k_1 Y^{\frac{1}{2}}. \end{aligned} \qquad (14)$$

A value of 100 is frequently substituted for k_1.

The (α', β', L') uniform-surface-color solid, in which

$$\Delta E = [(\Delta\alpha')^2+(\Delta\beta')^2+(\Delta L')^2]^{\frac{1}{2}}, \qquad (15)$$

is illustrated in Fig. 5. White is at the top of this solid with a value of L' equal to $k_1=100$. The chromaticity plane at an L' level of approximately 45 has been drawn. Its boundary was determined by finding the points representing colors of maximum saturation index [34] for apparent reflectance of 0.20 (corresponding closely to $L'=45$ for $k_1=100$, or a middle gray).

5. To the Hue Angle ϕ, the Saturation Index S, and the Lightness Index L

In the psychological surface-color solid, which is perhaps best exemplified in the Munsell color system, the two components of chromaticness—hue and saturation—combine in a polar-coordinate arrangement. To correlate with hue, a number must be a measure of angle; to correlate with saturation, a number must be a measure of radius [31, p. 353 and 33, p. 11]. To obtain numbers from photoelectric tristimulus settings which will correlate well with hue, saturation, and lightness of surface-color perceptions, the following definitions have proved useful:

$$\begin{aligned} &\phi \equiv \text{angle whose tangent is } \beta/\alpha, \\ &S \equiv ((\alpha^2+\beta^2)\,Y^{\frac{1}{2}})^{\frac{1}{2}}, \\ &L \equiv Y^{\frac{1}{2}}. \end{aligned} \tag{16}$$

The above quantities have been designated the hue angle, the saturation index, and the lightness index, respectively. It can be seen that the signs of both α and β must be known to place ϕ in the proper quadrant.

6. To Estimates in N.B.S. Units of the Hue, Saturation, and Lightness Components $\Delta H'$, $\Delta S'$, and $\Delta L'$ of a Perceived Surface-Color Difference

It is frequently valuable to compute not only an estimate of the size of the difference perceived between two surface colors, but also estimates of sizes of the separate hue, saturation, and lightness components of the difference.

To compute these separate components of color difference, it is necessary to convert the rectangular coordinates of the color solid defined by Eqs. (14) to cylindrical coordinates. The saturation attribute in this solid is measured by radius from the lightness axis as center:

$$S' \equiv (\alpha'^2+\beta'^2)^{\frac{1}{2}}.$$

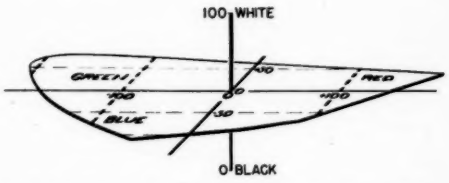

FIG. 5 Diagram of the (α', β', L') surface-color solid showing the chromaticity plane for $Y=0.20$.

The hue-difference component of color difference in this solid is measured by distance along the circumference which passes through the point midway between the points representing the two colors:

$$\Delta H' \equiv \frac{S_1'+S_2'}{2}\Delta\phi.$$

From these relations and Eqs. (14),

$$\begin{aligned} &\Delta H' = 12.2\,Y^{\frac{1}{2}}(\alpha^2+\beta^2)^{\frac{1}{4}}\cdot\Delta\phi \\ &\qquad \text{where } \Delta\phi \text{ is measured in degrees,} \\ &\Delta S' = 700\,Y^{\frac{1}{2}}\Delta((\alpha^2+\beta^2)^{\frac{1}{2}}), \\ &\Delta L' = k_1\Delta(Y^{\frac{1}{2}}), \end{aligned} \tag{17}$$

where the values which do not refer to difference measurements are taken as averages of the corresponding values for the two specimens concerned.

7. To Values of Whiteness W

The whiteness of a sample is assumed, for purposes of its measurement, to be proportional to the perceived degree of approach of its color to that of an ideal white surface. If MgO is assumed to approximate sufficiently well the ideal white, the whiteness of the unknown surface may be quantitatively defined by a relation suggested by Judd [32]:

$$W \equiv 1-\frac{\Delta E_{\text{MgO to specimen}}}{\Delta E_{\text{MgO to black}}}, \tag{18}$$

which gives a scale of whiteness from 1.00 for MgO to zero for black. Judd found that a proximity factor (k_1) of 20 yielded numerical ratings for the whiteness of surfaces in good accord with visual estimates. By substituting this value in Eq. (13), the color difference between MgO and black for the assumed conditions of whiteness grading is found to be 20 N.B.S. units. The above

equations for whiteness may therefore be written

$$W = 1 - \frac{1}{20}\Delta E_{\text{MgO to specimen}}.$$

Since the use of this equation is to be restricted to white and near white surfaces, Eq. (13) may be somewhat simplified when incorporated into the relation for whiteness. Within the range of apparent reflectances (0.60 to 1.00) covered by whites and near whites, $(7 \cdot Y^{\frac{1}{3}} \cdot 10^2)/20$ does not vary greatly from 30, and, for the $\Delta(Y^{\frac{1}{3}})$ component, $(1.00 - Y^{\frac{1}{3}})$ does not differ greatly from the more easily computed $(1.00 - Y)/2$. Since, in addition, the values of α and β for MgO are both zero, an approximate expression for whiteness of a white or near-white surface may be written:

$$W = 1 - \left\{ [30(\alpha^2 + \beta^2)^{\frac{1}{2}}]^2 + \left[\frac{(1.00 - Y)}{2}\right]^2 \right\}^{\frac{1}{2}}. \quad (19)$$

Whiteness evaluated by this expression differs from that by Eq. (18) by less than 0.025 for W greater than 0.80. This difference is less than the uncertainty of estimates of whiteness equality by direct visual inspection. In correlating visual estimates of whiteness of white papers, finishes, and other materials with colorimetric values of the samples examined, one frequently finds that magnesium oxide is not a suitable standard for whiteness. Judd [27] had fifteen experienced paper technologists each rate 29 pieces of paper for whiteness. As a result of the ratings supplied, he found that in the paper industry there are recognized apparently not one, but at least two "ideal whites." One ideal white is "natural paper white," a yellowish color representing the best grade of undyed paper. Another ideal white seems to possess almost the chromaticity of MgO; it is typical of papers "whitened" with blue dye. Some observers judge whiteness by one ideal, others by another.

The fact that some observers use ideal whites differing in color from MgO does not destroy the usefulness of relations for rating whiteness numerically. If the ideal white used by the graders of the material in question can be identified, Eq. (18) can be used by substituting the colorimetric coordinates of this ideal white for those of MgO.

8. To the Yellowness of a White or Near-White Surface

White and near-white surfaces are so frequently rated for degree of yellowness that it is convenient to have a scale which provides approximate psychophysical measures of yellowness. The equation,

$$\text{Yellowness} = (A - B)/G, \quad (20)$$

is similar to others which have been used for the same purpose [48, 49] and gives a scale of yellowness increasing from zero for MgO or any equally non-selective surface to positive values for yellowish surfaces and negative values for bluish surfaces.

V. STANDARDS FOR PHOTOELECTRIC TRISTIMULUS COLORIMETRY

For almost all photoelectric tristimulus measurements, regardless of the purpose for which they are made, a substitution method should be employed. That is, the specimens being measured should be exposed under the same circumstances as the standard with which they are compared. This standard may be either the actual reference standard, which for surface colors is usually a freshly smoked magnesium-oxide surface, or it may be a secondary or working standard such as a porcelain-enamel plaque which has been calibrated in terms of the reference standard. If simply the differences in color between the test specimens and a specimen designated as standard are of interest, this arbitrary standard often need not be calibrated.

The present photoelectric tristimulus method is subject to error because of the above-mentioned spectral inaccuracy of the source-filter photo-cell combinations. In the following section of this paper it will be shown that this error tends to increase in amount with the spectral dissimilarity between the specimens compared. Because of this tendency, it is advantageous to use wherever possible in photoelectric tristimulus colorimetry a working standard which is spectrally similar[19] to the samples being measured.

To calibrate a working standard for photo-

[19] By spectrally similar specimens are meant specimens which are not metamerically different (see text, p. 526).

electric tristimulus colorimetry without reference to a spectrally similar, previously calibrated standard, the spectrophotometric curve of the new standard is first obtained. From this curve, x, y, z, and Y are computed according to one of the customary methods [15, 25, 31, 45]. From these computed values, A_{std}, G_{std}, and B_{std} may be derived using Eqs. (21) which are derived from Eqs. (5) and (6):

$$A_{std}=\frac{Y}{y}(1.25x-0.1907z),$$
$$G_{std}=Y, \qquad (21)$$
$$B_{std}=\frac{Y}{y}0.8475z.$$

As a specific example of how values of A, G, and B may be assigned a working standard, the pink plaque used for the measurements demonstrated in Example 2 below, was given the following I.C.I. colorimetric values by spectrophotometry and computation:

$$x=0.3585,$$
$$y=0.3345,$$
$$z=0.3070,$$
$$Y=0.606.$$

Accordingly values of A, G, and B were computed for this working standard according to Eqs. (21):

$$Y/y \quad =1.81166,$$
$$1.25x \quad =0.448125$$
$$0.1907z=0.058545$$
$$\text{Dif.} \quad =0.389580,$$
$$A=\text{Dif.}\ (Y/y) \quad =0.7058,$$
$$G=Y \quad =0.606,$$
$$0.8475z=0.260182,$$
$$B=0.8475z(Y/y)=0.4714.$$

When, instead of I.C.I. values, values of α, β, and Y of the working standard are given, values of A, G, and B are computed by using equations which are essentially Eqs. (8) reversed:

$$A=Y\left(\frac{1.0+3.0\alpha+2.5\beta}{1.0-\alpha+2.5\beta}\right),$$
$$G=Y, \qquad (22)$$
$$B=Y\left(\frac{1.0-\alpha-7.5\beta}{1.0-\alpha+2.5\beta}\right).$$

To find the colors of a series of spectrally similar specimens, none of which can be used as a working standard because of unstable color, a stable plaque is assigned values of A, G, and B which relate to the impermanent specimens rather than to its own color. To calibrate such a working standard, one of the unstable specimens must be measured on a spectrophotometer and then compared immediately with the stable plaque on the tristimulus instrument.

TABLE VI. Amounts of change in chromaticity and color difference introduced by changes in instrument settings of 0.001.

		For a white surface reflecting 80%	For a yellow surface reflecting 35%
If settings of the instrument should be	A	0.800	0.500
	G	.800	.350
	B	.800	.050
But instead the instrument gives	A	.801	.501
	G	.799	.349
	B	.801	.051
Changes of the following magnitudes will result	in x	+.00024	+.00049
	in y	−.00054	−.00182
	in α	+.00062	+.00160
	in β	−.00025	−.00064
	in $(\alpha^2+\beta^2)^{\frac{1}{2}}$	.00067	.00172
	in ΔE (maximum, N.B.S. units)	±.45	±.94
	in W	−.0025	

VI. ERRORS IN PHOTOELECTRIC TRISTIMULUS MEASUREMENTS

In the paper describing the multipurpose reflectometer [18] eighteen potential sources of instrument error are listed. These eighteen sources include most of those which will be found in photoelectric tristimulus instruments and it is believed, therefore, that no further study of the errors of instruments is needed here. With special reference to the errors of photoelectric tristimulus colorimetry, however, there are several matters which merit attention. These matters are considered herein with particular reference to measurements with the author's three-filter multipurpose reflectometer.

It should be pointed out first that high precision is needed for useful photoelectric tristimulus measurements. In order to identify by an instrument, chromaticity differences as small as can be distinguished by an experienced observer, relative values of A, G, and B must be highly precise. To show what this precision must be, changes of 0.001 in the instrument settings on a hypothetical white surface and on a hypothetical yellow surface have been converted to corresponding changes in x, y, α, β, ΔE, and W by using the relations above. These are shown in Table VI.

Under favorable observing conditions, a trained inspector can usually distinguish as different the colors of two light-colored surfaces if

$$\Delta E = 0.3,$$

or if

$$[(\Delta\alpha)^2+(\Delta\beta)^2]^{\frac{1}{2}}=0.0005.$$

In general, it can therefore be said that a tristimulus colorimeter giving apparent reflectances imprecise by 0.001 will not serve to identify color differences as small as those which the trained color inspector can distinguish.

Although the individual settings of a multipurpose reflectometer are usually uncertain by more than 0.001, a technique is used to obtain settings with this instrument which ordinarily reduces the errors of the resulting values of x, y, α, β, ΔE, and W to considerably less than those given in Table VI. With this instrument the settings on each specimen with the three filters are made consecutively. By thus taking settings with the three filters almost simultaneously and without moving the specimen, the errors ordinarily introduced by temperature drift and by change of the position of the specimen between exposures are minimized in the computed *differences* between the settings.

It may be seen from Eqs. (8) above that the chromaticity measurement of a sample depends chiefly upon these differences between settings. These differences must be uncertain by less than 0.001 for precise photoelectric colorimetry, since changes in the differences between A, G, and B are relatively more important in determining chromaticity than changes in their magnitudes. The three readings of a sample would have to be simultaneously high, or simultaneously low by four times 0.001 (for a near-white sample) to cause a lightness-component error in ΔE as large as the chromaticity-component error caused by an inaccuracy in A-G of 0.001. Resort to Eq. (13) above will verify this conclusion.

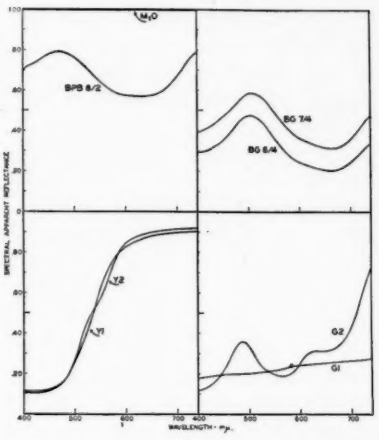

FIG. 6. Spectral curves of four pairs of specimens used for the study of amounts of error resulting from failure of the source-filter photo-cell combinations to be spectrally equivalent to the I.C.I. standard observer. Upper two pairs—curves representing essentially non-metameric differences; lower two pairs—curves representing differences in which there is appreciable metamerism.

1. Errors in Tristimulus Measurements of Chromaticity Difference Due to Spectral Inaccuracy of the Source-Filter Photo-Cell Combinations

The spectral inaccuracy of the source-filter photo-cell representation of the I.C.I. standard observer has been demonstrated above. Although the errors from this source were shown [18] to be not serious in measurements of luminous apparent reflectance, the errors from the same source are serious in measurements of chromaticity.

It was pointed out by Perry [40] that these chromaticity errors are small and can usually be tolerated when the photoelectric tristimulus method is used to measure differences in chromaticity between spectrally similar, or as he said, "spectrophotometrically similar" specimens. Under other circumstances, however, the chromaticity errors are frequently larger than can be tolerated. It can only be recommended, therefore, that the present method be used

to measure color differences between spectrally similar specimens.

Before undertaking quantitative evaluations of chromaticity errors, it seems desirable to explain in some detail what Perry meant when he spoke of "spectrophotometrically similar" specimens. Actually a word suggested by Ostwald [39], "non-metameric," seems to apply more specifically than either spectrally similar or spectrophotometrically similar to the property of the differences which is important. The stimuli produced by two illuminated specimens are metamers when there is a spectral difference between them which is of such a nature that they nevertheless have the same color. As an example, there is the frequently cited case of two specimens which have the same color under one illumination, but different colors under a second illumination. Under the first illumination, the two stimuli are metamers for the specimens have to be spectrally different to appear different in color under the second illumination.

In the present discussion, reference is made to "degree of metamerism." It is supposed that the spectral difference for two specimens under a given illumination can be separated into three components: (1) a factor of constant proportionality throughout the spectrum corresponding to the lightness difference, (2) a component which is responsible for the chromaticity difference, and (3) a metameric component yielding no color difference.

TABLE VII. Errors in measured chromaticity differences which result from substitution of photoelectric tristimulus combinations for the I.C.I. standard observer.

Specimens compared	Size of the chromaticity difference $[(\Delta\alpha)^2+(\Delta\beta)^2]^{\frac{1}{2}}$	Error in the photoelectrically measured chromaticity difference	
		Actual	Relative to size of difference (percent)
Munsell BPB 8/2 and MgO	0.0229	0.0013	6
BG 6/4 and *BG* 7/4	.0150	.0018	12
Yellow Y1 and Yellow *Y*2	.00187	.00043	(23)
Gray *G*1 and Gray *G*2	.0160	.0061	(38)

In general, the chromaticity error in photoelectric tristimulus measurement increases with the size of the latter two components. For pairs yielding no appreciable metameric component, therefore, the size of the chromaticity error is roughly proportional to the size of the chromaticity difference.

In order to find the approximate factor relating chromaticity error to size of non-metameric chromaticity difference, and to show also that this factor fails to evaluate the amount of error when there is appreciable metamerism, four chromaticity differences were carefully studied. The errors of these four differences were computed from the spectral curves of the eight specimens involved. With each of the four pairs, one specimen was assumed to represent a standard and the other an unknown sample. True (α, β) and approximate (photoelectric) values of chromaticity were computed using the spectral specifications of the I.C.I. observer and the source-filter photo-cell combinations, respectively. True chromaticity differences were then compared with the corresponding photoelectric-tristimulus chromaticity differences to obtain the errors of the latter values.

The spectral curves of the four pairs of specimens are shown in Fig. 6. With the top two pairs there is relatively little metamerism; with the bottom two there is significant metamerism. For the first pair, MgO and Munsell paper BPB 8/2 were chosen. The Munsell paper was chosen to represent a specimen which differed in chromaticity from MgO by about as much as any specimen which would be called "near white." Perry pointed out that because white and near-white specimens were relatively non-selective, significantly metameric differences between them were rare. Realizing that a photoelectric tristimulus colorimeter thus possessed special advantages for use on white materials, Perry named the device which he designed the Blancometer [40].

The two yellow papers, Y_1 and Y_2, are very nearly alike in color; in fact the perceived color difference between them will change in character with change from daylight to incandescent illuminant. Thus they represent a case in which the spectral difference is chiefly a metameric difference. The degree of metamerism is even

greater for the difference between the two gray samples, G_1 and G_2.

The true chromaticity differences and the computed errors of the photoelectric tristimulus method are given for the four pairs of specimens in Table VII. Since these data are computed from the spectral curves of the specimens, the errors shown are those due solely to the spectral inaccuracy of the source-filter photo-cell combinations. From Table VII it can be seen that if sample and standard are not metamerically different, photoelectric tristimulus measurements of chromaticity difference may be in error by roughly 10 percent of the difference measured. If there is appreciable metamerism, however, the error is not related to the size of the chromaticity difference. For this reason parentheses have been placed about the latter two "percent errors" in Table VII.

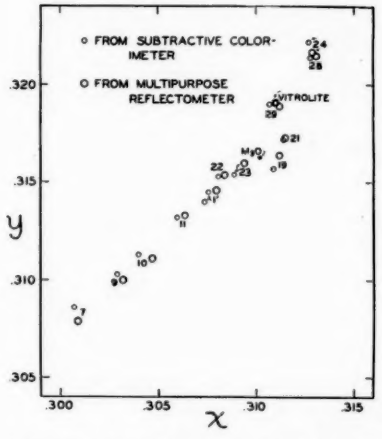

FIG. 7. Part of (x, y) diagram (outlined by rectangle in Fig. 2) showing x and y of a number of white porcelain-enamel plaques measured both with the visual subtractive colorimeter [29] and with the multipurpose reflectometer [18].

In Fig. 7 there is experimental confirmation of the conclusion that errors are small in the measurement of the chromaticities of white samples. Points representing twelve white porcelain-enamel plaques which were measured with both the multipurpose photoelectric reflectometer and the visual, subtractive colorimeter [29] are plotted in this figure. The plaques were compared in both instruments with a Vitrolite standard, for which the assigned chromaticity is shown. For none of the plaques is the disparity as great as 0.001 in $[(\Delta x)^2+(\Delta y)^2]^{\frac{1}{2}}$, even though it includes the errors of both instruments as well as the error due to spectral inaccuracy of the source-filter photo-cell combinations. To show how large a part of the total (x, y) diagram is covered by Fig. 7, its boundaries were plotted as a small rectangle near the center of Fig. 2.

The errors represented in Table VII and Fig. 7 have involved only small chromaticity differences. In Fig. 2, above, there is evidence which extends to large chromaticity differences the findings about errors given in Table VII for small differences. If distances between the different pairs of points representing the same colors are measured in Fig. 2, it will be found that they are, on the average, roughly one-tenth the respective distances from these points to the white point common to both diagrams. Since magnesium oxide, represented by the white point, was the standard against which the several specimens were measured, this average error of 1/10 the chromaticity difference is in good agreement with the errors of roughly 10 percent indicated in Table VII. Thus one may expect errors which will average about 10 percent of the measured chromaticity differences for large as well as small non-metameric differences.

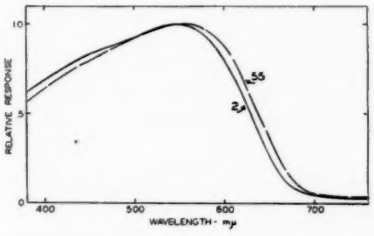

FIG. 8. Relative spectral responses of G. E. cells No. 55 and No. 2 used to demonstrate change in measured chromaticity which may result from change of the photo-cell in the instrument.

2. Changes in Measured Chromaticity Resulting from Change of Photo-Cell in an Instrument

Of the three components of each source-filter photo-cell combination, the photo-cell is in practice the most difficult to duplicate spectrally. In the absence of an evaluation of errors possible from all these components, it may be in-

structive to evaluate the changes in measured chromaticity which can result from change from one photo-cell in an instrument to another of the same manufacture. Of the several G.E. cells for which data were available, the cell most different in spectral response from cell No. 55 was cell No. 2. The relative spectral responses for these two cells are compared in Fig. 8.

The photoelectrically measured chromaticity difference for each pair of samples identified in Fig. 6 would change with substitution of cell No. 2 for cell No. 55. The amounts of these changes were computed in the same way as the errors reported in Table VII, and are given in Table VIII. It will be noted that the changes in computed chromaticity difference are somewhat smaller than the errors for the corresponding pairs reported in Table VII, but the changes are nevertheless large enough to be important.

3. Fluorescence Errors

The Institute of Paper Chemistry has shown [20, p. TS294] that fluorescence of a sample may cause error in any colorimetric instrument in which the energy striking the sample is spectrally different from that ordinarily used to observe the sample visually. A fluorescent sample has the power to change the spectral character of part of the energy striking it. In any instrument in which the incident energy does not possess the same spectral composition as the ordinary non-instrument illuminant, the energy leaving the sample may be altered in a manner different from that in the non-instrument situation. If, as in the multipurpose reflectometer, the energy is passed through a filter before incidence on the sample, fluorescence may cause the photo-cell exposed to the sample to receive energy of wave-lengths wholly excluded by the filter and therefore not supposed to be present for the particular measurements.

TABLE VIII. Changes in measured chromaticity difference which would result from the substitution of one photocell for another of the same type, but of different spectral response.

Specimens compared	Measured size of the chromaticity difference (with cell 55) $[(\Delta\alpha)^2+(\Delta\beta)^2]^{\frac{1}{2}}$	Change in the measured chromaticity difference with substitution of cell	
		Actual	Relative to size of difference (percent)
Munsell BPB 8/2 and MgO	0.0261	0.0016	6
BG 6/4 and *BG* 7/4	.0136	.0004	3
Yellow *Y*1 and Yellow *Y*2	.00224	.00035	(16)
Gray *G*1 and Gray *G*2	.0184	.0024	(13)

To illustrate the fluorescence error, the author selected a piece of phenol-formaldehyde resin found by Gibson and Keegan [12] to give a spectral curve significantly in error because of fluorescence when measured with the General Electric recording spectrophotometer. These authors showed that this pink plastic gave a strong reddish fluorescence when illuminated by the yellow-green part of the spectrum. On visual inspection, the pink plastic appeared red relative to Munsell paper RYR 5/6. This visual estimate, which was substantiated by measurement with the Judd subtractive colorimeter, is properly represented by the black dots in Fig. 9.

Measurements with the multipurpose instrument, represented by the open circles in Fig. 9, erroneously indicate, however, that the resin would be perceived as greener and weaker in color than the Munsell paper. The error, when evaluated by Eq. (13), amounted to 14 N.B.S. units of color difference and is about half the fluorescence error found by Gibson and Keegan when they measured the same sample with the G.E. spectrophotometer.

4. Short Cuts in Computation Which Produce only Small Errors

There are several short cuts which at times may be used to reduce the labor of computing tristimulus quantities from settings with the multipurpose reflectometer. The shortened procedures result in errors which diminish with the computed color difference between the specimens compared. With many small color differences, therefore, the short-cut computational errors are smaller than the errors introduced by lack of precision and are therefore unimportant. Even larger errors from this cause are unimportant if they are appreciably less than the maximum

error permitted for a successful solution of the problem.

As an example, short-cut errors are seldom serious when one is following the day-to-day change of the color of a paint or textile material due to fading or other cause. The highest accuracy is not necessary for such measurements so long as the day-to-day reproducibility is fairly good. The short-cut computational errors have negligible effect on this reproducibility.

(a) *Short-Cut A. Omitting Scale Corrections*

In practice, the apparent-reflectance scale supplied with a multipurpose reflectometer is not exact. Correction curves, which are found by calibration after the instrument is completed, are necessary to obtain accurate values with the device [18, p. 601; 18a, p. 548]. The corrections do not change value rapidly with scale reading for most parts of the scales employed. Therefore the omission of scale corrections usually produces only small changes in the computed color differences between samples of similar color. In all but one of the examples of tristimulus color measurement reproduced below, in Section VIII, scale corrections were omitted.

(b) *Short-Cut B. Neglect of the Difference Between the Known A, G, and B Values for the Standard and the Approximate Values Read Directly from the Instrument*

Because of the usual drift of instrument readings with time, the difficulty of making minute adjustments of photometric balance, and the frequent necessity of correcting readings for scale errors, the readings of a photoelectric tristimulus instrument seldom give accurate values of A, G, and B directly. Instead, values of A, values of G, and values of B each relative to those of the standard are obtained from instrument settings, after the effect of drift is balanced out in the manner illustrated in Examples 1, 3, 5, and 6, below. Thus if one exposes a standard and two samples for which the accurate tristimulus values are:

$$\begin{array}{lll} A_{std}, & G_{std}, & B_{std}, \\ A_1, & G_1, & B_1, \\ A_2, & G_2, & B_2, \end{array}$$

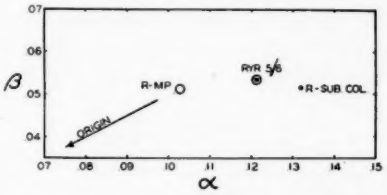

FIG. 9. Error in photoelectrically measured chromaticity due to fluorescence of the resin specimen R. When compared in the subtractive colorimeter [29] with Munsell paper RYR 5/6, the resin is properly assigned the chromaticity represented by the black dot, rather than the erroneous chromaticity assigned by the multipurpose reflectometer [18] and represented by the open circle.

he actually obtains from the corrected settings

$$\begin{array}{lll} k_aA_{std}, & k_gG_{std}, & k_bB_{std}, \\ k_aA_1, & k_gG_1, & k_bB_1, \\ k_aA_2, & k_gG_2, & k_bB_2. \end{array}$$

For many cases in which the highest accuracy is not required, it is not worthwhile to evaluate k_a, k_g, k_b; their departures from unity are found to be negligible. In Examples 3 and 4, Section VIII, use was made of this short-cut B.

One might suppose that a simple additive method could be used to compute accurate tristimulus values from instrument readings. If such a procedure were possible, one could take settings on a standard and sample, and from these settings compute values of x and y. From the computed and known values of x and y for the standard, the supposed additive corrections Δx and Δy, would be found. That such corrections applied additively are inexact, however, may easily be shown. An "uncorrected" value of x for the standard would be computed from the readings on it by:

$$x_{std(u)}=\frac{0.80k_aA_{std}+0.18k_bB_{std}}{0.80k_aA_{std}+k_gG_{std}+1.36k_bB_{std}},$$

whereas the true value of x would be:

$$x_{std}=\frac{0.80A_{std}+0.18B_{std}}{0.80A_{std}+G_{std}+1.36B_{std}}.$$

It will be seen that there is no simple function of $x_{std(u)}$ and x_{std} by which the factors k_a, k_g, and k_b can be eliminated.

TABLE IX. Percentage errors in computed values of color difference from using the suggested short-cuts.

	Errors in percent of total difference					
	For 2 pairs of white samples		For 2 pairs of blue samples		For 2 pairs of orange samples	
Short cut	$\Delta E = 1.8$	$\Delta E = 6.6$	$\Delta E = 1.0$	$\Delta E = 7.6$	$\Delta E = 1.4$	$\Delta E = 6.0$
Scale corrections omitted	0.6	1.1	0	4.1	4.2	4.8
Use of instrument values of A, G, and B having only relatively correct magnitudes	0	0	1.0	2.9	26.6	6.3
Use of 0.5 and 0.1 instead of true neutral-filter factors	—	—	3.9	3.6	7.7	1.0
Combination of above 3 short-cuts	0.6	0.3	0	8.7	27.3	4.8

(c) *Short-Cut C. Using 0.5 and 0.1 Instead of the Accurate Values for the Neutral-Filter Transmission Factors*

To extend its photometric range, the multipurpose reflectometer makes use of two neutral filters transmitting approximately 0.5 and 0.1, respectively, of the normally incident energy. Actually the transmissions of the two filters used in the author's instrument are not 0.5 and 0.1, nor are the filters ideally neutral. Instead the transmissions are as follows:

Nominal transmissions of "neutral" filters	Exact transmissions of "neutral" filters		
	For amber tristimulus filter	For green tristimulus filter (giving luminosity function)	For blue tristimulus filter
0.5	0.480	0.479	0.427
.1	.088	.086	.065

When the color differences between the specimens being compared are very small, or when accuracy is not needed, use of 0.5 and 0.1 instead of the proper filter factors is frequently permissible. It should be obvious, however, that these approximate factors should not be used for the computations if the neutral filter employed in conjunction with any one of the tristimulus filters was changed during the settings on the group of specimens. Example 4, Section VIII illustrates this third short-cut.

(d) *Amounts of Error from Using Short-Cut Methods of Computation*

To give an idea of the sizes of the errors which would be found in actual practice, instrument settings for six typical color differences were converted to amounts of color difference, first by the accurate computational procedure and then by using the short-cuts. Two white, two delphinium-blue, and two international-orange pairs of samples were chosen so that for each color there was one difference of about 1.5 N.B.S. units and one of about 7 units. For each color, pairs of samples were sought which seemed likely to give the most serious errors from the use of the short-cut methods. For these pairs, amounts of color difference were computed five times; first they were computed accurately, then each of the three short-cuts was used separately, and finally they were used together.

The errors are given in Table IX as percentages of the accurately computed differences. The size of each error depends upon the nature of the color difference involved as well as on the spectral selectivity of the samples and hence some of the differences are surprisingly small. In general, it will be seen that the errors become larger as the samples become more strongly colored. It will also be seen that the errors from the use of more than one short-cut are not always additive. By comparison of the percentage errors in Table IX with those in Table VII, above, it will be seen that most of these short-cut errors are smaller than the errors from spectral inaccuracy of the source-filter photo-cell combinations. For this reason the short-cuts can be recommended for use in many photoelectric tristimulus comparisons of color in which the highest accuracy possible is not needed.

VII. THE RELATION OF PERCEPTUAL IMPRESSIONS AND MEASURED VALUES OF COLOR

Because the I.C.I. standard observer was created from the color matches made by a number of normal observers [13, 51] the numerical description of a color difference in the I.C.I. or a related color system will, if possible interfering circumstances are eliminated, indicate the

EXAMPLE 1. Measurement of the I.C.I. values, x, y, z, and Y of four white painted plaques (see Eqs. (5) and (6), and Fig. 10).

Purpose—To test samples for compliance with color requirements given in Federal Specification TT-P-23a, [8] namely:

	x	y	z	Y
Minimum	—	—	0.355	0.85
Maximum	0.324	0.331	—	—

Computational short-cut—Scale corrections omitted.
Working standard—Vitrolite No. 1 ($A=0.906$, $G=0.909$, $B=0.890$).

Specimen	Standard	No. 1	No. 2	No. 3	No. 4
Blue settings	0.8985	0.8480	0.7900	0.7810	0.7080
	.8955	.8450	.7880	.7790	.7070
Mean	.8970	.8465	.7890	.7800	.7075
$B=\text{Mean}\times\frac{0.890}{0.8970}$		.8398	.7828	.7739	.7020
Amber settings	.9055	.8785	.8720	.8420	.8530
	.9030	.8770	.8680	.8400	.8520
Mean	.9042	.8778	.8700	.8410	.8525
$A=\text{Mean}\times\frac{0.906}{0.9042}$		.8795	.8717	.8427	.8542
Green settings	.9100	.8770	.8620	.8340	.8320
	.9070	.8740	.8585	.8320	.8310
Mean	.9085	.8755	.8602	.8330	.8315
$Y\doteq G=\text{Mean}\times\frac{0.909}{0.9085}$		.8760	.8607	.8335	.8320
$0.18\,B$		.1512	.1409	.1393	.1264
$1.18\,B$		.9910	.9237	.9132	.8284
$0.80\,A+0.18\,B$		.8548	.8383	.8135	.8098
Denom $(G+0.80\,A+1.36\,B)$		2.7218	2.6227	2.5602	2.4702
$x\doteq\frac{0.80\,A+0.18\,B}{\text{Denom}}$		.3141	.3196	.3177	.3278
$y\doteq G/\text{Denom}$		.3218	.3282	.3256	.3368
$z\doteq 1.18/\text{Denom}$		.3641	.3522	.3567	.3354
Result of test		pass	fail (z)	fail (Y)	fail (all)

character of the color difference perceived and described by the normal observer. With some of the methods of measuring color suggested in the present paper, however, numbers are given which, in addition to indicating the character of the difference, are intended to designate quantitatively the perceptual impression of the difference. Unfortunately there is at present little information on the success with which quantitative perceptual impressions are duplicated by these photoelectric tristimulus measurements. One bit of information may be noted. In a study of several methods for measuring color difference, Balinkin [1] compared the photoelectrically measured values of ΔE for ten pairs of green porcelain tiles with the averages of the visual estimates of the same differences by 60 observers. He found fairly good agreement between measured and estimated values with a correlation according to ranks of 0.86.

A number of the circumstances which may disturb the correspondence between visual estimates and photoelectric determinations of color and color difference are well known. Some of these circumstances relate to imperfections in the measuring method, others to imperfections in the observing situation. There follows a two-part list in which a number of the circumstances are

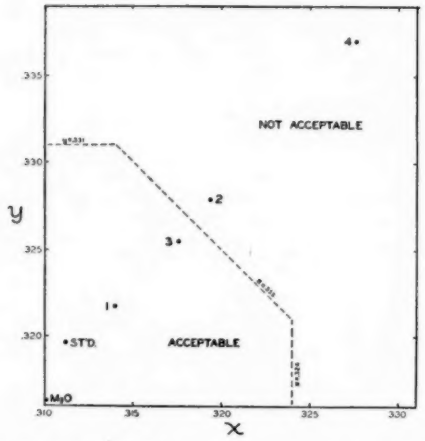

FIG. 10. Part of the (x, y) diagram showing chromaticities acceptable and chromaticities not acceptable according to Federal Specification TT-P-23a for white casein paints. The plotted points show values obtained with actual samples.

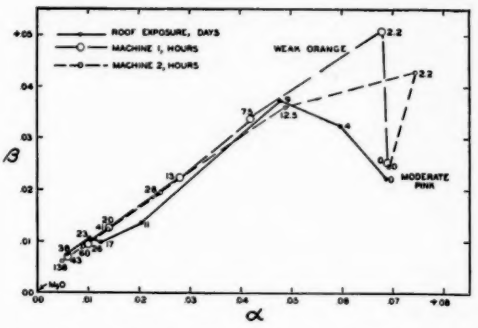

FIG. 11. Part of the (α, β) diagram used to show the changes of chromaticity of a pink-colored paint with exposure outdoors and in two machines designed to accelerate the changes produced in weathering.

given. It will be seen that each of those listed under "imperfections in the measuring method" was discussed above.

EXAMPLE 2. Measurement of the change of α and β of three painted plaques with exposure (see Eqs. (8) and Fig. 11).

Purpose—To follow the chromaticity changes of panels of the same paint exposed out of doors and in two machines which accelerate the changes produced by weathering.

Note—Only one of the many sets of computations used to obtain values of α and β is reproduced below.
Computational short-cut—Scale corrections omitted.
Working standard—Pink plaque ($A=0.7058$, $G=0.606$, $B=0.4714$).

Specimen	Standard	Roof (4 days)	Machine 1 (43 hours)	Machine 2 (41 hours)
Blue settings	0.4995 .501	0.300	0.685	0.597
Mean	.5002			
$B=\text{Setting}\times\frac{0.4714}{0.5002}$		.2827	.6453	.5626
Amber settings	.704 .704	.510	.7075	.675
Mean	.704			
$A=\text{Setting}\times\frac{0.7058}{0.704}$		.5113	.7093	.6767
Green settings	.620 .619	.424	.708	.656
Mean	.6195			
$G=\text{Setting}\times\frac{0.606}{0.6195}$		.4148	.6926	.6417
$A-G$		+.0965	+.0167	+.0350
$G-B$		+.1321	+.0473	+.0791
$0.4(G-B)$		+.0528	+.0189	+.0316
$B+A+2G=\text{Denom}$		1.6236	2.7398	2.5227
$\alpha \doteq (A-G)/\text{Denom}$		+.0594	+.0061	+.0139
$\beta \doteq 0.4(G-B)/\text{Denom}$		+.0325	+.0069	+.0125

EXAMPLE 3. Measurement of the amount of color difference ΔE between a standard and each of four similarly colored brown automobile pile fabrics (see Eq. (13)).

Purpose—To find which fabrics comply with the requirement that they differ from the standard by no more than one N.B.S. unit of color difference.

Computational short-cut—No calibrated standard used.
$k_l = 100$, $f_g = 1.00$.

Fabric	Standard	No. 1	No. 2	No. 3	No. 4
Blue settings (with 0.427 filter)	{0.1700 .1688	0.1744 .1738	0.1620 .1618	0.1690 .1686	0.2024 .2018
Mean (M)	.1694	.1741	.1619	.1688	.2021
Scale correction	−.0139	−.0138	−.0138	−.0136	−.0121
Corrected M	.1555	.1603	.1481	.1552	.1900
B = Above times 0.427	.0664	.0684	.0632	.0663	.0811
Amber settings (with 0.480 filter)	{.2098 .2082	.2144 .2142	.2022 .2018	.2042 .2036	.2524 .2520
Mean (M)	.2090	.2143	.2020	.2039	.2522
Scale correction	−.0120	−.0120	−.0120	−.0120	−.0113
Corrected M	.1970	.2023	.1900	.1919	.2409
A = Above times 0.480	.0946	.0971	.0912	.0921	.1156
Green settings (with 0.479 filter)	{.1916 .1900	.1946 .1944	.1848 .1844	.1882 .1876	.2300 .2302
Mean (M)	.1908	.1945	.1846	.1879	.2301
Scale correction	−.0127	−.0126	−.0130	−.0129	−.0122
Corrected M	.1781	.1819	.1716	.1750	.2179
$Y \doteq G$ = Above times 0.479	.0853	.0871	.0822	.0838	.1044
$A - G$	+.0093	+.0100	+.0090	+.0083	+.0112
$G - B$	+.0189	+.0187	+.0190	+.0175	+.0233
$0.4(G - B)$	+.0076	+.0075	+.0076	+.0070	+.0093
Denom $= B + A + 2G$	.3316	.3397	.3188	.3260	.4055
$\alpha \doteq (A - G)/\text{Denom}$	+.0280	+.0294	+.0282	+.0255	+.0276
$\beta \doteq 0.4(G - B)/\text{Denom}$	+.0229	+.0221	+.0238	+.0215	+.0229
$\Delta\alpha = \alpha - \alpha_{std}$		+.0014	+.0002	−.0025	−.0004
$\Delta\beta = \beta - \beta_{std}$		−.0008	+.0009	−.0014	0
$[(\Delta\alpha)^2 + (\Delta\beta)^2 \cdot 10^2]^{\frac{1}{2}}$		.16	.09	.29	.04
$Y^{\frac{1}{2}}$	.292	.295	.287	.289	.323
$7(Y^{\frac{1}{2}})$*	3.78				3.98
$\Delta C = 7(Y^{\frac{1}{2}})[(\Delta\alpha)^2 + (\Delta\beta)^2 \cdot 10^2]^{\frac{1}{2}}$		.60	.34	1.10	.16
$\Delta Y^{\frac{1}{2}}$		+.003	−.005	−.003	+.031
$\Delta L = k_l(\Delta Y^{\frac{1}{2}})$		.3	.5	.3	3.1
$\Delta E/f_g = [(\Delta C)^2 + (\Delta L)^2]^{\frac{1}{2}}$		.67	.60	1.14	3.11
ΔE		0.7	0.6	1.1	3.1

* Compute $7(Y^{\frac{1}{2}})$ for standard and for any samples for which the value of Y differs from that of the standard by more than 10° percent. For the latter samples, use the mean of the two values of $7(Y^{\frac{1}{2}})$; for others, use the value for the standard.

List of Circumstances Which May Interfere with Correlation Between Visually Estimated and Photoelectrically Measured Values of Color and Color Difference

A. Imperfections in the Measuring Method

1. Error from spectral inaccuracy of source-filter photo-cell combinations.

2. Error from fluorescence of sample.

3. Error from photometric inaccuracy of measuring instrument.

4. Failure of the empirically chosen scales for chromaticity, surface-color difference, and lightness to represent appropriate scales for these quantities.

B. Imperfections in the Observing Situation

1. Spectral difference between illuminant used for observations and I.C.I. Illuminant *C*.

2. Angular difference between directions of illuminating and viewing used for the visual observations and those used for the measure-

EXAMPLE 4. Measurement of the hue-difference estimate, $\Delta H'$, the saturation-difference estimate, $\Delta S'$, and the lightness-difference estimate, $\Delta L'$, between an actual earth sample and two modified earths (see Eqs. (17)).

Purpose—To find how the modified earths differ in color from the actual earth.

Computational short-cuts—Scale corrections omitted, no calibrated standard used, and the factor 0.5 used instead of the actual transmissions of the neutral filter.
$k_l = 100$, $f_0 = 1.00$.

Specimen	Earth Mixture	Modification No. 1	Modification No. 2
Blue settings	0.295	0.260	0.370
B = Above times 0.5	$.147_5$	.130	.185
Amber settings	.496	.446	.575
A = Above times 0.5	.248	.223	$.287_5$
Green settings	.428	.386	.508
$Y \doteq G$ = Above times 0.5	.214	.193	.254
$L = Y^{\frac{1}{2}} \doteq G^{\frac{1}{2}}$	.463	.439	.504
$\Delta L' = k_l \Delta(Y^{\frac{1}{2}})$	—	−2.4	+4.1
$A - G$ (note sign)	+.034	+.030	+.0335
$G - B$ (note sign)	+.0665	+.063	+.069
$0.4(G - B)$	+.0266	+.0252	+.0276
Denom $= B + A + 2G$	.8235	.739	.9805
$\alpha \doteq (A - G)/\text{Denom}$	+.0413	+.0406	+.0342
$\beta \doteq 0.4(G - B)/\text{Denom}$	+.0323	+.0341	+.0281
$(\alpha^2 + \beta^2)^{\frac{1}{2}}$	.0525	.0528	.0443
$\Delta(\alpha^2 + \beta^2)^{\frac{1}{2}}$		+.0003	−.0082
$700\, Y^{\frac{1}{2}}$*		470.	487.
$\Delta S' = 700\, Y^{\frac{1}{2}} \Delta(\alpha^2 + \beta^2)^{\frac{1}{2}}$		+0.14	−3.99
β/α	+.782	+.840	+.822
ϕ = angle whose tan is β/α	38.03°	40.03°	39.42°
$\Delta\phi$		+2.00°	+1.39°
$12.2\, Y^{\frac{1}{2}}$*		8.06	8.34
$12.2\, Y^{\frac{1}{2}}(\alpha^2 + \beta^2)^{\frac{1}{2}}$*		.424	.404
$\Delta H' = 12.2\, Y^{\frac{1}{2}}(\alpha^2 + \beta^2)^{\frac{1}{2}} \cdot \Delta\phi$		+0.85	+0.56
Color of modification relative to that of actual earth, according to the measurements		Darker, greener, slightly stronger	Lighter, weaker, slightly greener
$\Delta E = [(\Delta L')^2 + (\Delta S')^2 + (\Delta H')^2]^{\frac{1}{2}}$		2.6	5.8

* Values which are average for the two specimens being compared should be entered in those rows marked by an asterisk.

ments. (This factor frequently affects the correlation if appreciable specularly reflected light is present in one case, but is eliminated in the other.)

3. Differences in texture and shape of the specimens being compared.

4. Non-uniformity of color from point to point on some of the specimens. (For instrument measurements of pairs of specimens, central areas are usually used; for visual comparisons, the colors of the immediately adjacent areas of the specimens have the greatest influence on estimated color difference.)

5. Failure to take proper account in the measured values of the character of the dividing line, separating pattern, or background used during visual observation.

6. Abnormality of the observer, either temporary as from fatigue, or permanent as with an observer having abnormal color vision.

VIII. EXAMPLES

To demonstrate uses of the photoelectric tristimulus method, and to illustrate forms for recording the corresponding data, six examples have been prepared. These examples represent multipurpose reflectometer measurements made at the National Bureau of Standards for purposes which have been identified on each of the forms which is shown. All of the steps leading from the initially recorded settings to the desired values for color have been duplicated. The number of settings taken on each sample and the short-cuts permitted in the reduction of the

EXAMPLE 5. Measurement of the whiteness W of one new and two laundered sheeting specimens (see Eq. (19)).
Purpose—To measure the effect of repeated laundering on the whiteness of new sheeting material.
Computational short-cut—Scale corrections omitted.
$k_l = 20$, $f_g = 1.00$.
Working standard—Vitrolite No. 1 ($A = 0.906$, $G = 0.909$, $B = 0.890$).

Specimen	Standard	New	1L	20L
Blue settings	0.898	0.837	0.845	0.765
	.892	.850	.852	.787
Mean	.895	.8435	.8485	.776
$B = \text{Mean} \times \frac{0.890}{0.895}$		.8388	.8438	.7717
Amber settings	.9085	.892	.912	.826
	.906	.904	.912	.836
Mean	.9072	.898	.912	.831
$A = \text{Mean} \times \frac{0.906}{0.9072}$		.8968	.9108	.8299
Green settings	.9055	.884	.900	.812
	.903	.894	.900	.824
Mean	.9042	.889	.900	.818
$G = \text{Mean} \times \frac{0.909}{0.9042}$		.8937	.9048	.8223
$A - G$		.0031	.0060	.0076
$2.5(A - G)$		.0078	.0150	.0190
$G - B$		.0549	.0610	.0506
$\alpha \doteq 2.5(A - G)/10G$		.0009	.0017	.0023
$\beta \doteq (G - B)/10G$		.0061	.0067	.0062
$(\alpha^2 + \beta^2)^{\frac{1}{2}}$		.0062	.0069	.0066
$W_C = 30(\alpha^2 + \beta^2)^{\frac{1}{2}}$		.186	.207	.198
$1.00 - G$		.106	.095	.178
$W_L = (1.00 - G)/2$		.053	.048	.089
$(W_C^2 + W_L^2)^{\frac{1}{2}}$		.193	.213	.217
$W = 1 - \text{above}$		.807	.787	.783

data were decided in each case by a consideration of the needs for precision and accuracy of the problem at hand. Whenever two readings were made with each filter for every specimen, the order of readings was: Std., No. 1, No. 2, No. 3, . . ., No. 3, No. 2, No. 1, Std. This symmetrical order, which was used to eliminate some of the error of drift, was mentioned above. The equations used in the accompanying examples are given in Table III and in the text above.

One fact is worthy of comment in connection with the changes of chromaticity accompanying fading of the paint illustrated in Fig. 11. At the start of exposure, a change in the paint from moderate pink to weak orange took place. This pronounced hue change is unusual in fading; paints, textile, and other materials are usually perceived to become merely weaker in color as the result of exposure to light, heat, and humidity. The usual curve of chromaticity change with time of exposure is therefore merely a curve directed toward the origin of the (α, β) diagram, similar to the curves of Fig. 11 beyond the points showing the initial hue change.

IX. SUMMARY

Photoelectric tristimulus measurements are well-suited for comparisons of the colors of

EXAMPLE 6. Measurement of the yellowness of four near-white porcelain-enamel specimens (Eq. (20)).
Purpose—To find which of several enamel specimens are yellowish (+ values) and which are bluish (− values).
Computational short-cut—Scale corrections omitted.
Working standard—Vitrolite No. 1 ($A=0.906$, $G=0.909$, $B=0.890$).

Plaque No.	Standard	1	10	22	24
Blue settings	0.8955	0.7540	0.7760	0.8238	0.7804
	.8920	.7490	.7716	.8222	.7780
Mean	.8938	.7515	.7738	.8230	.7792
$B=\text{Mean}\times\frac{0.890}{0.8938}$		.7483	.7705	.8195	.7759
Amber settings	.8945	.7276	.7236	.7990	.7980
	.8936	.7222	.7176	.7962	.7962
Mean	.8940	.7249	.7206	.7976	.7971
$A=\text{Mean}\times\frac{0.906}{0.8940}$		.7346	.7303	.8083	.8078
Green settings	.9037	.7370	.7364	.8094	.8046
	.9030	.7316	.7324	.8074	.8030
Mean	.9034	.7343	.7344	.8084	.8038
$G=\text{Mean}\times\frac{0.909}{0.9034}$		.7389	.7390	.8134	.8088
$A-B$		−.0137	−.0402	−.0112	+.0319
Yellowness $=(A-B)/G$ (Eq. 20)		−.0185	−.0544	−.0138	+.0394

spectrally similar specimens. In commerce there seem to be many situations in which such measurements may prove to be useful: (1) in the day-to-day control of the colors of materials in production, (2) in obtaining compliance of materials with color-tolerance requirements, (3) in making modifications of color to produce matches, and (4) in the measurements of color changes accompanying fading. For problems of this general character, it is believed that photoelectric tristimulus measurements will prove to be useful.

Table X has been prepared to summarize the advantages and disadvantages of photoelectric tristimulus colorimetry. The directness of the method and the small number of computational steps necessary to give numbers indicative of the color of measured specimens recommend the method. Its inaccuracy because of failure of source-filter photo-cell combinations to be spectrally equivalent to the I.C.I. standard observer is its most important defect. Nevertheless it can be reasonably expected that the use of photoelectric tristimulus colorimetry will increase as the combinations of elements used are improved in spectral character.

X. REFERENCES

(1) I. A. Balinkin, "Industrial color tolerances," Am. J. Psychol. **52**, 428 (1939).
(2) B. T. Barnes, "A four-filter photoelectric colorimeter," J. Opt. Soc. Am. **29**, 448 (1939).
(3) F. C. Breckenridge and W. R. Schaub, "Rectangular uniform-chromaticity-scale coordinates," J. Opt. Soc. Am. **29**, 370 (1939).
(4) A. Dresler and H. G. Frühling, "Uber ein photoelektrisches Dreifarbenmessgerät," Das Licht **8**, 238 (1938).
(5) R. S. Estey, "The selection of color temperature altering filters," J. Opt. Soc. Am. **26**, 293 (1936).
(6) Federal Standard Stock Catalog, Procurement Division, Washington, D. C., Federal Specification TT-P-53 for paint; outside, ready-mixed, medium-chrome-yellow (Feb. 12, 1937).
(7) Federal Standard Stock Catalog, Procurement Division, Washington, D. C., Federal Specification TT-P-59 for paint; ready-mixed, international-orange (June 17, 1937).

TABLE X. Advantages and disadvantages of photoelectric tristimulus colorimetry.

Advantages	Disadvantages
1. Small number of settings required for each sample.	1. Errors resulting from the inaccurate spectral response of the source-filter photo-cell combinations used.
2. Small number of computational steps required to obtain x, y, and Y, or α, β, and Y.	2. The necessity for working standards which are spectrally similar to the samples measured.
3. Simplicity and inexpensiveness of apparatus.	3. The necessity for special precautions to attain the high precision required if the tristimulus method is to equal the eye in power to discriminate colors.
4. Opportunity to convert settings rapidly to numbers giving size and character of color difference perceived between samples.	4. Failure of tristimulus measurements to provide the physical description of a color stimulus such as is given by a spectrophotometric curve.
5. Correspondence between values of α, β, and Y, and positions of points representing colors in the uniformly spaced surface-color solid.	

(8) Federal Standard Stock Catalog, Procurement Division, Washington, D. C., Federal Specification TT-P-23a for paint; cold-water, interior, light-tints and white (March 22, 1940).

(9) H. P. Gage, "Color filters for altering color temperature. Pyrometer absorption and daylight glasses," J. Opt. Soc. Am. **23**, 46 (1933).

(10) General Electric Company, The G. E. light-sensitive cell, Catalog GEA-2467 (1936); see also R. H. Mighell, "The light-sensitive cell," Gen. Elec. Rev. **40**, 372 (1937).

(11) K. S. Gibson, "Photoelectric photometers and colorimeters," Instruments **9**, 309 and 335 (1936); see also Nat. Bur. Stand. Letter Circular LC545, "Photoelectric colorimeters" (March 8, 1939).

(12) K. S. Gibson and H. J. Keegan, "On the magnitude of the error resulting from fluorescence in spectrophotometric measurements," J. Opt. Soc. Am. **28**, 180 (1938).

(13) J. Guild, "The colorimetric properties of the spectrum," Phil. Trans. Roy. Soc. **A230**, 149 (1931).

(14) J. Guild, "The instrumental side of colorimetry," J. Sci. Inst. **11**, 69 (1934).

(15) A. C. Hardy, *Handbook of Colorimetry*, The Technology Press (Cambridge, 1936).

(16) R. S. Hunter, "Progress in developing a photoelectric method for measuring color difference," Bull. Am. Ceramic Soc. **18**, 121 (1939).

(17) R. S. Hunter, "Further progress in developing a photoelectric method for measuring color difference," Bull. Am. Ceramic Soc. **19**, 133 (1940).

(18) R. S. Hunter, "A multipurpose photoelectric reflectometer," J. Research, Nat. Bur. Stand. **25**, 581 (1940) RP1345; also [18a] J. Opt. Soc. Am. **30**, 536 (1940).

(19) R. S. Hunter, "Photoelectric tristimulus colorimetry," part of *Symposium on Color*, published by the A.S.T.M., Philadelphia, Pennsylvania (1941).

(20) Institute of Paper Chemistry, Instrumentation studies, XX, A study of photoelectric instruments for the measurements of color, reflectance, and transmittance, Paper Trade J. **105**, TS293 (1937).

(21) Institute of Paper Chemistry, Instrumentation studies XIII, Adaptability of the G. E. reflection meter as a color analyzer, Paper Trade J. **104**, TS245 (1937).

(22) International Commission on Illumination, Proceedings of the 8th Session, Commission Internationale de l'Éclairage, Cambridge, pp. 19–29 (Sept. 1931); see also reference [25].

(23) H. E. Ives, "A precision artificial eye," Phys. Rev. **6**, 334 (1915).

(24) L. A. Jones, "Colorimetry; preliminary draft of a report on nomenclature and definitions," J. Opt. Soc. Am. **27**, 207 (1937).

(25) D. B. Judd, The 1931 I.C.I. standard observer and coordinate system for colorimetry, J. Opt. Soc. Am. **23**, 359 (1933).

(26) D. B. Judd, "A Maxwell triangle yielding uniform chromaticity scales," J. Research Nat. Bur. Stand. **14**, 41 (1935), RP756; also J. Opt. Soc. Am. **25**, 24 (1935).

(27) D. B. Judd, "A method for determining whiteness of paper, II, Paper Trade J. **103**, TS154 (1936); also Tech. Assoc. Papers, Series 19, 359 (1936).

(28) D. B. Judd, "Specification of color tolerances at the National Bureau of Standards," Am. J. Psychol. **52**, 418 (1939).

(29) D. B. Judd, "Specification of uniform color tolerances for textiles," Textile Research **9**, 253, 292 (1939).

(30) D. B. Judd, "Hue, saturation, and lightness of surface colors with chromatic illumination," J. Research Nat. Bur. Stand. **24**, 293 (1940) RP1285, and J. Opt. Soc. Am. **30**, 2 (1940).

(31) D. B. Judd, "Color systems and their inter-relation," Illum. Eng. **36**, 336 (1941).

(32) D. B. Judd, "Whiteness of light surface-colors," J. Opt. Soc. Am. **31**, 462 (1941).

(33) D. B. Judd, "Introduction to Color," part of *Symposium on Color*, published by the A.S.T.M., Philadelphia, Pennsylvania (1941).

(34) D. L. MacAdam, "Maximum visual efficiency of colored materials," J. Opt. Soc. Am. **25**, 361 (1935).

(35) National Bureau of Standards, Letter Circular LC547, "Preparation and colorimetric properties of a magnesium oxide reflectance standard" (1939).

(36) National Bureau of Standards, Commercial standards CS62–38, "Colors for kitchen accessories," and CS63–38, "Colors for bathroom accessories" (1937).

(37) S. M. Newhall, "Preliminary report of the O.S.A. Subcommittee on the spacing of the Munsell colors," J. Opt. Soc. Am. **30**, 617 (1940).

(38) D. Nickerson, "Use of I.C.I. tristimulus values in disk colorimetry," U. S. Department of Agriculture, Bureau of Agricultural Economics, Washington, D. C. (May, 1938).

(39) W. Ostwald, *Colour Science; Part II, Colour Measurement and Colour Harmony* (English trans.) p. 35, Winsor and Newton (London, 1933).

(40) J. W. Perry, "The objective measurement of color," J. Sci. Inst. **15**, 270 (1938).

(41) I. G. Priest, "Apparatus for the determination of color in terms of dominant wave-length, purity, and brightness," J. Opt. Soc. Am. **8**, 173 (1924).

(42) F. Scofield, D. B. Judd, and R. S. Hunter, "A proposed method of designating color," A.S.T.M. Bulletin No. 110, p. 19 (May, 1941).

(43) F. W. Sears, "An improved calculator for obtaining tristimulus values from spectrophotometric curves," J. Opt. Soc. Am. **29**, 77 (1939).

(44) J. F. Skogland, "Tables of spectral energy distribution and luminosity for use in computing light transmissions and relative brightnesses from spectrophotometric data," Bur. Stand. Misc. Pub. No. 86 (1929); M86.

(45) T. Smith and J. Guild, "The C.I.E. colorimetric standards and their use," Trans. Opt. Soc. London **33**, 74 (1931).

(46) F. Twyman and J. Perry, "Improvements in or relating to colorimeters," British Patent Spec. No. 324, 351, (Jan. 20, 1930); Application dated Aug. 18, 1928.

(47) J. A. Van den Akker, "Chromaticity limitations of the best physically realizable three-filter photoelectric colorimeter," J. Opt. Soc. Am. **27**, 401 (1937).

(48) A. W. VanHeuckeroth, "Effect of several factors upon the yellowing of some protective coatings," Sci. Sec. Cir. No. 407 of the Nat. Paint, Varnish, and Lacquer Assn., Washington, D. C. (1932).

(49) S. Werthan, A. C. Elm, and R. H. Wien, "Yellowing of interior gloss paints and enamels," Ind. Eng. Chem. **22**, 772 (1930).

(50) G. T. Winch and E. H. Palmer, "A direct reading photoelectric trichromatic colorimeter," Trans. Illum. Eng. Soc. London **2**, 137 (1937).

(51) W. D. Wright, "A re-determination of the trichromatic coefficients of the spectral colours," Trans. Opt. Soc. **30**, 141 (1928–29); "A re-determination of the trichromatic mixture data," Medical Research Council, Reports of the Committee upon the Physiology of Vision, VII, Special Report Series No. 139, London, 1929.

Illumination from Arrays of Rectangular Sources

DOMINA EBERLE SPENCER
Massachusetts Institute of Technology, Cambridge, Massachusetts
(Received June 18, 1942)

1. INTRODUCTION

ONE of the most common methods of lighting large rooms is by rectangular sources arranged in some kind of an orderly pattern. Various arrangements are used, such as a two-dimensional array of rectangular sources (lens plates set in the ceiling, luminous panels, commercial fluorescent luminaires); a set of long, parallel, luminous strips (troffer lighting); or a series of rectangular windows. The illumination from any such array can be calculated by repeated use of the well-known formulae for rectangular sources,[1] but this method is inherently time-consuming and becomes almost hopelessly complex if a great number of sources are employed.

When the luminaires are regularly spaced, which usually occurs in practice, some simplification can be effected by writing equations for the total illumination produced by N sources instead of making separate calculations for each source alone. This procedure has been carried out in the present paper, and exact formulae are given for the luminous flux density produced on any suitably oriented surface by arrays of rectangular sources. These sources are regularly spaced and their helios[2] is assumed to be independent of the angle at which they are viewed. Further simplification of the formulae is desirable, which is obtained by making the simplest possible approximation. The array of sources is imagined to be replaced by a single uniform source and the error introduced by this approximation is investigated. It is gratifying to find that these very convenient approximations give extraordinarily accurate results while markedly shortening the labor involved.

2. ILLUMINATION FROM A SINGLE RECTANGULAR SOURCE

The luminous flux density[2] on a horizontal or vertical plane at a given point P (Fig. 1) is obtainable by the *unit sphere* or *solid angle* method. The illumination is produced by a single rectangular source. Two assumptions are made:

(1) The helios[2] H is constant for all rays reaching P from the light source.

(2) There are no interreflections in the room.

The flux density at P on any plane is then

$$D=(H/\pi)\sigma''. \tag{1}$$

The rectangle is projected stereometrically onto the sphere to give the area σ' and the resulting figure is then projected orthogonally onto the illuminated plane. The area of the final figure is called σ''.

By Eq. (1),

$$\begin{aligned} D_x&=(H/2\pi)[(\theta_{12}-\theta_{22})\cos\beta_2-(\theta_{11}-\theta_{21})\cos\beta_1];\\ D_y&=(H/2\pi)[(\zeta_{21}-\zeta_{22})\cos\gamma_2-(\zeta_{11}-\zeta_{12})\cos\gamma_1];\\ D_z&=(H/2\pi)[(\theta_{11}-\theta_{21})\sin\beta_1+(\zeta_{11}-\zeta_{12})\sin\gamma_1-(\theta_{12}-\theta_{22})\sin\beta_2-(\zeta_{21}-\zeta_{22})\sin\gamma_2]; \end{aligned} \tag{2}$$

where D_x, D_y, and D_z are components of the *flux density vector* **D**. The subscripts refer to the directions of the normal to the illuminated surface. The four corners of σ' are designated by the numbers 11, 12, 21, and 22, the first number of each pair giving the subscript of γ and the second giving the subscript of β. The distance on the sphere from M to any corner ij is designated by θ_{ij}, while the distance from N is designated by ζ_{ij}.

[1] Parry Moon and D. E. Spencer, "Illumination from a non-uniform sky," Illum. Eng. (in press).
[2] Parry Moon, "A system of photometric concepts," J. Opt. Soc. Am. **32**, 348 (1942).

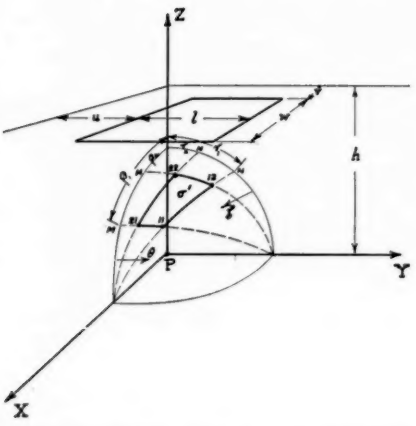

FIG. 1. Single rectangular source, arbitrarily placed with respect to the point P at which the flux density is to be calculated.

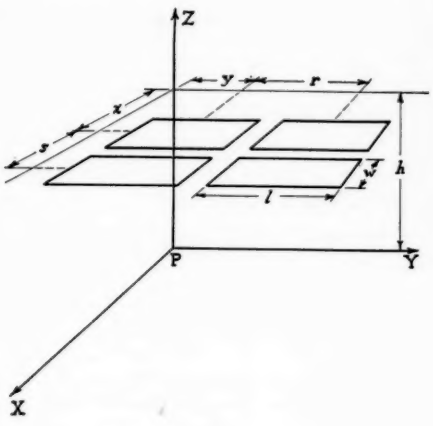

FIG. 2. A two-dimensional array of rectangular sources.

From the geometry of Fig. 1,

$$\begin{aligned}
&\tan\zeta_{11}=\cos\gamma_1\tan\beta_1, \quad \tan\theta_{11}=\tan\gamma_1\cos\beta_1;\\
&\tan\zeta_{12}=\cos\gamma_1\tan\beta_2, \quad \tan\theta_{12}=\tan\gamma_1\cos\beta_2;\\
&\tan\zeta_{21}=\cos\gamma_2\tan\beta_1, \quad \tan\theta_{21}=\tan\gamma_2\cos\beta_1;\\
&\tan\zeta_{22}=\cos\gamma_2\tan\beta_2, \quad \tan\theta_{22}=\tan\gamma_2\cos\beta_2.
\end{aligned} \tag{3}$$

It will be convenient to express the equations for D_x, D_y, and D_z in terms of four new variables:

$$e=(w+v)/h, \quad f=v/h, \quad g=(u+l)/h, \quad q=u/h. \tag{4}$$

Then it is obvious from Fig. 1 that

$$\begin{aligned}
&\sin\beta_1=e(1+e^2)^{-\frac{1}{2}}, \quad \cos\beta_1=(1+e^2)^{-\frac{1}{2}}, \quad \tan\beta_1=e,\\
&\sin\beta_2=f(1+f^2)^{-\frac{1}{2}}, \quad \cos\beta_2=(1+f^2)^{-\frac{1}{2}}, \quad \tan\beta_2=f,\\
&\sin\gamma_1=g(1+g^2)^{-\frac{1}{2}}, \quad \cos\gamma_1=(1+g^2)^{-\frac{1}{2}}, \quad \tan\gamma_1=g,\\
&\sin\gamma_2=q(1+q^2)^{-\frac{1}{2}}, \quad \cos\gamma_2=(1+q^2)^{-\frac{1}{2}}, \quad \tan\gamma_2=q.
\end{aligned} \tag{5}$$

Substitution of Eqs. (5) and (3) in (2) yields the final equations for a single rectangular source:

$$\begin{aligned}
D_x&=\frac{H}{2\pi}\left\{(1+f^2)^{-\frac{1}{2}}\left[\tan^{-1}\frac{g}{(1+f^2)^{\frac{1}{2}}}-\tan^{-1}\frac{q}{(1+f^2)^{\frac{1}{2}}}\right]-(1+e^2)^{-\frac{1}{2}}\left[\tan^{-1}\frac{g}{(1+e)^{\frac{1}{2}}}-\tan^{-1}\frac{q}{(1+e^2)^{\frac{1}{2}}}\right]\right\};\\
D_y&=\frac{H}{2\pi}\left\{(1+q^2)^{-\frac{1}{2}}\left[\tan^{-1}\frac{e}{(1+q^2)^{\frac{1}{2}}}-\tan^{-1}\frac{f}{(1+q^2)^{\frac{1}{2}}}\right]-(1+g^2)^{-\frac{1}{2}}\left[\tan^{-1}\frac{e}{(1+g^2)^{\frac{1}{2}}}-\tan^{-1}\frac{f}{(1+g^2)^{\frac{1}{2}}}\right]\right\};\\
D_z&=\frac{H}{2\pi}\left\{e(1+e^2)^{-\frac{1}{2}}\left[\tan^{-1}\frac{g}{(1+e^2)^{\frac{1}{2}}}-\tan^{-1}\frac{q}{(1+e^2)^{\frac{1}{2}}}\right]-f(1+f^2)^{-\frac{1}{2}}\left[\tan^{-1}\frac{g}{(1+f^2)^{\frac{1}{2}}}-\tan^{-1}\frac{q}{(1+f^2)^{\frac{1}{2}}}\right]\right.\\
&\quad\left.+g(1+g^2)^{-\frac{1}{2}}\left[\tan^{-1}\frac{e}{(1+g^2)^{\frac{1}{2}}}-\tan^{-1}\frac{f}{(1+g^2)^{\frac{1}{2}}}\right]-q(1+q^2)^{-\frac{1}{2}}\left[\tan^{-1}\frac{e}{(1+q^2)^{\frac{1}{2}}}-\tan^{-1}\frac{f}{(1+q^2)^{\frac{1}{2}}}\right]\right\}.
\end{aligned} \tag{6}$$

3. TWO-DIMENSIONAL ARRAYS OF RECTANGULAR SOURCES

I. Exact Formulae

Figure 2 indicates a portion of an array of rectangular sources. The spacing in the y direction is r while the spacing in the x direction is s. The origin of the coordinate system is taken at the point P where the flux density is to be determined, and the distances x and y to the center of the nearest source are entirely arbitrary. Ordinarily there will be sources also on the other side of P. It is simpler, however, and entails no loss in generality to consider the array to be entirely in one quadrant. The flux density in the most general case is then obtained by adding the flux densities obtained from sources in the separate quadrants.

The array of Fig. 2 will be considered as made up of M equally spaced sources in the y direction and N equally spaced sources in the x direction. An arbitrary source will be specified by the numbers (m, n) where $m=1, 2, \cdots, M$ and $n=1, 2, \cdots, N$. Then by Eq. (4),

$$\begin{aligned} e&=\frac{(n-1)s+x+w/2}{h}, \quad f=\frac{(n-1)s+x-w/2}{h}, \quad n=1, 2, \cdots, N, \\ g&=\frac{(m-1)r+y+l/2}{h}, \quad q=\frac{(m-1)r+y-l/2}{h}, \quad m=1, 2, \cdots, M, \end{aligned} \tag{7}$$

where e, f, g, q, *are restricted to non-negative values.* These quantities are always positive except for $n=1$ or $m=1$, when they may sometimes be negative. A negative value means that part of the light source is in another quadrant. Since only the portion of the array that is in one quadrant is considered, the rule may be stated that *if* $e, f, g,$ *or* q *appears as a negative number, it is taken as zero.*

It is convenient to introduce the further change of variable:

$$\lambda=l/h, \quad \mu=s/h, \quad \nu=w/h, \quad \xi=x/h, \quad \omega=y/h, \quad \sigma=r/h. \tag{8}$$

Substitution of Eq. (8) in (7) gives

$$\begin{aligned} e&=(n-1)\mu+\xi+\nu/2, \quad f=(n-1)\mu+\xi-\nu/2, \quad n=1, 2, \cdots, N, \\ g&=(m-1)\sigma+\omega+\lambda/2, \quad q=(m-1)\sigma+\omega-\lambda/2, \quad m=1, 2, \cdots, M. \end{aligned} \tag{9}$$

Then, according to Eq. (6), an array of N by M rectangular sources will give the flux densities:

$$\begin{aligned} D_x=\frac{H}{2\pi}\sum_{n=1}^{N}\sum_{m=1}^{M}\Bigg\{&(1+f^2)^{-\frac{1}{2}}\left[\tan^{-1}\frac{g}{(1+f^2)^{\frac{1}{2}}}-\tan^{-1}\frac{q}{(1+f^2)^{\frac{1}{2}}}\right] \\ &-(1+e^2)^{-\frac{1}{2}}\left[\tan^{-1}\frac{g}{(1+e^2)^{\frac{1}{2}}}-\tan^{-1}\frac{q}{(1+e^2)^{\frac{1}{2}}}\right]\Bigg\}; \\ D_y=\frac{H}{2\pi}\sum_{n=1}^{N}\sum_{m=1}^{M}\Bigg\{&(1+q^2)^{-\frac{1}{2}}\left[\tan^{-1}\frac{e}{(1+q^2)^{\frac{1}{2}}}-\tan^{-1}\frac{f}{(1+q^2)^{\frac{1}{2}}}\right] \\ &-(1+g^2)^{-\frac{1}{2}}\left[\tan^{-1}\frac{e}{(1+g^2)^{\frac{1}{2}}}-\tan^{-1}\frac{f}{(1+g^2)^{\frac{1}{2}}}\right]\Bigg\}; \end{aligned} \tag{10}$$

$$D_z=\frac{H}{2\pi}\sum_{n=1}^{N}\sum_{m=1}^{M}\left\{e(1+e^2)^{-\frac{1}{2}}\left[\tan^{-1}\frac{g}{(1+e^2)^{\frac{1}{2}}}-\tan^{-1}\frac{q}{(1+e^2)^{\frac{1}{2}}}\right]\right.$$
$$-f(1+f^2)^{-\frac{1}{2}}\left[\tan^{-1}\frac{g}{(1+f^2)^{\frac{1}{2}}}-\tan^{-1}\frac{q}{(1+f^2)^{\frac{1}{2}}}\right]$$
$$+g(1+g^2)^{-\frac{1}{2}}\left[\tan^{-1}\frac{e}{(1+g^2)^{\frac{1}{2}}}-\tan^{-1}\frac{f}{(1+g^2)^{\frac{1}{2}}}\right]$$
$$\left.-q(1+q^2)^{-\frac{1}{2}}\left[\tan^{-1}\frac{e}{(1+q^2)^{\frac{1}{2}}}-\tan^{-1}\frac{f}{(1+q^2)^{\frac{1}{2}}}\right]\right\}.$$

It is often sufficient to calculate the flux densities for the following special cases:

(A) Point P midway between a pair of sources in the x direction ($\xi=\mu/2$, $\omega=0$). In this case,

$$e=\frac{(2n-1)\mu+\nu}{2},\quad f=\frac{(2n-1)\mu-\nu}{2},\quad n=1, 2, \cdots, N,$$
$$g=\frac{2(m-1)\sigma+\lambda}{2},\quad q=\frac{2(m-1)\sigma-\lambda}{2},\quad m=1, 2, \cdots, M. \tag{11}$$

(B) Point P midway between a pair of sources in the y direction ($\xi=0$, $\omega=\sigma/2$). Then

$$e=\frac{2(n-1)\mu+\nu}{2},\quad f=\frac{2(n-1)\mu-\nu}{2},\quad n=1, 2, \cdots, N,$$
$$g=\frac{(2m-1)\sigma+\lambda}{2},\quad q=\frac{(2m-1)\sigma-\lambda}{2},\quad m=1, 2, \cdots, M. \tag{12}$$

(C) Point P beneath the center of a source ($\xi=0$, $\omega=0$):

$$e=(n-1)\mu+\nu/2,\quad f=(n-1)\mu-\nu/2,\quad n=1, 2, \cdots, N,$$
$$g=(m-1)\sigma+\lambda/2,\quad q=(m-1)\sigma-\lambda/2,\quad m=1, 2, \cdots, M. \tag{13}$$

II. Approximate Formulae

The simplest way of approximating Eqs. (10) is to replace the array of rectangular sources by a single rectangular source having the proper helios. Let H_u be the helios of the uniform source which replaces the array of rectangular sources having the helios H_a. Then the average helios over the area used for the single uniform source is

$$H_u=H_a\frac{[(N-1/2)\nu+\xi][(M-1/2)\lambda+\omega]}{[(N-1/2)\mu+\xi][(M-1/2)\sigma+\omega]}\quad \text{if } \xi<\nu,\ \omega<\lambda;$$
$$H_u=H_a\frac{[(N-1/2)\nu+\xi]M\lambda}{[(N-1/2)\mu+\xi][(M-1/2)\sigma+\omega]}\quad \text{if } \xi<\nu,\ \omega\geq\lambda;$$
$$H_u=H_a\frac{[(M-1/2)\lambda+\omega]N\nu}{[(N-1/2)\mu+\xi][(M-1/2)\sigma+\omega]}\quad \text{if } \xi\geq\nu,\ \omega<\lambda; \tag{14}$$
$$H_u=H_a\frac{NM\lambda\mu}{[(N-1/2)\mu+\xi][(M-1/2)\sigma+\omega]}\quad \text{if } \xi\geq\nu,\ \omega\geq\lambda.$$

If

$$e=(N-1/2)\mu+\xi, \quad g=(M-1/2)\sigma+\omega; \tag{15}$$

then

$$D_x=\frac{H_u}{2\pi}\left[\tan^{-1} g-(1+e^2)^{-\frac{1}{2}}\tan^{-1}\frac{g}{(1+e^2)^{\frac{1}{2}}}\right];$$

$$D_y=\frac{H_u}{2\pi}\left[\tan^{-1} e-(1+g^2)^{-\frac{1}{2}}\tan^{-1}\frac{e}{(1+g^2)^{\frac{1}{2}}}\right]; \tag{16}$$

$$D_z=\frac{H_u}{2\pi}\left[e(1+e^2)^{-\frac{1}{2}}\tan^{-1}\frac{g}{(1+e^2)^{\frac{1}{2}}}+g(1+g^2)^{-\frac{1}{2}}\tan^{-1}\frac{e}{(1+g^2)^{\frac{1}{2}}}\right].$$

For the special cases cited in Part I of this section, Eq. (15) assumes the following simple forms:

(A) Point P midway between a pair of sources in the x direction ($\xi=\mu/2$, $\omega=0$):

$$e=N\mu, \quad g=(M-1/2)\sigma. \tag{17}$$

(B) Point P midway between a pair of sources in the y direction ($\xi=0$, $\omega=\sigma/2$):

$$e=(N-1/2)\mu, \quad g=M\sigma. \tag{18}$$

(C) Point P beneath center of source ($\xi=0$, $\omega=0$):

$$e=(N-1/2)\mu, \quad g=(M-1/2)\sigma. \tag{19}$$

Another interesting special case is that in which *the rectangular array is very long* in one direction or the other, or in both directions. If $N\to\infty$, Eqs. (14) and (16) become

$$H_u=H_a\frac{\nu[(M-1/2)\lambda+\omega]}{\mu[(M-1/2)\sigma+\omega]}, \quad \omega=\lambda; \quad H_u=H_a\frac{M\lambda\nu}{\mu[(M-1/2)\sigma+\omega]}, \quad \omega\geq\lambda; \tag{20}$$

and

$$D_x=(H_u/2\pi)\tan^{-1} g; \quad D_y=(H_u/4)[1-(1+g^2)^{-\frac{1}{2}}]; \quad D_z=(H_u/4)g(1+g^2)^{-\frac{1}{2}}. \tag{21}$$

If $M\to\infty$, the equations become

$$H_u=H_a\frac{\lambda[(N-1/2)\nu+\xi]}{\sigma[(N-1/2)\mu+\xi]}, \quad \xi<\nu; \quad H_u=H_a\frac{N\lambda\nu}{\sigma[(N-1/2)\mu+\xi]}, \quad \xi\geq\nu; \tag{22}$$

and

$$D_x=(H_u/4)[1-(1+e^2)^{-\frac{1}{2}}]; \quad D_y=(H_u/2\pi)\tan^{-1} e; \quad D_z=(H_u/4)e(1+e^2)^{-\frac{1}{2}}. \tag{23}$$

If $M\to\infty$ and $N\to\infty$, the formulae reduce to

$$H_u=H_a\lambda\nu/\sigma\mu, \tag{24}$$

and

$$D_x=D_y=D_z=H_u/4. \tag{25}$$

In practice the two-dimensional array is ordinarily in the ceiling of the room while the point P is at desk level. Under these conditions the distance h is usually greater than r or s and the approximate formulae give results of sufficient accuracy for engineering use. The approximation used in this section is of the same type that will be described later in connection with arrays of long, narrow strip sources, where the errors introduced by the approximate formulae can be shown to be very small. The order of magnitude of the errors found in the case of strip sources can be inferred to be valid also for the two-dimensional arrays of the present section. That is, *for all situations encountered in illuminating engineering practice, the approximate formulae give results that are correct to within one percent or better.* The exact equations are needed only if unusually high accuracy is required or if P is close to the plane of the array.

4. ONE-DIMENSIONAL ARRAYS OF RECTANGULAR WINDOWS

I. Exact Formulae

Section 3 treated the flux density produced by the general array of sources extending in both x and y directions. In many cases the array extends in one direction only and the previous equations can be considerably simplified. Figure 3 shows a one-dimensional array of rectangular sources such as a set of evenly spaced windows in the wall of a factory or office. For the nth source, according to Eq. (4),

$$e=\frac{(n-1)s+x+w/2}{h},\quad f=\frac{(n-1)s+x-w/2}{h},\quad g=\frac{u+l}{h},\quad q=u/h,\quad n=1, 2, \cdots, N, \tag{26}$$

where $e, f, g,$ *and* q *are restricted to non-negative values* as before. If the new variables defined by Eq. (8) are again used,

$$e=(n-1)\mu+\xi+\nu/2,\quad f=(n-1)\mu+\xi-\nu/2,\qquad g=\omega+\lambda,\quad q=\omega,\quad n=1, 2, \cdots, N. \tag{27}$$

The flux densities produced by the complete array of N rectangular sources is then, according to Eq. (6),

$$D_x=\frac{H}{2\pi}\sum_{n=1}^{N}\left\{(1+f^2)^{-\frac{1}{2}}\left[\tan^{-1}\frac{g}{(1+f^2)^{\frac{1}{2}}}-\tan^{-1}\frac{q}{(1+f^2)^{\frac{1}{2}}}\right]\right.$$
$$\left.-(1+e^2)^{-\frac{1}{2}}\left[\tan^{-1}\frac{g}{(1+e^2)^{\frac{1}{2}}}-\tan^{-1}\frac{q}{(1+e^2)^{\frac{1}{2}}}\right]\right\};$$

$$D_y=\frac{H}{2\pi}\sum_{n=1}^{N}\left\{(1+q^2)^{-\frac{1}{2}}\left[\tan^{-1}\frac{e}{(1+q^2)^{\frac{1}{2}}}-\tan^{-1}\frac{f}{(1+q^2)^{\frac{1}{2}}}\right]\right.$$
$$\left.-(1+q^2)^{-\frac{1}{2}}\left[\tan^{-1}\frac{e}{(1+g^2)^{\frac{1}{2}}}-\tan^{-1}\frac{f}{(1+g^2)^{\frac{1}{2}}}\right]\right\}; \tag{28}$$

$$D_z=\frac{H}{2\pi}\sum_{n=1}^{N}\left\{e(1+e^2)^{-\frac{1}{2}}\left[\tan^{-1}\frac{g}{(1+e^2)^{\frac{1}{2}}}-\tan^{-1}\frac{q}{(1+e^2)^{\frac{1}{2}}}\right]\right.$$
$$-f(1+f)^{-\frac{1}{2}}\left[\tan^{-1}\frac{g}{(1+f^2)^{\frac{1}{2}}}-\tan^{-1}\frac{q}{(1+f^2)^{\frac{1}{2}}}\right]+g(1+g^2)^{-\frac{1}{2}}\left[\tan^{-1}\frac{e}{(1+g^2)^{\frac{1}{2}}}-\tan^{-1}\frac{f}{(1+g^2)^{\frac{1}{2}}}\right]$$
$$\left.-q(1+q^2)^{-\frac{1}{2}}\left[\tan^{-1}\frac{e}{(1+q^2)^{\frac{1}{2}}}-\tan^{-1}\frac{f}{(1+q^2)^{\frac{1}{2}}}\right]\right\}.$$

It is often sufficient to calculate the flux density in two special cases:

(A) Point P midway between a pair of windows ($\xi=\mu/2$). Then

$$e=\frac{(2n-1)\mu+\nu}{2},\quad f=\frac{(2n-1)\mu-\nu}{2},\quad g=\omega+\lambda,\quad q=\omega,\quad n=1, 2, \cdots, N. \tag{29}$$

(B) Point P opposite the center of a window ($\xi=0$):

$$e=\frac{2(n-1)\mu+\nu}{2},\quad f=\frac{2(n-1)\mu-\nu}{2},\quad g=\omega+\lambda,\quad q=\omega,\quad n=1, 2, \cdots, N. \tag{30}$$

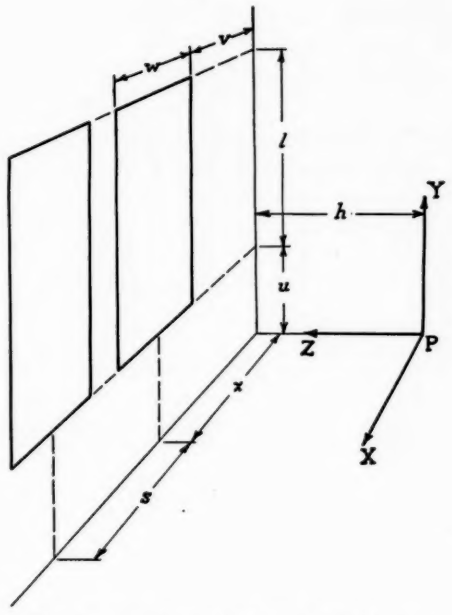

FIG. 3. A one-dimensional array of windows.

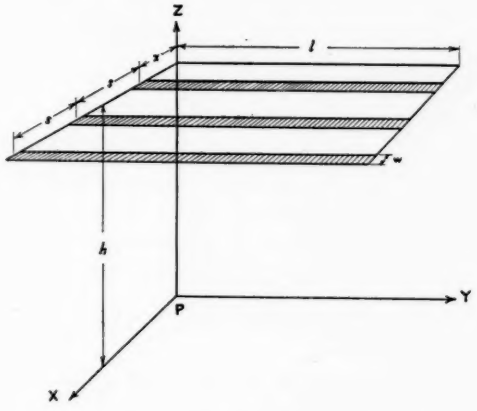

FIG. 4. A one-dimensional array of narrow luminous strips.

II. Approximate Formulae

(a) *Points Sufficiently Far from Windows*

If the point P at which the flux density is to be calculated is not too near the windows, a good approximation can be obtained by considering a single uniform window with an appropriate uniform helios. Let H_u be the helios of the equivalent uniform window and H_w that of the actual system of windows. Then

$$H_u = H_w \frac{(N-1/2)\nu+\xi}{(N-1/2)\mu+\xi} \quad \text{if } \xi<\nu; \quad H_u = H_w \frac{N\nu}{(N-1/2)\mu+\xi} \quad \text{if } \xi\geq\nu. \tag{31}$$

If

$$e=(N-1/2)\mu+\xi, \quad g=\omega+\lambda, \quad q=\omega, \tag{32}$$

Eq. (6) gives

$$\begin{aligned}
D_x &= \frac{H_u}{2\pi}\left\{\tan^{-1} g-\tan^{-1} q(1+e^2)^{-\frac{1}{2}}\left[\tan^{-1}\frac{g}{(1+e^2)^{\frac{1}{2}}}-\tan^{-1}\frac{q}{(1+e^2)^{\frac{1}{2}}}\right]\right\};\\
D_y &= \frac{H_u}{2\pi}\left\{(1+q^2)^{-\frac{1}{2}}\tan^{-1}\frac{e}{(1+q^2)^{\frac{1}{2}}}-(1+g^2)^{-\frac{1}{2}}\tan^{-1}\frac{e}{(1+g^2)^{\frac{1}{2}}}\right\};\\
D_z &= \frac{H_u}{2\pi}\left\{e(1+e^2)^{-\frac{1}{2}}\left[\tan^{-1}\frac{g}{(1+e^2)^{\frac{1}{2}}}-\tan^{-1}\frac{q}{(1+e^2)^{\frac{1}{2}}}\right]+g(1+g^2)^{-\frac{1}{2}}\tan^{-1}\frac{e}{(1+g^2)^{\frac{1}{2}}}\right.\\
&\qquad \left.-q(1+q^2)^{-\frac{1}{2}}\tan^{-1}\frac{e}{(1+q^2)^{\frac{1}{2}}}\right\}.
\end{aligned} \tag{33}$$

For the two special cases, the values of e, g, and q to be used in Eq. (33) are as follows:

(A) Point P midway between light sources ($\xi=\mu/2$):

$$e=N\mu, \quad g=\omega+\lambda, \quad q=\omega. \tag{34}$$

(B) Point P opposite center of a light source ($\xi=0$):

$$e=(N-1/2)\mu, \quad g=\omega+\lambda, \quad q=\omega. \tag{35}$$

Another special case that is of some importance is that in which the number of windows is very large. Then $N\to\infty$ and Eqs. (33) become

$$D_x=\frac{H_u}{2\pi}\tan^{-1}g; \quad D_y=\frac{H_u}{4}[(1+q^2)^{-\frac{1}{2}}-(1+g^2)^{-\frac{1}{2}}]; \quad D_z=\frac{H_u}{4}\left[\frac{g}{(1+g^2)^{\frac{1}{2}}}-\frac{q}{(1+q^2)^{\frac{1}{2}}}\right]. \tag{36}$$

(*b*) *Points Near the Windows*

When the distance h between P and the plane of the windows is sufficiently small, the approximation (*a*) is no longer accurate. If P is opposite a window, a large part of the luminous flux is from this one window and the approximation (*a*) gives too low a value of flux density. Conversely, if P is between a pair of windows, the value of flux density calculated from (*a*) is too high.

This difficulty is obviated by considering the wall to be divided into two windows instead of the single fictitious window of (*a*). An exact calculation is then made for the window or rectangular portion of wall nearest the point P, and the flux density from the remainder of the array is approximated by the use of an equivalent uniform window of helios H_u.

Case I. The point P is opposite a window of helios H_w. Then $\xi\leq\nu/2$ and

$$H_u=H_w\frac{2(N-1)\nu}{2(N-1/2)\mu-\nu}. \tag{37}$$

The quantities e, g, and q are defined by Eq. (32); and from Eq. (6),

$$\begin{aligned}
D_x=\frac{1}{2\pi}\Bigg\{&H_w[\tan^{-1}g-\tan^{-1}q]-H_u(1+e^2)^{-\frac{1}{2}}\left[\tan^{-1}\frac{g}{(1+e^2)^{\frac{1}{2}}}-\tan^{-1}\frac{q}{(1+e^2)^{\frac{1}{2}}}\right]\\
&+\frac{(H_u-H_w)}{(1+(\xi+\nu/2)^2)^{\frac{1}{2}}}\left[\tan^{-1}\frac{g}{(1+(\xi+\nu/2)^2)^{\frac{1}{2}}}-\tan^{-1}\frac{\omega}{(1+(\xi-\nu/2)^2)^{\frac{1}{2}}}\right]\Bigg\};\\
D_y=\frac{1}{2\pi}\Bigg\{&(1+q^2)^{-\frac{1}{2}}\left[H_u\tan^{-1}\frac{e}{(1+q^2)^{\frac{1}{2}}}-(H_w-H_u)\tan^{-1}\frac{\xi+\nu/2}{(1+q^2)^{\frac{1}{2}}}\right]\\
&-(1+g^2)^{-\frac{1}{2}}\left[H_u\tan^{-1}\frac{e}{(1+g^2)^{\frac{1}{2}}}-(H_w-H_u)\tan^{-1}\frac{\xi+\nu/2}{(1+g^2)^{\frac{1}{2}}}\right]\Bigg\};\\
D_z=\frac{1}{2\pi}\Bigg\{&H_ue(1+e^2)^{-\frac{1}{2}}\left[\tan^{-1}\frac{g}{(1+e^2)^{\frac{1}{2}}}-\tan^{-1}\frac{q}{(1+e^2)^{\frac{1}{2}}}\right]\\
&+(H_w-H_u)(\xi+\nu/2)(1+(\xi+\nu/2)^2)^{-\frac{1}{2}}\left[\tan^{-1}\frac{g}{(1+(\xi+\nu/2)^2)^{\frac{1}{2}}}-\tan^{-1}\frac{q}{(1+(\xi+\nu/2)^2)^{\frac{1}{2}}}\right]\\
&+g(1+g^2)^{-\frac{1}{2}}\left[H_u\tan^{-1}\frac{e}{(1+g^2)^{\frac{1}{2}}}+(H_w-H_u)\tan^{-1}\frac{\xi+\nu/2}{(1+g^2)^{\frac{1}{2}}}\right]\\
&-q(1+q^2)^{-\frac{1}{2}}\left[H_u\tan^{-1}\frac{e}{(1+q^2)^{\frac{1}{2}}}+(H_w-H_u)\tan^{-1}\frac{\xi+\nu/2}{(1+q^2)^{\frac{1}{2}}}\right]\Bigg\}.
\end{aligned} \tag{38}$$

In the special case in which the point P is opposite the center of a light source, Eq. (38) continues to apply, but e, g, and q are defined by Eq. (35).

If the number of windows is very large, $N\to\infty$ and Eqs. (37) and (38) give

$$D_x=\frac{H_w}{2\pi}\left\{\tan^{-1}(\omega+\lambda)-\tan^{-1}\omega+\left(\frac{\nu}{\mu}-1\right)(1+(\xi+\nu/2)^2)^{-\frac{1}{2}}\right.$$
$$\left.\times\left[\tan^{-1}\frac{\omega+\lambda}{(1+(\xi+\nu/2)^2)^{\frac{1}{2}}}-\tan^{-1}\frac{\omega}{(1+(\xi-\nu/2)^2)^{\frac{1}{2}}}\right]\right\};$$

$$D_y=\frac{H_w}{2\pi}\left\{(1+\omega^2)^{-\frac{1}{2}}\left[\frac{\pi\nu}{2\mu}-\left(1-\frac{\nu}{\mu}\right)\tan^{-1}\frac{\xi+\nu/2}{(1+\omega^2)^{\frac{1}{2}}}\right]\right.$$
$$\left.-(1+(\omega+\lambda)^2)^{-\frac{1}{2}}\left[\frac{\pi\nu}{2\mu}-\left(1-\frac{\nu}{\mu}\right)\tan^{-1}\frac{\xi+\nu/2}{(1+(\omega+\lambda)^2)^{\frac{1}{2}}}\right]\right\}; \quad (39)$$

$$D_z=\frac{H_w}{2\pi}\left\{\left(1-\frac{\nu}{\mu}\right)(\xi+\nu/2)(1+(\xi+\nu/2)^2)^{-\frac{1}{2}}\left[\tan^{-1}\frac{\omega+\lambda}{(1+(\xi+\nu/2)^2)^{\frac{1}{2}}}-\tan^{-1}\frac{\omega}{(1+(\xi+\nu/2)^2)^{\frac{1}{2}}}\right]\right.$$
$$+(\omega+\lambda)(1+(\omega+\lambda)^2)^{-\frac{1}{2}}\left[\frac{\pi\nu}{2\mu}+\left(1-\frac{\nu}{\mu}\right)\tan^{-1}\frac{\xi+\nu/2}{(1+(\omega+\lambda)^2)^{\frac{1}{2}}}\right]$$
$$\left.-(1+\omega^2)^{-\frac{1}{2}}\left[\frac{\pi\nu}{2\mu}+\left(1-\frac{\nu}{\mu}\right)\tan^{-1}\frac{\xi+\nu/2}{(1+\omega^2)^{\frac{1}{2}}}\right]\right\}.$$

For sufficiently large distances h from the window, $(\xi+\nu/2)$ becomes very small and Eqs. (39) approach Eqs. (33) of approximation (a).

Case II. The point P is between a pair of windows ($\xi\geq\nu/2$). Then

$$H_u=H_wN\nu/(N-1/2)\mu. \quad (40)$$

The quantities e, g, and q are defined by Eq. (32). From Eq. (6), the flux densities are

$$D_x=\frac{H_u}{2\pi}\left\{(1+(\xi-\nu/2)^2)^{-\frac{1}{2}}\left[\tan^{-1}\frac{g}{(1+(\xi-\nu/2)^2)^{\frac{1}{2}}}-\tan^{-1}\frac{q}{(1+(\xi-\nu/2)^2)^{\frac{1}{2}}}\right]\right.$$
$$\left.-(1+e^2)^{-\frac{1}{2}}\left[\tan^{-1}\frac{g}{(1+e^2)^{\frac{1}{2}}}-\tan^{-1}\frac{q}{(1+e^2)^{\frac{1}{2}}}\right]+2(\tan^{-1}g-\tan^{-1}q)\right\};$$

$$D_y=\frac{H_u}{2\pi}\left\{(1+q^2)^{-\frac{1}{2}}\left[\tan^{-1}\frac{e}{(1+q^2)^{\frac{1}{2}}}+\tan^{-1}\frac{\xi-\nu/2}{(1+q^2)^{\frac{1}{2}}}\right]-(1+q^2)^{-\frac{1}{2}}\left[\tan^{-1}\frac{e}{(1+g^2)^{\frac{1}{2}}}+\tan^{-1}\frac{\xi-\nu/2}{(1+g^2)^{\frac{1}{2}}}\right]\right\}; \quad (41)$$

$$D_z=\frac{H_u}{2\pi}\left\{e(1+e^2)^{-\frac{1}{2}}\left[\tan^{-1}\frac{g}{(1+e^2)^{\frac{1}{2}}}-\tan^{-1}\frac{q}{(1+e^2)^{\frac{1}{2}}}\right]\right.$$
$$+(\xi-\nu/2)(1+(\xi-\nu/2)^2)^{-\frac{1}{2}}\left[\tan^{-1}\frac{g}{(1+(\xi-\nu/2)^2)^{\frac{1}{2}}}-\tan^{-1}\frac{q}{(1+(\xi-\nu/2)^2)^{\frac{1}{2}}}\right]$$
$$\left.+g(1+g^2)^{-\frac{1}{2}}\left[\tan^{-1}\frac{e}{(1+g^2)^{\frac{1}{2}}}+\tan^{-1}\frac{(\xi-\nu/2)}{(1+g^2)^{\frac{1}{2}}}\right]-q(1+q^2)^{-\frac{1}{2}}\left[\tan^{-1}\frac{e}{(1+q^2)^{\frac{1}{2}}}+\tan^{-1}\frac{(\xi-\nu/2)}{(1+q^2)^{\frac{1}{2}}}\right]\right\}.$$

In the special case in which the point P is midway between windows, e, g, and q are defined by Eq. (34).

If the number of windows is very large, $N\to\infty$ and Eq. (40) and (41) give the following equations:

$$D_x=\frac{H_w\nu}{2\pi\mu}\left\{(1-(\xi-\nu/2)^2)^{-\frac{1}{2}}\left[\tan^{-1}\frac{\omega+\lambda}{(1+(\xi-\nu/2)^2)^{\frac{1}{2}}}-\tan^{-1}\frac{\omega}{(1+(\xi-\nu/2)^2)^{\frac{1}{2}}}\right]\right.$$
$$\left.+2[\tan^{-1}(\omega+\lambda)-\tan^{-1}\omega]\right\};$$
$$D_y=\frac{H_w\nu}{2\pi\mu}\left\{(1+\omega^2)^{-\frac{1}{2}}\left[\frac{\pi}{2}+\tan^{-1}\frac{\xi-\nu/2}{(1+\omega^2)^{\frac{1}{2}}}\right]-(1+(\omega+\lambda)^2)^{-\frac{1}{2}}\left[\frac{\pi}{2}+\tan^{-1}\frac{\xi-\nu/2}{(1+(\omega+\lambda)^2)^{\frac{1}{2}}}\right]\right\};\tag{42}$$
$$D_z=\frac{H_w\nu}{2\pi\mu}\left\{(\xi-\nu/2)(1+(\xi-\nu/2)^2)^{-\frac{1}{2}}\left[\tan^{-1}\frac{\omega+\lambda}{(1+(\xi-\nu/2)^2)^{\frac{1}{2}}}-\tan^{-1}\frac{\omega}{(1+(\xi-\nu/2)^2)^{\frac{1}{2}}}\right]\right.$$
$$\left.+(\omega+\lambda)(1+(\omega+\lambda)^2)^{-\frac{1}{2}}\left[\frac{\pi}{2}+\tan^{-1}\frac{(\xi-\nu/2)}{(1+(\omega+\lambda)^2)^{\frac{1}{2}}}\right]-\omega(1+\omega^2)^{-\frac{1}{2}}\left[\frac{\pi}{2}+\tan^{-1}\frac{(\xi-\nu/2)}{(1+\omega^2)^{\frac{1}{2}}}\right]\right\}.$$

As in Section 3, the excellence of the approximations can be inferred from the results of another paper.[3]

5. ARRAYS OF TROFFERS

I. Exact Formulae for the Flux Density from a One-Dimensional Array of Finite Troffers

Illumination is produced by an array of long, narrow, luminous strips (Fig. 4). Such arrays are common in modern lighting practice and may consist of luminous panels of diffusing glass set in the ceiling, built-in ceiling reflectors with fluorescent lamps (troffers[3]), or long continuous rows of fluorescent luminaires hung from the ceiling. For the nth source in a complete array of N,

$$e=\frac{(n-1)s+x+w/2}{h},\quad f=\frac{(n-1)s+x-w/2}{h},\quad g=l/h,\quad q=0,\quad n=1,2,\cdots,N,\tag{43}$$

where e, f, g, *and* q *are restricted to non-negative values*. If the variables of Eq. (8) are introduced, Eq. (43) becomes

$$e=(n-1)\mu+\xi+\nu/2,\quad f=(n-1)\mu+\xi-\nu/2,\quad g=\lambda,\quad q=0,\quad n=1,2,\cdots,N.\tag{44}$$

For the array of N sources, according to Eq. (6),

$$D_x=\frac{H}{2\pi}\sum_{n=1}^{N}\left[(1+f^2)^{-\frac{1}{2}}\tan^{-1}\frac{g}{(1+f^2)^{\frac{1}{2}}}-(1+e^2)^{-\frac{1}{2}}\tan^{-1}\frac{g}{(1+e^2)^{\frac{1}{2}}}\right];$$
$$D_y=\frac{H}{2\pi}\sum_{n=1}^{N}\left\{\tan^{-1}e-\tan^{-1}f-(1+g^2)^{-\frac{1}{2}}\left[\tan^{-1}\frac{e}{(1+g^2)^{\frac{1}{2}}}-\tan^{-1}\frac{f}{(1+g^2)^{\frac{1}{2}}}\right]\right\};\tag{45}$$
$$D_z=\frac{H}{2\pi}\sum_{n=1}^{N}\left\{g(1+g^2)^{-\frac{1}{2}}\left[\tan^{-1}\frac{e}{(1+g^2)^{\frac{1}{2}}}-\tan^{-1}\frac{f}{(1+g^2)^{\frac{1}{2}}}\right]\right.$$
$$\left.+e(1+e^2)^{-\frac{1}{2}}\tan^{-1}\frac{g}{(1+e^2)^{\frac{1}{2}}}-f(1+f^2)^{-\frac{1}{2}}\tan^{-1}\frac{g}{(1+f^2)^{\frac{1}{2}}}\right\}.$$

[3] D. E. Spencer, "Exact and approximate formulae for the calculation of illumination from troffers," Illum. Eng. (in press).

As previously stated, it is ordinarily sufficient to calculate the flux density for two special cases:

(A) At point P between troffers ($\xi=\mu/2$):

$$e=\frac{(2n-1)\mu+\nu}{2},\quad f=\frac{(2n-1)\mu-\nu}{2},\quad g=\lambda,\quad n=1, 2, \cdots, N. \tag{46}$$

(B) At a point P beneath the center of the troffer ($\xi=0$):

$$e=\frac{2(n-1)\mu+\nu}{2},\quad f=\frac{2(n-1)\mu-\nu}{2},\quad g=\lambda,\quad n=1, 2, \cdots, N, \tag{47}$$

where e, f, and g are again restricted to non-negative values.

II. Exact Formulae for the Flux Density from an Array of Infinite Troffers

If the sources are very long compared with their mounting height they may be considered of infinite length. For the nth source, Eq. (43) becomes

$$e=\frac{2(n-1)s+x+w/2}{h},\quad f=\frac{2(n-1)s+x-w/2}{h},\quad n=1, 2, \cdots, N, \tag{48}$$

where e and f are as usual restricted to non-negative values. Then the introduction of the variables of Eq. (8) into (43) gives

$$e=(n-1)\mu+\xi+\nu/2,\quad f=(n-1)\mu+\xi-\nu/2,\quad n=1, 2, \cdots, N. \tag{49}$$

For a system of N troffers of infinite length, Eq. (45) reduces to

$$\begin{aligned} D_x&=\frac{H}{4}\sum_{n=1}^{N}[(1+f^2)^{-\frac{1}{2}}-(1+e^2)^{-\frac{1}{2}}];\\ D_y&=\frac{H}{2\pi}\sum_{n=1}^{N}[\tan^{-1}e-\tan^{-1}f]; \\ D_z&=\frac{H}{4}\sum_{n=1}^{N}[e(1+e^2)^{-\frac{1}{2}}-f(1+f^2)^{-\frac{1}{2}}]. \end{aligned} \tag{50}$$

The special cases are the same as in I, and e and f are given by Eqs. (46) and (47).

III. Approximate Formulae for Illumination from a One-Dimensional Array of Finite Troffers

The simple approximation effected by the use of an equivalent uniform source will now be developed. Let H_u be the helios of the uniform source which is substituted in place of the system of troffers having helios H_t. Then

$$H_u=H_t\frac{(N-1/2)\nu+\xi}{(N-1/2)\mu+\xi}\quad\text{if } \xi<\nu;\quad H_u=H_t\frac{N\nu}{(N-1/2)\mu+\xi}\quad\text{if } \xi\geq\nu, \tag{51}$$

and from Eq. (6),

$$e=(N-1/2)\mu+\xi,\quad g=\lambda. \tag{52}$$

The flux densities are therefore

$$D_x=\frac{H_u}{2\pi}\left\{\tan^{-1} g-(1+e^2)^{-\frac{1}{2}}\tan^{-1}\frac{g}{(1+e^2)^{\frac{1}{2}}}\right\};$$

$$D_y=\frac{H_u}{2\pi}\left\{\tan^{-1} e+(1+g^2)^{-\frac{1}{2}}\tan^{-1}\frac{e}{(1+g^2)^{\frac{1}{2}}}\right\}; \tag{53}$$

$$D_z=\frac{H_u}{2\pi}\left\{e(1+e^2)^{-\frac{1}{2}}\tan^{-1}\frac{g}{(1+e^2)^{\frac{1}{2}}}+g(1+g^2)^{-\frac{1}{2}}\tan^{-1}\frac{e}{(1+g^2)^{\frac{1}{2}}}\right\}.$$

If the number of troffers is large, $N\to\infty$ and Eq. (53) reduces to

$$D_x=\frac{H_u}{2\pi}\tan^{-1} g;\quad D_y=\frac{H_u}{4}[1-(1+g^2)^{-\frac{1}{2}}];\quad D_z=\frac{H_u}{4}g(1+g^2)^{-\frac{1}{2}}. \tag{54}$$

If $N\to\infty$ and $g\to\infty$, corresponding to conditions in an extremely large room,

$$D_x=D_y=D_z=H_u/4, \tag{55}$$

which is the well-known result for the flux density from one-quarter of a uniform sky.

For the two kinds of special cases considered in previous sections, Eq. (52) gives for an array of troffers,

(A) At a point midway between troffers ($\xi=\mu/2$):

$$e=N\mu,\quad g=\lambda. \tag{56}$$

(B) At a point beneath the center of a troffer ($\xi=0$):

$$e=(N-1/2)\mu,\quad g=\lambda. \tag{57}$$

IV. Approximate Formulae for Flux Density from One-Dimensional Arrays of Infinite Troffers

If the luminous strip sources are very long compared with their mounting height, they may be considered as of infinite length and may be replaced by a single uniform window of infinite length. The equations of III then assume the following simple forms:

$$H_u=H_t\frac{(N-1/2)\nu+\xi}{(N-1/2)\mu+\xi}\quad\text{if } \xi<\nu;\quad H_u=H_t\frac{N\nu}{(N-1/2)\mu+\xi}\quad\text{if } \xi\geq\nu. \tag{58}$$

Also,

$$e=(N-1/2)\mu+\xi. \tag{59}$$

The flux densities are

$$D_x=\frac{H_u}{4}[1-(1+e^2)^{-\frac{1}{2}}];\quad D_y=\frac{H_u}{2\pi}\tan^{-1} e;\quad D_z=\frac{H_u}{4}e(1+e^2)^{-\frac{1}{2}}. \tag{60}$$

If the number of troffers is infinite, Eqs. (55) are again obtained. For the usual special cases, Eq. (59) gives

(A) At a point midway between troffers ($\xi+\mu/2$):

$$e=N\mu. \tag{61}$$

(B) At a point P beneath the center of a troffer ($\xi=0$):

$$e=(N-1/2)\mu. \tag{62}$$

TABLE I. Effect of number of troffers. Troffers of infinite length. Illumination on a horizontal plane at a point midway between troffers. $\mu=0.2$, $\nu=0.1$.

N	D_z/H_i Exact	Approx.	Difference	Error (percent)
1	0.024 601	0.024 515	-86×10^{-6}	0.35
2	0.046 554	0.046 424	−130	0.28
3	0.064 443	0.064 312	−131	0.20
4	0.078 196	0.078 087	−109	0.14
5	0.088 471	0.088 388	− 83	0.094
6	0.096 088	0.096 028	− 60	0.063
7	0.101 760	0.101 717	− 43	0.043
8	0.106 031	0.106 000	− 31	0.030
9	0.109 292	0.109 268	− 24	0.021
10	0.111 820	0.111 803	− 17	0.015
11	0.113 808	0.113 796	− 12	0.011
12	0.115 394	0.115 384	− 10	0.008
∞	—	0.125 000		

An idea of the magnitude of the errors introduced by the use of these approximate formulae can be gained from Table I, and the subject is discussed in greater detail in another paper.[3] It is shown that for the range of values encountered in illuminating engineering practice, the approximate formulae give values of flux density that are within one percent of the correct values. The error is practically independent of the position of the point P in a horizontal plane. Effect of number of troffers and of troffers spacing are also considered, and it is found that the error remains less than one percent throughout the range of practical importance, i.e., for N from 1 to ∞ and for μ ranging from 0.1 to 1.0. Even in the extreme case of a single troffer with $\mu=0.5$, the error is less than 2 percent.

6. CONCLUSIONS

Arrays of rectangular sources are of great practical importance in the lighting of rooms. Previous methods of calculating at any point the luminous flux density from such arrays have been rather haphazard and have usually entailed the application of the rectangular-window formula for each source of the array. The present paper develops for the first time equations of complete generality, applying to two-dimensional and one-dimensional arrays of any number of elements and giving flux densities on horizontal and on vertical surfaces.

These formulae allow exact calculations to be made in a straightforward and systematic manner. The equations are inherently cumbersome, however, and hence it is desirable to derive approximate formulae. It is found that by imagining the array to be replaced by an equivalent uniform window of appropriate helios, the calculations are immensely simplified. The errors introduced by this approximation are investigated and are found to be less than one percent for the range of values occurring in illuminating engineering practice.

The formulae presented in the paper give the flux densities on horizontal and on vertical planes. The vector method of calculation[4] then *allows the determination of the flux density on any tilted plane.* If the illuminated plane cuts the plane of the array in such a way that the equivalent uniform source is rectangular, the formulae of this paper are directly applicable. In the rather unusual case that the equivalent uniform source is not rectangular, the results of a paper on triangular sources are used.[5]

An important consequence is that the methods can be extended to the problem of interreflections in rooms. Methods are available[6] for the calculation of the *average* flux density in rooms lighted by uniform ceilings and having interreflections. This work can now be extended to rooms lighted by arrays of rectangular sources by the simple procedure of obtaining the helios H_u of the equivalent uniform ceiling and imagining the true lighting system to be replaced[3] by an indirect system having this helios.

[4] Parry Moon, "Basic principles in illumination calculations," J. Opt. Soc. Am. **29**, 108 (1939).
[5] D. E. Spencer, "Calculation of illumination from triangular sources," J. Opt. Soc. Am. **32**, 274 (1942).
[6] Parry Moon, "Interreflections in rooms," J. Opt. Soc. Am. **31**, 374 (1941).

A Fundamental Criterion of Uniform* Representability of Equiluminous Colors on a Geometrical Surface†

LUDWIK SILBERSTEIN
Kodak Research Laboratories, Eastman Kodak Company, Rochester, New York
(Received June 12, 1942)

CONSIDER the two-dimensional manifold of all colors of equal luminance (or brightness), each defined by two independent stimuli-coordinates, x, y (with z co-determined by x, y). Any two colors just distinguishable from each other or, in technical language, of least perceptible chromaticity difference, will be called next neighbors or simply *neighbors*.

Any color $P(x, y)$, unless it be a boundary color, is surrounded by a closed continuous (one-dimensional) set of neighbors $Q(x+\Delta x, y+\Delta y)$. In any graphical representation, on a plane or some other surface, the color $P(x, y)$ will be represented by a point P and the whole set of its neighbors Q by a closed line or circuit. The shape and size of this line will depend of course on the choice of the system of stimuli-coordinates and on the scheme adopted for their graphical representation (which need not so far be "uniform").

Let Q_1 be one of the Q colors. It has, on the Q line, two neighbors. Let Q_2 (Fig. 1) be one of them. From Q_2 pass on to its neighbor Q_3, thence to Q_4, and so on. Suppose, for instance, that the next neighbor of Q_6 is the starting color Q_1 itself. Then we shall say that P has just six *distinct neighbors* (or, equivalently, that the Q circuit around P is just completed by six chromaticity steps). Generally, *mutatis mutandis*, we shall say that a color P has n *distinct neighbors* (or as many "steps" around it). Notice that this number n need not be an integer. In fact, it might happen that Q_7 (say) does not coincide with Q_1, but falls somewhere between Q_1 and Q_2. Such being the case, let Q_7 be followed by $Q_8, \cdots, Q_{11}$, and suppose, e.g., that Q_{12} coincides with the starting point Q_1. Then, since the circuit was completed twice over (in eleven steps), we shall say that $n=11/2=5.5$. In fine, the number n may turn out (experimentally) to have any value (not less than 2, of course) integer or not.

Moreover, the value of n need not, *a priori*, be the same for (i.e., around) all colors P, but may be different in different parts of our color domain. To provide for this, we may denote it by $n(P)$ or $n(x, y)$.

We shall, however, assume for the sequel that n does not change appreciably in passing from a color to any of its *next* neighbors, e.g., that $n(P) \doteqdot n(Q_1)$. It shall, also, be taken for granted that the value found for $n(P)$ is independent of the choice of the starting point (Q_1) on the Q line and of the sense in which the Q circuit has been traversed. Thus, $n(P)$, constant or not, will at least be a one-valued function of "position" in the color twofold.

Now, whereas the shape of the Q line surrounding a color P depends on the choice of the coordinate system, the number $n(P)$ of its neighbors, as defined above, is manifestly independent of any such choice. It is an intrinsic property of the color domain itself in relation to perceptibility of chromaticity differences, of course for a given eye, given field size and field brightness. It can be evaluated experimentally for any color P independently of, and, in fact, without the aid of, any graphical representation at all.

Suppose, now, that this has actually been accomplished and let it be required to represent

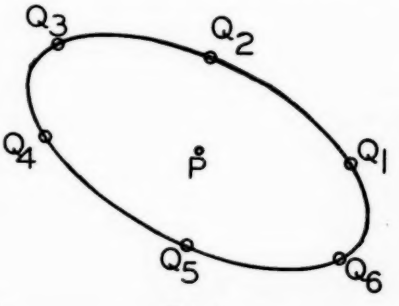

FIG. 1.

* I.e., with chromaticity difference proportional to distance.

† Communication No. 860 from the Kodak Research Laboratories.

the whole color twofold on a geometrical surface in such a way that, with a proper choice of the coordinate system, the chromaticity difference of every two colors shall be proportional to the distance of the corresponding two points on that surface (i.e., the length of the geodesic between them).

We can say that then the properties of such a surface at or around any point P corresponding to a color $P(x, y)$ will be determined by the number $n(P)$ belonging to this color, namely, $n(P)$ will determine *the curvature* of the surface at the point P.

In fact, let the points P, Q_1, and Q_2 correspond to the color P and its two neighbors, as defined above in connection with Fig. 1. Then, by requirement,

$$PQ_1 = Q_1Q_2 = PQ_2,$$

so that the geodesic triangle PQ_1Q_2 (Fig. 2) will be an equilateral triangle with the angle at P equal $2\pi/n$ and, since by assumption $n(Q_1) \doteq n(Q_2) \doteq n(P)$, each of its angles will be equal to $2\pi/n$.** Thus, the excess of its angle sum over two right angles will be $\Delta = 6\pi/n - \pi$ or

$$\Delta = \pi(6/n - 1). \qquad (1)$$

But this excess (positive or negative) is, by Gauss' well-known theorem, *the total curvature* of the geodesic triangle PQ_1Q_2. If we agree to consider the (psychologically elementary) triangle as "infinitesimal," which amounts only to assuming that the properties of the surface do not vary appreciably within it, and if we denote its area by σ, then Δ/σ will be just *the curvature* K of the surface at the point P,

$$K = (\pi/\sigma)(6/n - 1), \qquad (2)$$

where n may vary from point to point, intrinsically, while σ will depend also on the arbitrary scale of the map.

The simple formula (1) or (2) gives directly the criterion announced in the title of the paper.

The formula teaches us that the necessary and sufficient condition of the required uniform representability of the color twofold on a surface of any constant curvature at all is the constancy of n, i.e., the equality of the number $n(P)$ for all colors P of the contemplated twofold up to its boundary.

If this number is constant and smaller than six, the required surface is of constant positive curvature or a sphere, of radius $R = 1/K^{\frac{1}{2}}$, and if it is greater than six, a surface of constant negative curvature (like the plane of hyperbolic geometry or its familiar model, the pseudosphere, not unlike a champagne glass). It can be an ordinary plane (or developable upon it) if, and only if, the number n is just equal to six, or practically so.

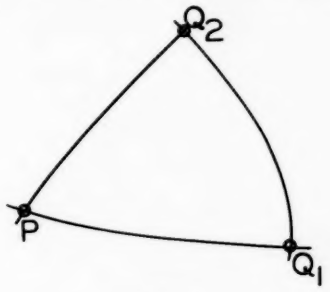

FIG. 2.

How nearly and whether at all such is the case or not, we are far from being able to say. In this respect we should like to mention only an excellent paper by Deane B. Judd of the Bureau of Standards on "*A Maxwell triangle yielding uniform chromaticity scales.*"[1] Judd claims to have found by trial and error a colorimetric coordinate system whose "Maxwell triangle [a *plane* triangle of course] has the useful property that the length of any line on it is a close measure of the chromaticity difference between the stimuli represented at the extremes of the line." To support his claim, Judd tests it very carefully and impartially on a wealth of available experimental data, namely, pertaining to sensibility to change in dominant wave-length (Λ) at constant purity, sensibility to change in purity at constant Λ, sensibility to change in color temperature, and sensibility to change in the so-called "Lovibond number." The degree of agreement is, in several instances, encouraging but, admittedly, far from being perfect.

** Notice that on a surface of variable curvature (as, e.g., an egg's surface) the angles of an equilateral triangle need not, in general, be equal.

[1] D. B. Judd, J. Opt. Soc. Am. **25**, 24–35 (1935).

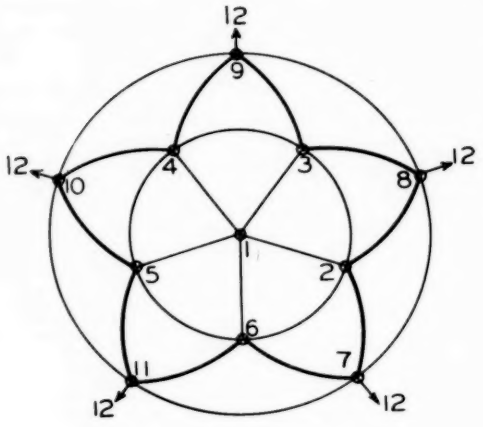

FIG. 3.

All these tests are, no doubt, relevant and valuable, but rather indirect. A most direct and conclusive test of Judd's contention would consist in experimentally evaluating the number n of distinct neighbors of a point (color) in various parts of the Maxwell triangle and showing that it does not differ appreciably from $n=6$.[2]

We do not know whether such counts have ever been made or not. They would, no doubt, imply very laborious experiments and delicate observations. Such, however, was also the price of some of the experimental data already available and utilized by Judd. And the evaluation of the n number at various places well distributed over the color twofold would have the advantage of offering a fundamental and most direct test of its uniform representability by a plane diagram. Perhaps some experts in experimental colorimetry will find it worth their while to take up this difficult but not unattractive task.

In the meantime, and without any intention of prejudging its outcome (for or against $n=6$), we should like to draw the reader's attention to some conclusions which may easily be derived from our curvature formula (2).

Suppose, for simplicity, that the number n has some unique, constant value up to the very borders of the color twofold. Then all the elementary triangles or natural meshes (such as PQ_1Q_2 above) are congruent and σ is a constant area depending only on the scale chosen, and the curvature K of the surface has some constant value.

Now, if n is *equal* to or *greater* than 6, the surface is an ordinary Euclidean plane or some model of a hyperbolic (Lobatchevskyan) plane, of constant negative curvature and, both of these surfaces being infinite, the number of elementary triangles or meshes is (*a priori*) unlimited, that is to say, the network of such meshes may be continued indefinitely and, colorimetrically, can be extended up to the natural boundary of the color twofold, no matter how great the number of meshes actually discernible to the most trained eye. In this respect, then, n might have any value greater than six without impairing the correctness of the color map.

The situation in the alternative case is altogether different. In fact, if $n<6$, then the representative surface is a sphere, of radius R say, such that, by (2),

$$1/R^2=(\pi/\sigma)(6/n-1).$$

It is, manifestly, in our power to make this radius as big (and thus the curvature of the surface as small) as we please, but then the triangular meshes will be correspondingly large. All this depends on the scale whose choice is perfectly arbitrary. But the total number N of meshes which can be spread over the sphere is governed only by the value of n and has thus an intrinsic meaning, independent of the scale chosen. In fact, $4\pi R^2$ being the total area of the sphere, this number is $4\pi R^2/\sigma$ or

$$N=4n/(6-n), \qquad (3)$$

a function of n alone. This simple formula can give us some interesting information about the possibilities of the proposed mapping of the color domain.

Thus, for instance, it enables us to say that, if such a map is to be practicable, the number n cannot be as small as 5. For, if it were equal to 5,

[2] In a paper entitled "Solid geometry in color space," J. Opt. Soc. Am., **31**, 461–462 (1941), I. A. Balinkin assumed that chromaticity differences can be represented adequately in the manner suggested by Judd and that the principle can be extended to the representation in Euclidean space of co-existent differences of luminance and chromaticity. From these assumptions Balinkin claims to have demonstrated that only twelve colors can be chosen which are as different from each other as from any given central color.

the whole sphere would be covered by a network consisting of only

$$N=20$$

triangular meshes, spread between 12 points‡‡ or colors, and since within the color twofold many more color meshes and points (several hundred) can be distinguished, only a small portion of the twofold at a time could be mapped on the sphere. For the whole twofold a good many spheres would be necessary. Moreover, the actual neighbor-relations of the colors, even on any of these partial maps, would be coarsely misrepresented, unless some of its 12 points were discarded. To see this, imagine one color placed at the corner 1 of the icosahedron. Its five neighbors occupy then as many corners, 2 to 6, placed on a circle around 1. Each of these five colors, having already three neighbors, must be given two more neighbors. Let those of 2 be labelled 7 and 8. These must be each other's neighbors, and since 7, 8, 3, 1, 6 is to be a ring of neighbors, 7 must also be the neighbor of 6, and 8 of 3. The color 3 has now four neighbors (see the merely schematic Fig. 3); its fifth neighbor 9 must also (as before) be the neighbor of 4; similarly, 4 and 5 have the common neighbor 10, and 5 and 6 the common neighbor 11. The five colors 7 to 11 now form a ring of neighbors which, on the proper sphere, are distributed evenly on a circle equal and parallel to the circle 23456. Each of the five colors 7 to 11, having already its four neighbors, calls just for one more. Let 12 be this missing neighbor of 7, say. Then, for the same reason as before, 12 must also be directly linked to 8 and to 11 and thus also to 9 and 10. Herewith, the point 12 which, on the sphere, is the antipode of 1, is already provided with its five neighbors 7, 8, $\cdots$, 11. Each of the twelve points has now a complete ring of five neighbors, the network is closed, and there is no way of continuing it. The twelve points form obviously $5\times12:3=20$ triangular meshes, as stated above (but here found again, quite regardless of metrics). There is now no room left on the sphere for other colors distinguishable from those twelve. Moreover, the actual neighbor-relationships of some of these twelve colors are not correctly represented. For the five colors 7, 8, $\cdots$, 11, each two steps away from 1, have been given a *common* neighbor (*viz.*, 12), which manifestly is a coarse misrepresentation of the actual relations. Thus, as stated above, some of the twelve colors would have to be relegated from even this partial spherical map of the color twofold. In fact, to avoid radically all misrepresentation (for any $n<6$), only a hemisphere could be utilized. For, beyond the equator, with 1 as pole, the parallel circles, which have to represent loci of colors equidistant from 1, would begin to decrease (instead of increasing) with increasing distance from the pole.

The situation would not be much improved if, instead of $n=5$, we had $n=11/2=5.5$. In fact, formula (3) would then give $N=44$ meshes, and for the available hemisphere, only 22 meshes. Similarly, $n=17/3=5\frac{2}{3}$ would give $N=68$ or, for the hemisphere, 34 meshes only, and so on.††

Needless to say, for $n<5$, the total number of meshes possible on a proper sphere would be much smaller still. Thus, e.g., $n=4$ would give $N=8$, an octahedron, and $n=3$ would give $N=4$, a tetrahedron, with 6 and 4 corner points (or distinguishable colors), respectively. Such low values of n, however, seem quite unlikely.

Without indulging any longer in these academic niceties, we may conclude by saying that, if the number n is at all constant and perceptibly

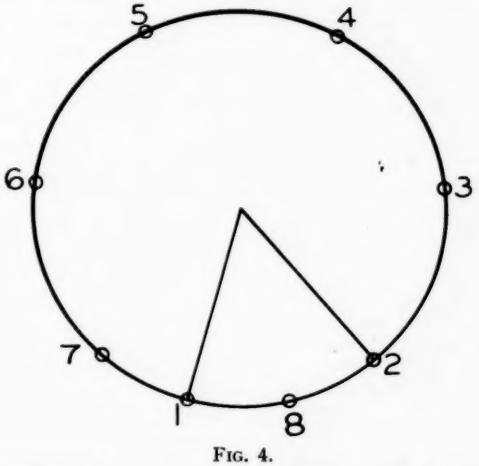

FIG. 4.

‡‡ The corners of a regular *icosahedron*. (20 faces.)

†† If $n=6$ exactly, the formula gives of course $N=\infty$, without overlappings or lacunes.

smaller than six, a uniform mapping of the color twofold on one or several globes is, to all purposes, impracticable. If $n \doteqdot 6$, very nearly, as seems to be implied by Judd's results, we may overlook the little difference and represent the twofold on a plane chart, and if n exceeds 6 considerably, on some saddle-shaped surface.

The main purpose of this paper, however, was to bring out the fundamental and intrinsic nature of the number $n(P)$ as an attribute of the color twofold, leading directly to the formula (2), (3), and to urge its evaluation by actual experiments and observations.

ACKNOWLEDGMENT

Our thanks are due to David L. MacAdam for reading the manuscript of this paper and for many valuable comments.

Note. Our coincidence method of ascertaining the generally non-integral value of the number n can be used for measuring an angle without the aid of a goniometer, only with rigidly clamped compasses. Let a circle, Fig. 4, centered at the vertex, cut the sides of the angle in 1, 2. The legs of the compasses being clamped down so as to fit the point pair 1, 2, apply the compasses successively to 1, 2; 2, 3, and so on until the starting point 1 is (perceptibly) reached again. Then, if k be the total number of steps made in m round trips, the angle is equal to $2\pi m/k$ radians or $360m/k$ degrees. On trial, the reader will find that this method is capable of considerable accuracy.

Richard B. Brown, Jr., Boston Illuminating Engineer, Elected President of Illuminating Engineering Society

RICHARD B. BROWN, JR., illuminating engineer, Boston Edison Company, 39 Boylston Street, Boston, Massachusetts, has been elected President of the Illuminating Engineering Society, and will assume his new office on October 1, according to a recent announcement by the Society.

Other national officers recently elected are: *Vice President* until September 30, 1944—S. B. Williams, Editor, *Electrical World*, 330 West 42 Street, New York; *General Secretary*—Oscar P. Cleaver, Westinghouse Lamp Division, Bloomfield, N. J.; *Treasurer*—A. F. Wakefield, F. W. Wakefield Brass Company, Vermilion, Ohio; *Directors* until September 30, 1945—A. A. Brainerd, Philadelphia Electric Company, 900 Sansom Street, Philadelphia, Pennsylvania; and R. W. Staud, Benjamin Electric Mfg. Company, Des Plaines, Illinois.

In addition, the following Regional Vice Presidents were elected for two-year terms ending September 30, 1944—Carl T. Bremicker, Northern States Power Company, Minneapolis, Minnesota, representing the Mid-Western Region; G. R. Baumgartner, General Electric Company, Nela Park, Cleveland, Ohio, representing the Great Lakes Region; Fred J. Wellhouse, Westinghouse Electric and Mfg. Company, 1 Montgomery Street, San Francisco, California, representing the Pacific Coast Region; and Clarence C. Keller, Holophane Company, Inc., New York, New York, representing the Northeastern Region.